NAVAL POSTGRADUATE SCHOOL

MONTEREY, CALIFORNIA

THESIS

OPTIMAL SCHEDULING OF TIME-SHIFTABLE ELECTRIC LOADS IN EXPEDITIONARY POWER GRIDS

by

John G. Sprague

September 2015

Thesis Advisor:	Emily M. Craparo
Second Reader:	Daniel A. Nussbaum

THIS PAGE INTENTIONALLY LEFT BLANK

REPORT DOCUMENTATION PAGE

Form Approved OMB No. 0704–0188

1. AGENCY USE ONLY *(Leave Blank)*	2. REPORT DATE	3. REPORT TYPE AND DATES COVERED
	09-25-2015	Master's Thesis 01-06-2015 to 09-25-2015

4. TITLE AND SUBTITLE

OPTIMAL SCHEDULING OF TIME-SHIFTABLE ELECTRIC LOADS IN EXPEDITIONARY POWER GRIDS

5. FUNDING NUMBERS

6. AUTHOR(S)

John G. Sprague

7. PERFORMING ORGANIZATION NAME(S) AND ADDRESS(ES)

Naval Postgraduate School
Monterey, CA 93943

8. PERFORMING ORGANIZATION REPORT NUMBER

9. SPONSORING / MONITORING AGENCY NAME(S) AND ADDRESS(ES)

Office of Naval Research

10. SPONSORING / MONITORING AGENCY REPORT NUMBER

11. SUPPLEMENTARY NOTES

The views expressed in this document are those of the author and do not reflect the official policy or position of the Department of Defense or the U.S. Government. IRB Protocol Number: N/A.

12a. DISTRIBUTION / AVAILABILITY STATEMENT

Approved for public release; distribution is unlimited

12b. DISTRIBUTION CODE

13. ABSTRACT *(maximum 200 words)*

Environmental control on the battlefield enhances readiness, reduces casualties, and protects the sensitive equipment upon which U.S. doctrine relies. Purchase and delivery of fuel necessary to provide this service was responsible for an estimated $1.4 billion in costs and 33 resupply convoy casualties per year at the peak of U.S. wars in Iraq and Afghanistan.

It is well understood that the current semi-autonomous mode of environmental control unit (ECU) operation results in generators operating at low average loads—and low fuel efficiency—to accommodate periodic unmanaged spikes in peak load. We propose a mechanism to reduce costs through optimal prescriptive management of these ECUs.

We exploit the fact that ECU operation is time-shiftable to develop a mixed-integer linear programming (MILP) model that optimally schedules ECUs to eliminate unmanaged peak demand, reduce generator peak-to-average power ratios, and facilitate a persistent shift to higher fuel efficiency. Using sensitivity analysis, we quantitatively demonstrate how grid composition, temperature band tolerance, and energy storage capabilities contribute to fuel efficiency under this approach.

14. SUBJECT TERMS

expeditionary, energy, optimization, deferrable, fuel, mixed integer linear program

15. NUMBER OF PAGES 121

16. PRICE CODE

17. SECURITY CLASSIFICATION OF REPORT	18. SECURITY CLASSIFICATION OF THIS PAGE	19. SECURITY CLASSIFICATION OF ABSTRACT	20. LIMITATION OF ABSTRACT
Unclassified	Unclassified	Unclassified	UU

NSN 7540-01-280-5500

Standard Form 298 (Rev. 2–89)
Prescribed by ANSI Std. 239–18

THIS PAGE INTENTIONALLY LEFT BLANK

Approved for public release; distribution is unlimited

OPTIMAL SCHEDULING OF TIME-SHIFTABLE ELECTRIC LOADS IN EXPEDITIONARY POWER GRIDS

John G. Sprague
Lieutenant Commander, United States Navy
B.S., University of Maryland, 2002

Submitted in partial fulfillment of the
requirements for the degree of

MASTER OF SCIENCE IN OPERATIONS RESEARCH

from the

NAVAL POSTGRADUATE SCHOOL
September 2015

Author: John G. Sprague

Approved by: Emily M. Craparo
Thesis Advisor

Daniel A. Nussbaum
Second Reader

Patricia A. Jacobs
Chair, Department of Operations Research

THIS PAGE INTENTIONALLY LEFT BLANK

ABSTRACT

Environmental control on the battlefield enhances readiness, reduces casualties, and protects the sensitive equipment upon which U.S. doctrine relies. Purchase and delivery of fuel necessary to provide this service was responsible for an estimated $1.4 billion in costs and 33 resupply convoy casualties per year at the peak of U.S. wars in Iraq and Afghanistan.

It is well understood that the current semi-autonomous mode of environmental control unit (ECU) operation results in generators operating at low average loads—and low fuel efficiency—to accommodate periodic unmanaged spikes in peak load. We propose a mechanism to reduce costs through optimal prescriptive management of these ECUs.

We exploit the fact that ECU operation is time-shiftable to develop a mixed-integer linear programming (MILP) model that optimally schedules ECUs to eliminate unmanaged peak demand, reduce generator peak-to-average power ratios, and facilitate a persistent shift to higher fuel efficiency. Using sensitivity analysis, we quantitatively demonstrate how grid composition, temperature band tolerance, and energy storage capabilities contribute to fuel efficiency under this approach.

THIS PAGE INTENTIONALLY LEFT BLANK

Table of Contents

List of Figures

THIS PAGE INTENTIONALLY LEFT BLANK

List of Tables

List of Acronyms and Abbreviations

AC	alternating current
AKSSS	Alaska Small Shelter System
AMMPS	Advanced Medium Mobile Power Sources
AutoDISE	Automatic Distribution Illumination System, Electrical
BTU	British thermal unit
CFM	cubic feet per minute
COC	combat operations center
DC	direct current
DCAC	direct current air conditioner
DLA-E	Defense Logistics Agency - Energy
DOD	Department of Defense
DSM	demand side management
ECU	environmental control unit
EV	electric vehicle
EXFOB	Experimental Forward Operating Base
FY	fiscal year
GAMS	General Algebraic Modeling System
GREENS	Ground Renewable Expeditionary Energy Network System
GBOSS	Ground Based Operation Surveillance System
GB	gigabyte

GWh	gigawatt-hour
HI-Power	Hybrid Intelligent Power
HVAC	heating, ventilation, and air conditioning
IECU	Improved Environmental Control Unit
IPDISE	Improved Power Distribution System, Electrical
kW	kilowatt
kWh	kilowatt-hour
LAMPS	Large Advanced Mobile Power Sources
LAMS	Large Area Maintenance Shelter
LGCY	legacy unmanaged
MAGTF	Marine Air Ground Task Force
MEB-A	Marine Expeditionary Battalion - Afghanistan
MEHPS	Mobile Electric Hybrid Power Sources
MEPDIS-R	Mobile Electric Power Distribution-Replacement
MILP	mixed integer linear program
MIT	Massachusetts Institute of Technology
MW	megawatt
NTV	non-tactical vehicle
OEF	Operation Enduring Freedom
OIF	Operation Iraqi Freedom
PDISE	Power Distribution Illumination System, Electrical

PFK-FM perfect future knowledge, full management

PFK-GSM perfect future knowledge, generator and storage management

PFK-SOM perfect future knowledge, storage-only management

PV photovoltaic

RH-PFK rolling horizon with perfect future knowledge

RH-U rolling horizon with uncertainty

RMIP relaxed mixed integer program

SOS2 specially ordered set, type 2

TEMPER Tent Extendable Modular Personnel

TOC tactical operations center

TQG Tactical Quiet Generator

USA United States Army

USAF United States Air Force

USMC United States Marine Corps

V volts

VSP village stability platform

W watt

WTE waste-to-energy

THIS PAGE INTENTIONALLY LEFT BLANK

Executive Summary

Heating, ventilation, and air conditioning (HVAC) on the battlefield enhances readiness and mission effectiveness, reduces combat and non-combat casualties, and protects the sensitive technology upon which an U.S. doctrine and military might increasingly relies. HVAC in expeditionary environments is provided by electric air conditioners and environmental control units (ECUs) that are commonly powered by diesel generators. ECUs account for up to 70% of total expeditionary electricity consumption, and the purchase and delivery of the fuel required to operate these generators places enormous financial, logistical, and human costs on the U.S. military [1]. Data from fiscal year 2007 suggest that HVAC fuel requirements in Iraq and Afghanistan were responsible for $1.4 billion in costs and 33 resupply convoy casualties in a single year [2], [3].

We propose a mechanism to reduce these costs by controlling ECU operation in a manner that optimizes generator fuel consumption while maintaining environmental conditions within desired parameters.

ECUs currently act independently under local thermostatic control. This semi-autonomous operation requires that the electrical grid have sufficient generation capacity to support the peak demand that would occur if all connected loads required power at the same instant. In practice, however, most electrical loads are not operating at all times and average electrical demand is often well below peak demand. Multiple studies by the U.S. Army and U.S. Marine Corps indicate that half of all generators in the field operate at less than 32% average load [4].

Sizing generators for the peak demand which *might* occur, yet operating them only at the actual demand that *does* occur from intermittent loads is a significant driver of fuel consumption. Generator efficiency is non-linear, highest when loaded near rated capacity and dropping rapidly as load declines below 50% [4]. Frequent operation at low power—and low fuel efficiency—is the price paid for the constant readiness to supply unmanaged demand.

We address this issue by prescriptively managing ECU operation. We exploit the fact that ECU events are *time-shiftable*, or capable of being advanced or deferred by small incre-

ments with no impact to the mission, and show that ECUs can be optimally scheduled to eliminate unmanaged peak demand, improve generator peak-to-average power ratios, and reduce total fuel consumption.

Analysis was conducted using discrete-time simulation to model shelter thermal characteristics and ECU operation under existing control schemes, followed by mixed-integer linear programming (MILP) to assess potential fuel savings under various optimization policies. Notable findings include:

- Fuel consumption in the baseline optimally scheduled ECU grid is 28% lower than legacy ECU policies
- The greatest benefit to ECU optimization occurs when ECU duty cycle (the proportion of time that ECUs are operating) is low. Optimal and legacy results converge as duty cycle approaches 100%
- Energy storage offers very little benefit in the grid configurations tested, with only 2% to 6% of generator output stored. Optimal solutions overwhelmingly choose to do ECU work in advance rather than store energy, at a loss, to do work later.
- Generator clustering, i.e., deploying two 30 kW generators rather than a single 60 kW generator, permits a broader range of optimization alternatives that can deliver greater fuel economy under certain load conditions.

.

List of References

[1] M. Schwartz, K. Blakely, and R. O'Rourke, "Department of Defense Energy initiatives: Background and issues for Congress," Congressional Research Service, Washington, DC, CRS Report R42558, June 2012.

[2] S. B. Siegel, S. Bell, S. Dicke, and P. Arbuckle, "Sustain the mission project: Energy and water costing methodology and decision support tool," Army Environmental Policy Institute, Arlington, VA, Final Technical Report, Mar. 2008.

[3] D. S. Eady, S. B. Siegel, R. S. Bell, and S. H. Dicke, "Sustain the mission project: Casualty factors for fuel and water resupply convoys," Army Environmental Policy Institute, Arlington, VA, Final Technical Report CTC-CR-2009-163, Sep. 2009.

[4] S. B. Van Broekhoven, E. Shields, S. V. T. Nguyen, E. R. Limpaecher, and C. M. Lamb, "Tactical power systems study ," Lincoln Laboratory, Massachusetts Institute of Technology, Lexington, MA, Technical Report 1181, May 2014.

THIS PAGE INTENTIONALLY LEFT BLANK

Acknowledgments

I am deeply indebted to the entire faculty and staff of the Operations Research Department at the Naval Postgraduate School. Their profound expertise and unrelenting commitment to education and national security is inspiring, and I am endlessly grateful for having had the opportunity to study under their guidance.

My advisor, Assistant Professor Emily Craparo, deserves special mention. Her patience, thoughtful analysis, critical review, and tireless coaching were indispensable. Visiting Professor Daniel Nussbaum graciously consented to act as my second reader, bringing a sharp eye for detail, discerning judgment, and deep knowledge of the subject matter.

Several external contributors kindly shared their knowledge, data, and feedback. These include Mr. John Vavrin of the U.S. Army Corps of Engineers, LTC Sundiata-Walker of the U.S. Army Program Executive Office - Combat Support and Combat Service Support, Mr. Eric Shields of the Naval Surface Warfare Center - Carderock Division, and Mr. Chris Bolton of the U.S. Army Program Manager for Expeditionary Energy and Sustainment Systems.

I was fortunate to be among an amazingly diverse and talented cohort of officer students at the Naval Postgraduate School. They are too numerous to list, but I would be remiss not to thank Mark Fitzgerald, Kerry Hogan, Abbie Merkl, Abaigeal Pacholk, Rob Salire, and Matt Miller for their friendship, encouragement, and camaraderie.

Finally, I owe my wife, Shawna, and our children, Alex and Kimberly, an immeasurable amount of gratitude for their patience and support over the past two years.

THIS PAGE INTENTIONALLY LEFT BLANK

CHAPTER 1:
Introduction and Research Objectives

An essential component of U.S. military power is the ability to conduct sustained operations in every area of the globe. When these operations occur in extreme climatic regions, preserving combat effectiveness and minimizing incidence of combat and non-combat casualties depend heavily upon protecting military forces from the physical and psychological effects of environmental extremes [1]. Personnel and equipment are safeguarded from bitter cold and blazing heat by expeditionary shelter systems consisting of structures with heating, ventilation, and air conditioning (HVAC) systems supported by electrical generation and distribution equipment.

This thesis evaluates the cost of providing environmental protection, reviews related literature, and proposes a mechanism to reduce costs by exploiting specific characteristics of HVAC loads and the generators that power them.

1.1 Operational Energy

The Department of Defense (DOD) is the largest energy consumer within the U.S. government, accounting for 80% of all federal energy consumption [2]. As shown in Table 1.1, operational energy[1] demands for fiscal year (FY) 2015 are estimated at 96.2 million barrels of refined petroleum products, or more than 263,000 barrels per day [5]. To put this figure in perspective, DOD operational energy requirements are greater than that of the entire nation of Austria, the world's 53rd largest consumer of petroleum [6].

[1] Operational energy is defined in law as "the energy required for training, moving, and sustaining military forces and weapons platforms for military operations. The term includes energy used by tactical power systems and generators and weapons platforms" [3]. This is distinct from facility energy, described by [4] as the energy to power fixed installations, enduring locations, and non-tactical vehicles (NTVs).

		Historical					*Estimated*	
		FY09	**FY10**	**FY11**	**FY12**	**FY13**	**FY14**	**FY15**
Operational Energy Demand, Million Barrels	Army	18.9	18.9	20.1	16.1	12.7	22.3	21.7
	Navy	29.5	30.0	31.0	31.5	28.4	36.1	33.7
	Air Force	61.7	63.0	61.4	55.8	47.8	42.4	36.8
	USMC	0.6	0.4	0.3	0.2	0.2	1.5	1.2
	Other DoD	0.5	0.5	0.5	0.4	0.7	2.3	2.5
	Total Demand	**111.2**	**112.8**	**113.3**	**104.0**	**89.8**	**104.6**	**96.2**
	Expenditures, $ Billion	**$ 10.3**	**$ 13.3**	**$ 16.8**	**$ 16.4**	**$ 14.8**	**$ 16.0**	**$ 15.0**

Table 1.1: DOD operational energy demand, FY09 through FY15, from [5].

Globally, aircraft account for an estimated 75% of this usage with ships, ground vehicles, and support operations consuming the remaining 25% [7]. This mix changes in active combat zones, where large cargo aircraft are less likely to be refueled on the ground, up-armored tactical ground vehicles are heavier and less fuel-efficient, and a greater portion of electricity is supplied by local generation rather than a municipal grid. A 2009 United States Marine Corps (USMC) study of 5.2 million gallons of fuel consumed by Marine Expeditionary Battalion - Afghanistan (MEB-A) in March, June, September, and December discovered that 32% of the fuel usage was devoted to electrical power generation [8]. Figure 1.1 displays a summary result from this study.

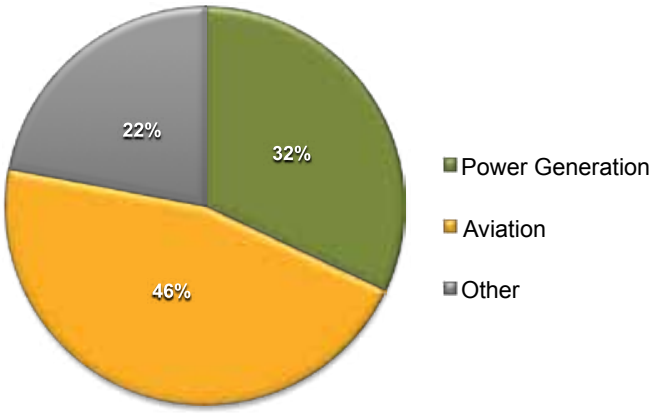

Figure 1.1: MEB-A bulk fuel consumption, August 2009, from [9].

The majority of this generated electricity is used for environmental control, i.e., HVAC systems. Figure 1.2 shows results from a USMC study of Marine Air Ground Task Force (MAGTF) organizational equipment inventories that found air conditioners and environmental control units (ECUs) accounted for 57% of expeditionary power demand [9]. Similarly, research conducted over a 48-hour period on an instrumented expeditionary camp at Fort Blevins showed that 97.7% of total electricity consumption was devoted to maintaining desirable temperatures in occupied areas [10]. In a 2012 survey of multiple studies, the Congressional Research Service cited a range of 57% to 70% of generator power output committed to expeditionary environmental control [2]. We adopt a value of 60% for further analysis.

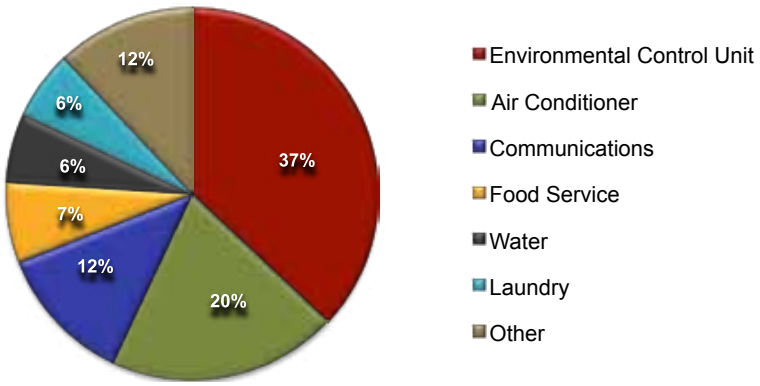

Figure 1.2: Analysis of MAGTF equipment power demands. Environmental control equipment accounts for 57% of electrical power consumption, from [9].

1.2 The Cost of Heating and Cooling

Operational energy costs and risks have been the subject of Congressional hearings, contributed to the creation of a presidentially-appointed Assistant Secretary of Defense for Operational Energy Plans and Programs, and received more than $4 billion to support demand reduction and supply diversification efforts [11], [12]. Examination of consumption, cost, and casualty data for a sample year illustrates the magnitude of resources required to fulfill expeditionary heating and cooling demands.

1.2.1 Monetary Costs

In FY2007, the Army Petroleum Center purchased 590 million gallons of fuel to supply U.S. forces operating in Iraq and Afghanistan [13]. Applying USMC estimates that 32% of this fuel was directed to electrical power generation, and that 60% of the resulting electricity was utilized for environmental control, we estimate that nearly 20% of the 2007 fuel requirement, or 113 million gallons, were devoted to heating and cooling. Additionally, contractor activities—including prime power generation for U.S. forces—require substantial fuel whose cost is embedded in the contract price rather than in DOD consumption figures, resulting in underestimation of actual operational fuel requirements [2].

Applying the 2007 Defense Logistics Agency - Energy (DLA-E) standard price of $2.00 per gallon for diesel fuel, we establish a floor of $226M in heating and cooling costs for Operation Iraqi Freedom (OIF)-Operation Enduring Freedom (OEF) in 2007 [14]. At the present standard price of $3.15 per gallon, the minimum cost to duplicate this effort rises to more than $356M.

DLA-E figures merely represent the fuel commodity price "at the pump" and do not adequately capture the true cost of delivery to the point of ultimate consumption. Escalation factors include security, delivery and maintenance personnel, delivery, storage and distribution equipment, and the fuel consumed in the delivery process. A survey of computational methodologies by the Congressional Research Service reported that fully burdened costs for a gallon of fuel ranged from $3 to $45 per gallon if delivered by land, and $29 to $45 per gallon if delivered by air [2]. Among these was an Army Environmental Policy Institute 2008 calculation for the fully burdened cost of fuel in Iraq of $14.13 per gallon. Incorporating this estimate reveals a final cost of $1.6 billion for heating and cooling in FY2007 alone [15].

1.2.2 Human Costs

Resupply convoys are an inviting target and significant operational vulnerability, and logistic convoy personnel account for many of the killed and wounded in recent conflicts. Figure 1.3 shows resupply casualty levels in Iraq and Afghanistan from 2003 to 2007.

Applying 2007 convoy casualty factors[2], 33 killed or wounded personnel in a single year are attributable to our demand for heating and cooling [13].

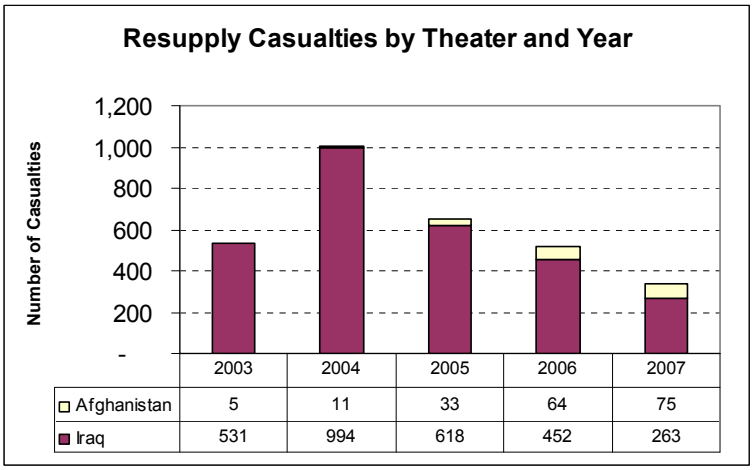

Figure 1.3: Casualties from resupply convoys in Iraq and Afghanistan, 2003-2007, from [13].

1.3 Efficiency and Availability Trade-off

Cyclical loads such as ECUs present a unique and significant obstacle to achieving maximum efficiency in an expeditionary energy system. Though frequently idle and drawing little power, the defining characteristic of these loads is that they *could* activate at any moment. Thermostats monitoring temperature within each facility issue control signals to associated ECUs without regard to existing or pending demands imposed upon the grid. We label these loads, which are permitted to act locally appropriate but are globally naïve, as *unmanaged*. Such demand-side autonomy requires the grid to maintain sufficient online capacity to support unilateral load decisions or risk an overload condition. As a result of these design choices, the system suffers from chronic overgeneration, underutilization, and suboptimal fuel efficiency.

1.3.1 Peak and Average Loads

Expeditionary energy system design currently begins with analysis of electrical demands under the following framework:

[2]One casualty per 3.762 million gallons of delivered fuel in Iraq. One casualty per 2.329 million gallons of fuel delivered in Afghanistan.

1. Determine the type, quantity, and characteristics of connected loads in each structure or facility.
2. Calculate the theoretical maximum power requirement of a facility if all connected equipment is simultaneously operating.
3. Adjust this maximum value by applying a demand factor (≤ 1) representing an assessment of the realistic portion of facility equipment that would simultaneously operate.
4. Add allowances for future growth [16].

Demand factors for air conditioning loads are specified at 1.0, indicating that an appropriately designed power system must be capable of immediately meeting the full, simultaneous demands of all connected units [16].[3] Actual ECU duty cycles[4] depend on factors such as structure characteristics and current environmental conditions, and are often well below 1.0 [17].

Simulation results for generator output with connected loads operating at 75% and 25% duty cycles are presented in Figure 1.4 to illustrate the relationship between ECU duty cycle and generator loading. When connected loads operate at 75% duty cycle, average power demand is 21.6 kilowatt (kW) and peak demand is 28.8 kW. Generator utilization is high, and unused capacity (indicated by white space) is low. At 25% duty cycle, average power demand is only 7.2 kW while peak demand remains 28.8 kW. Utilization is much lower, substantial capacity is wasted, and the generator frequently runs below 30% load, leading to inefficient and potentially damaging operation [18]. Field observations at multiple sites have repeatedly observed this effect [18], [19]. Figure 1.5 displays historical generator load at a village stability platform (VSP) camp in Afghanistan over 96 hours in June 2012.

[3] Other demand factors include laundry (0.8), base operations (0.7), communications (0.7), billeting (1.0), latrines (0.8), warehouse (0.6), and kitchen facilities (0.9) [16].

[4] Duty cycle is the fraction of a time period that a particular unit is operational. For example, a unit that runs six minutes out of every ten has a duty cycle of 0.6.

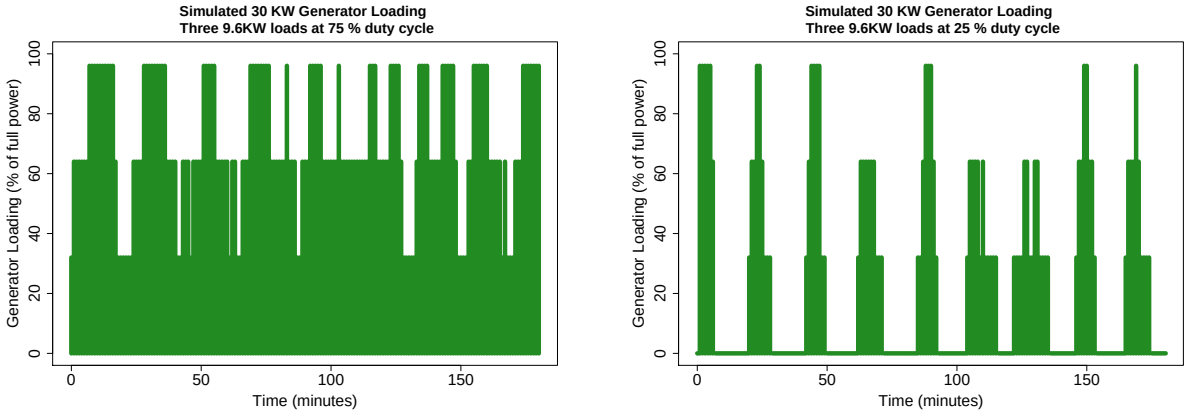

Figure 1.4: Simulated 30 kW generator operation with loads at 75% and 25% duty cycles.

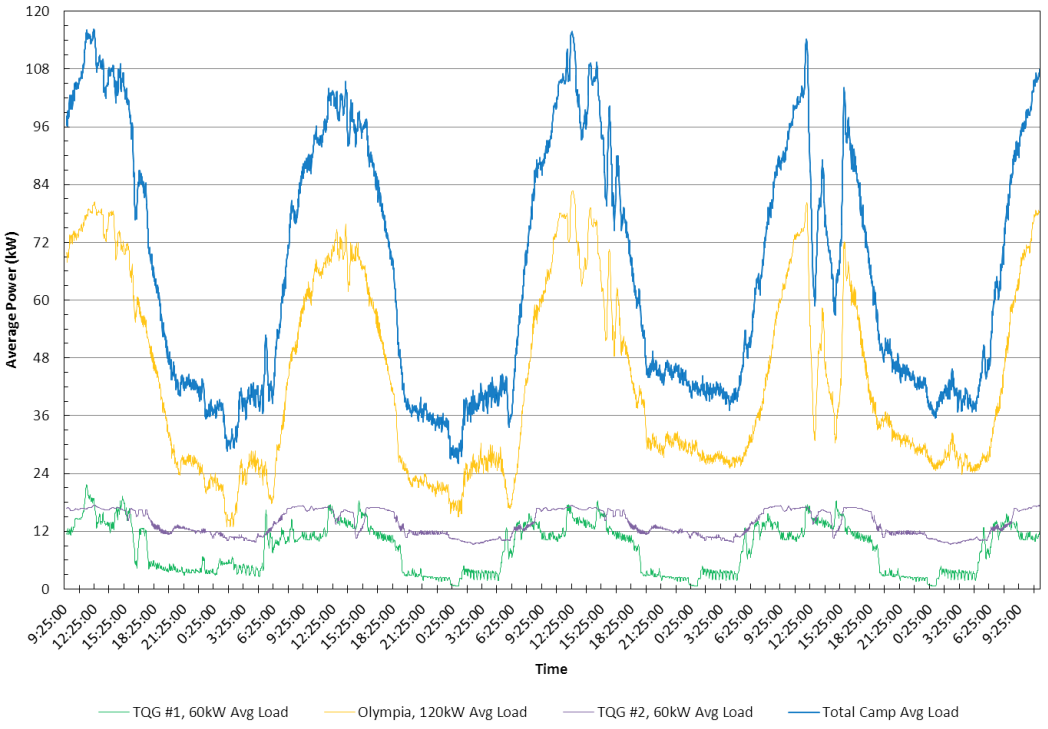

Figure 1.5: U.S. Forces Afghanistan camp electrical demand over a 96-hour period in June 2012. Three generators and site cumulative are displayed, from [19]

.

These demand peaks establish the minimum amount of power that the generation network must constantly be prepared to deliver. Failure to have sufficient online capacity may overload generators, causing voltage and frequency instability that can damage sensitive equipment or trip protective circuits and immediately disconnect serviced loads.[5] Though a generator may, on the average, be capable of powering additional devices, the brief periods of peak demand from those loads already being serviced prevent the connection of any further equipment.

1.3.2 Generator Fuel Efficiency

Generator efficiency (η) is the fraction of chemical energy from fuel that is converted to usable electrical energy [18]. Efficiency is generally greater for larger units and rises nonlinearly with load factor[6] for all sizes of generators. Figure 1.6 depicts the relationship between load factor and fuel efficiency for five sizes of Tactical Quiet Generators (TQGs).

Maximum system efficiency is achieved by selecting the smallest generator capable of providing the required power. For example, a single 40 kW load is better served by a 60 kW generator operating at 0.67 load factor ($\eta \approx 32\%$) than a 200 kW generator running at 0.20 load factor ($\eta \approx 25\%$).

[5] We recognize that military specification generators may operate reliably up to 150% of rated power for limited periods under certain conditions [20]. Unless explicitly specified, we adopt nameplate ratings as the upper limit of generator capacity for two reasons. First, we treat this robustness of military generators as an operational risk mitigator reserved for the benefit of those in the field. Second, many generators used in combat theaters are not military specification and offer no assurance of similar overload capacity.

[6] Generator load factor is power output as a percentage of maximum continuous rated load. For example, a generator rated for 100 kW presently supplying 70 kW is operating at 0.70 load factor

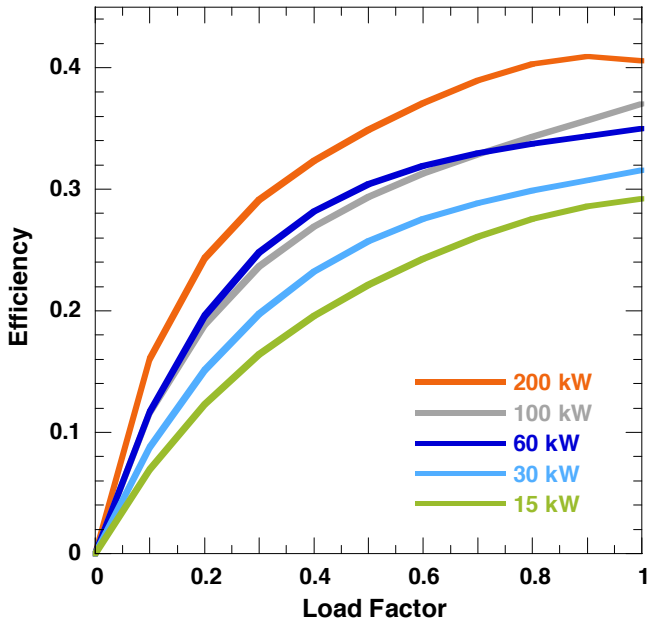

Figure 1.6: Fuel efficiency of U.S. military TQGs as a function of generator size and load factor, from [18].

.

The present requirement to size generators based on peak, rather than average, power demand leads us to provision high-capacity generators from which we tolerate substantial periods of inefficient, low power operation as the price to be paid for peak readiness. The Chief, Technical Management Division at the United States Army (USA) Program Manager for Expeditionary Energy and Sustainment Systems reports that most generator sets used for non-critical applications run at 25-30% average load. Raising that figure while still allowing for peak power operation is described as one the organization's most significant challenges [20].

1.4 Research Objectives

We propose a mechanism in which time-shiftable, non-critical electrical loads in an expeditionary energy grid are optimally scheduled to minimize fuel consumption. We combine information on current load and generator status, generator fuel efficiencies, and shelter conditions and characteristics in a mixed integer linear program (MILP) that prescriptively

defines operational schedules. We construct scenarios with perfect future knowledge to establish optimal upper bounds on improvements to fuel efficiencies, and use simulation of unmanaged systems to establish our lower bounds. Finally, we employ rolling-horizon optimization to determine how a fielded system might perform relative to these bounds.

1.4.1 Scope

Though the model is extensible to an arbitrary number of power sources and loads, computational restrictions limit our exploration to systems of no more than four power sources and nine time-shiftable loads.

We investigate the risks and benefits of a prescriptive operating model under varying:

- Environmental conditions
- Equipment configuration
- Energy storage capabilities

Limitations and assumptions accompany our mathematical model in Section 4.1

1.4.2 Thesis Contributions and Outline

Significant achievements and ongoing efforts by government and industry have produced tactical hybrid energy systems, improved load efficiency, and reduced overall demand. This thesis aims to complement these efforts by introducing optimized, intelligent demand side management (DSM) to the tactical energy grid using concepts and practices from the commercial utility sector and electric vehicle manufacturers.

In Chapter 2, we review the academic, commercial, and government literature that inform the present research. Chapter 3 provides an overview of expeditionary energy systems to establish the background for our mathematical optimization model proposed in Chapter 4. Our findings are presented in Chapter 5 and Chapter 6, and conclusions and future work are contained in Chapter 7.

CHAPTER 2:
Literature Review

This thesis lies at the intersection of three fields of research and application. The first are efforts, led by the U.S. military and supported by industry and academia, to improve the efficiency of fielded generators, ECUs, and structures through engineering and procedural solutions. The second is hybrid microgrid architectures incorporating renewable production, uncertain demand, and energy storage for use in remote military and civil applications. Finally, we examine academic literature on deferrable electric load management in commercial and residential scenarios.

2.1 Military Energy Efficiencies

Motivated by the expeditionary energy costs discussed in Section 1.2, the DOD has aggressively explored HVAC energy efficiency and conservation efforts.

Power production has improved with the introduction of more efficient generators and addition of hybrid power plants. The Advanced Medium Mobile Power Sources (AMMPS) series of 5-60 kW generators, fielded in FY2011, are smaller, lighter, and 21% more fuel efficient than the preceding TQG series [21], [22]. The USMC Experimental Forward Operating Base (EXFOB) technology demonstration event, conducted at least once per year since 2010, has led to the adoption of two hybrid systems as programs of record. The Ground Renewable Expeditionary Energy Network System (GREENS) combines solar panels and energy storage sufficient to power a battalion combat operations center (COC), while the Mobile Electric Hybrid Power Sources (MEHPS) merges batteries, solar panels, and generators to save up to 50% in fuel while reducing generator run time by as much as 80% [23].

Research efforts directed at consumption efficiencies have produced radiant barriers that double the insulative value of tent walls to reduce thermal load [23]. Application of closed-cell spray foam to tent exteriors, common in Iraq and Kuwait, is estimated to reduce ECU operation and subsequent fuel consumption by up to 50%, while research into high per-

formance, lightweight aerogel compounds show potential for 35% fuel savings over an uninsulated tent [24], [25]. Fielding of the Improved Environmental Control Unit (IECU) in sizes from 9,000 to 60,000 British thermal units (BTUs), begun in 2011, offers fuel savings of 6% to 28% depending upon size [26].

Insulation and other demand-side conservation methods reduce average power demand without lowering peak demand. While this yields desirable fuel savings, it also serves to increase the peak-to-average power ratios that our present research attempts to address. Prior efforts to integrate hybrid generation with intelligent load control include the Hybrid Intelligent Power (HI-Power) system, a $3.5 million research and development effort awarded in 2010 and demonstrated in 2012 [27], [28]. As of 2014, the development of systemic solutions to address the generator-load inefficiency remained a top recommendation from the Tactical Power Systems study conducted by the Lincoln Laboratory at the Massachusetts Institute of Technology (MIT) [18].

2.2 Hybrid Smart Microgrids

For clarity, we begin by articulating the features and characteristics that distinguish micro, hybrid, and smart grids.

Microgrids combine multiple potentially dissimilar generation sources with various loads through a network of controllers, distribution panels, and cabling [29]. Properly designed microgrids save fuel by aggregating numerous small loads for servicing with a fewer number of larger, more efficient power sources. In one example, the USA observed fuel savings of 17% by replacing thirteen 60 kW TQGs at Bagram Airfield, Afghanistan with a one megawatt (MW) microgrid in August 2011 [11].

Hybrid power systems combine two or more dissimilar energy sources into a single composite source intended to provide greater efficiency or increased resilience over single-source generation systems [18]. Components of an expeditionary hybrid system may include reciprocating diesel generators, photovoltaic (PV) solar arrays, wind turbines, and battery storage.

Smart grids utilize information about energy sources, loads, and storage devices to improve grid efficiency and reliability [30]. This basic information can be augmented with additional data on user behavior, environmental conditions, or forecasts to enhance renewable integration and make predictive management decisions.

Existing microgrid optimization literature focuses on minimizing costs via long-term infrastructure investment or short-term supply-side dispatch decisions. Bouaicha [31] examines minimum-cost fulfillment of specified demand by incorporating estimates of near-term renewable generation forecasts. Ulmer [32] extends this work by maximizing the endurance of an isolated grid at a fixed location by using renewable generation estimates to inform capital planning decisions. Ongoing work by Newman [33] focuses on development of a decision support tool to aid in pre-deployment equipment provisioning selections to minimize DOD total mission lifecycle costs. Sadiqi, Pahwa, and Miller [34] conduct similar analysis for rural community electric hybrid power systems in Afghanistan.

2.3 Demand-Side Management

Load-following electrical grids treat energy demands of connected loads as immutable parameters that must be completely satisfied if the grid is to remain stable. Generator output will vary, storage devices will charge and discharge, and additional production resources will be brought online or placed offline to match supply to demand.

Introducing basic smart grid features permits demand side management (DSM), a feedback and control mechanism to reshape the demand profile to match available supply. DSM implementations vary by provider, customer, and connected load. The least intrusive solutions merely notify consumers of an opportunity to reduce costs by limiting demand, while the most prescriptive programs allow the grid to explicitly permit or deny operation of a particular device [35]. Candidate loads for DSM control must be *time-shiftable*, or capable of being satisfied within a range of time periods, and *cyclical*, or naturally subject to alternating on / off periods.[7] Substantial research has been performed on the application of DSM to electric vehicle (EV) charging and to commercial and residential appliance control, and

[7] *Deferrable* is commonly used in the literature to describe loads that may be delayed to a more advantageous time. We adopt the convention that *time-shiftable* loads include not only deferrable loads, but also those demands that may be fulfilled earlier.

various DSM approaches have been successfully implemented to reduce costs and manage peak demand.

2.3.1 Electric Vehicle Charging

The electric vehicle charging problem seeks to minimize electricity cost while delivering a sufficiently charged vehicle on a schedule that meets the customer's demands. Alizadeh, Kesidis, and Scaglione [36] compare heuristic and near-optimal scheduling alternatives for known demands and unconstrained supply. Chen, Ji, and Tong [37] propose a heuristic to meet demand on a known schedule while subject to uncertain renewable sources. Mohsenian-Rad and Ghamkhari [38] express a closed-form solution to minimize cost under a constantly available supply but with uncertain vehicle departure times. Xu and Pan [39] address both uncertain arrival times and renewable production in a multiple EV charging lot that incentivizes incoming drivers who are less time-sensitive to return onboard vehicle energy to the grid to support the immediate charging—at a premium—of more time-sensitive customers. Sherif, Zhu, and Lambotharan [40] formulate an optimization model that integrates EVs into a residential smart grid with the objective of minimizing neighborhood peak-to-average power ratio by using vehicle onboard batteries as both loads and power sources.

2.3.2 Appliance Control

Prescriptive residential and commercial DSM constitutes a bargain between energy suppliers and customers in which customers surrender a degree of control over the timing of demand satisfaction in exchange for lower utility rates or other incentives. Suppliers exert this control to stabilize demand across multiple customers during peak periods. The ability to level demand reduces the risk of overloading portions of the grid, permits increased renewable penetration, and potentially reduces the amount of spinning reserve[8] that a utility must maintain [35].

Loads most suitable for shifting include HVAC, water heating, clothes and dish washing appliances, and EV charging. Vlot, Knigge, and HanSlootweg [42] find that 12% of Dutch

[8]Spinning reserve is unused production capacity available to compensate for dramatic load changes or generation outages. It is online, synchronized to the grid, and capable of reaching full power within 10 minutes [41].

national electricity usage is suitable for residential load shifting, and that investment in a nationwide smart grid would have the effect of adding 700 MW of generation and 5 gigawatt-hours (GWhs) of storage to the grid with a cost recovery period of less than seven years. In their stochastic optimization of energy bidding strategies in community microgrids, Nguyen and Le [43] show that flexible HVAC scheduling can significantly reduce costs while enabling increased renewable participation. Similarly, Tarasak, Chai, Kwok, and Oh [44] show that a notional hotel participating in a demand bidding program[9] can more than double peak monetary rewards by scheduling HVAC loads.

Barriers to adoption of DSM include capital investment costs for grid integration, lack of standardized communication and negotiation protocols between sources, loads, and storage, and undeveloped cost and reward sharing arrangements between energy suppliers and customers [35], [46], [47]. The DOD has begun limited work to establish communications protocols through the HI-Power and Alternative Energy Demonstration Project [27], [48]. Further protocol development and implementation was a top recommendation of the 2014 MIT Lincoln Laboratory study [18].

[9]Demand bidding programs are utility-managed programs that encourage large customers to commit to future demand reductions if called upon by the utility during peak periods. See [45] for details of one program.

THIS PAGE INTENTIONALLY LEFT BLANK

CHAPTER 3:
Expeditionary Energy Systems

This chapter provides an overview of expeditionary energy systems and components. We intend to equip readers with sufficient knowledge to comprehend the model we will propose in Chapter 4, understand the related constraints and assumptions, and interpret the findings presented in Chapter 5 and Chapter 6. Readers interested in further technical and operating information for the diverse array of DOD and service-specific equipment are directed to the referenced sources.

We limit our examination to tactical power only, excluding prime and commercial power production and distribution. Prime power is utility-grade power production and distribution to support major bases, airfields, and other large requirements. Prime power generators are those larger than 200 kW and with output voltages up to 4,160 volts (V) [49]. Installation, operation, and maintenance of these systems require highly trained personnel found in specialized units such as the 249th Prime Power Battalion. The size, capability, and complexity of these systems place them beyond the reach of forward tactical units and outside the scope of our research. Figure 3.1 shows the relationship between tactical, prime, and commercial power.

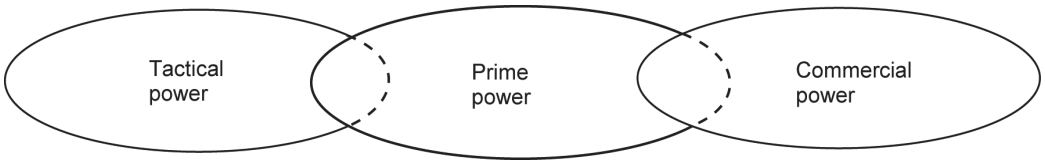

Figure 3.1: The expeditionary power continuum, from [49]. We limit our study to tactical power.

3.1 Energy System Architectures

At a minimum, an expeditionary energy system consists of power sources, electrical loads, and the distribution equipment required for interconnection. Specific site configurations vary based upon the nature of the power requirement, equipment and personnel available, and the type and duration of the mission being supported.

3.1.1 Spot Generation

The simplest configuration is spot generation, in which a single generator provides power to a set of connected loads. Figure 3.2 depicts a simplified spot generation line diagram.

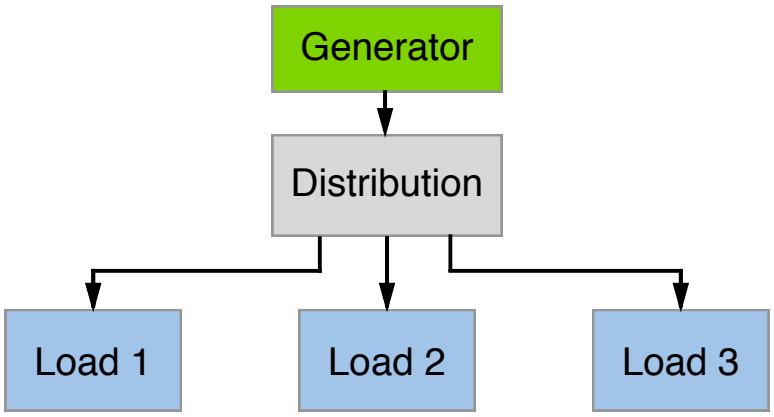

Figure 3.2: Notional spot generation configuration.

Spot generation is appropriate when:

- Total power requirement is within capacity of a single generator.
- Isolated power is required due to geographic or reliability considerations.
- Mission duration is short.

The single generator is sized to accommodate peak demand. Actual demand may fluctuate significantly, causing high peak-to-average ratios and low utilization. Many spot generation systems operate with an average load factor less than 30% [18].

3.1.2 Multiple Generator Systems

Some shortcomings of spot generation can be overcome by using a multiple generator configuration as illustrated in Figure 3.3. Generators are selected so that their combined output is sufficient to satisfy peak demand. One or more generators are designated as the primary generator(s) and the others as standby units; once power demand exceeds the capacity of the primary generators the standby generators will start, warm up, synchronize frequency and phase with the primaries, and begin supplying power to the loads.

Military specification generators are sufficiently robust to permit overloading of the primary generator for several minutes until the standby generator comes online [18], [20]. Control logic monitors the system load and can be configured to shut down the standby generator(s) when demand is once again within the capacity of the primary generator.

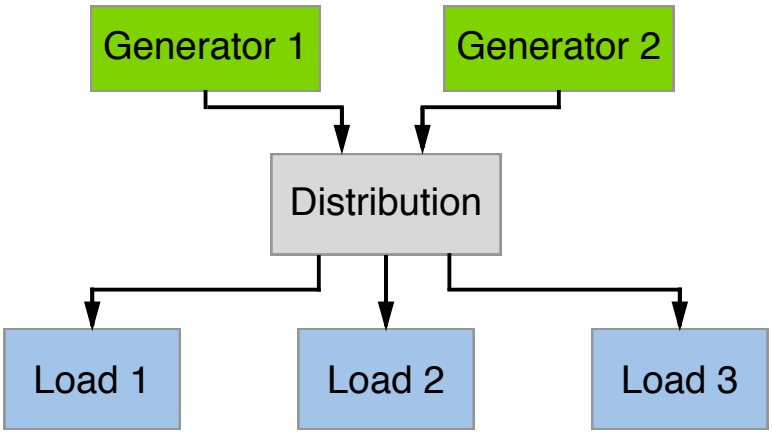

Figure 3.3: Notional two generator configuration.

Peak-to-average ratios are the same as a spot generation configuration, but because the standby generators only operate when load is high, properly configured multiple generator systems achieve higher average utilization. Multiple generator arrangements are also more reliable, allowing the system to operate at diminished capacity in the event of mechanical failure of a single generator.

3.1.3 Hybrid Systems

Hybrid systems aggregate multiple types of power sources into a single composite supply. Power sources in a hybrid grid may include two or more of the following:

- Reciprocating diesel generators
- PV solar arrays
- Wind turbines
- Energy storage

Figure 3.4 illustrates a simplified hybrid power system incorporating energy storage and renewable production. Though a single-generator system is represented, the architecture is extensible to include multiple generators, alternative sources, and storage capabilities.

Control logic manages generator operation, storage replenishment and depletion, and renewable contributions. In general, demands are preferentially met by current perishable production (e.g., solar or wind), then with available storage capacity, and finally by generator output. Production in excess of demand is used to replenish storage as required.

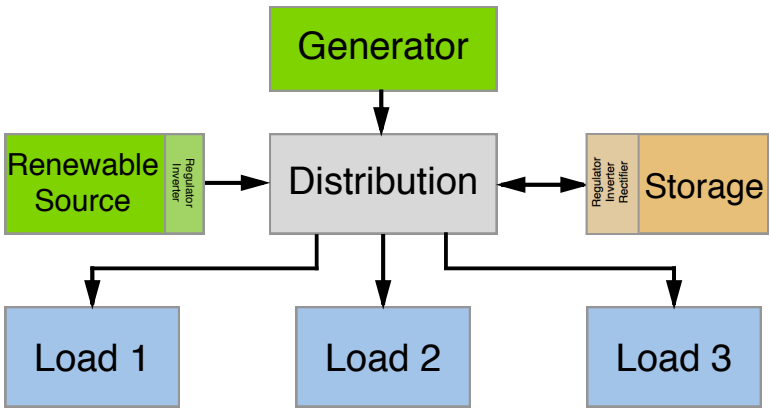

Figure 3.4: Notional single generator hybrid configuration.

Examples of currently available hybrid systems are the Earl Energy FlexGen and ZeroBase H-Series, combining diesel generation, battery storage, and PV renewable components to form modular systems with capacities from 3 kW to 240 kW [50], [51].

3.1.4 Mixed Configurations

In practice, electrical generation and distribution at forward locations is often accomplished by an ad-hoc arrangement of available equipment that has been assembled over the months or years that a site has been in operation [19], [48], [52], [53], [54], [55]. Grid topology may be the result of the most expedient courses of action rather than the most effective or efficient. High priority loads such as tactical operations centers (TOCs) or medical treatment areas are frequently assigned a dedicated generator in an attempt to increase reliability at those locations.

3.1.5 Smart Grid

A smart grid is one that gathers and acts on information to improve the efficiency and reliability of electricity production and distribution [56]. Application of smart grid principles to tactical power systems is the subject of ongoing efforts to articulate requirements, balance

costs, and assess reliability and vulnerability risks [57]. Specific benefits of a smart tactical power grid are expected to include:

- Lower fuel consumption
- Reduced maintenance and aural signature due to fewer generator operating hours
- Priority load shedding that drops non-critical loads when necessary to preserve continuity of power to critical loads
- Reduced equipment requirements as loads are aggregated on to fewer generators
- Simplified configuration and management
- Increase penetration and efficiency of renewable resources [18]

Figure 3.5 represents a hybrid grid enhanced through addition of bidirectional communication and control channels that permit each node to broadcast current status, send or receive commands, and signal upcoming events.

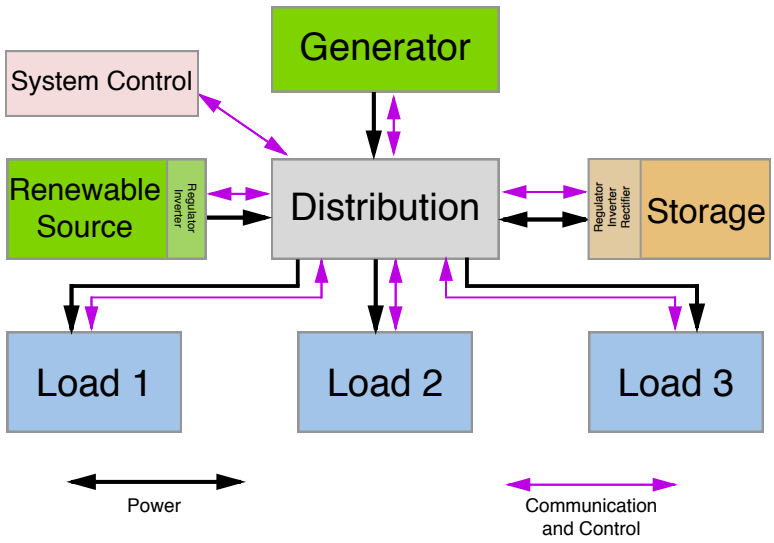

Figure 3.5: Notional smart grid configuration. The control node monitors conditions and adjusts loads and sources to maximize efficiency.

Existing or developmental systems that provide a limited subset of smart grid capabilities include the Improved Power Distribution System, Electrical (IPDISE) and the DRASH Intelligent Power Technology family of equipment [58], [59]. These solutions focus almost exclusively on supply-side management by offering generator control, supply consolida-

tion, and phase balancing.[10] With the exception of load shedding, they do not offer DSM capabilities.

Optimized time-shiftable load management as envisioned in this research requires a minimum foundation of smart grid capabilities that include ECU and generator control, and environmental monitoring of shelters serviced by the ECUs.

3.2 Energy Production

3.2.1 Diesel Generators

Reciprocating diesel generators provide a robust, reliable source of tactical power in sizes from 5 kW to 200 kW. The Advanced Medium Mobile Power Sources (AMMPS) series of medium tactical generators, detailed in Figure 3.6 and Table 3.1, supply tactical power requirements from 5 kW to 60 kW across the DOD.

Figure 3.6: Advanced Medium Mobile Power Sources generators, 5 kW, 10 kW, 15 kW, 30 kW, and 60 kW, from [60].

[10]Three-phase power incorporates three alternating current (AC) signals, each 120 degrees out of phase with the others. Loads may be designed to use all three phases, or they may be powered from only a single of these phases. Multiple single-phase loads must be apportioned among the three source phases to prevent imbalances. Failure to properly balance will lead to degraded performance or permanent equipment damage.

	5/60	5/400	10/60	10/400	15/60	15/400	30/60	30/400	60/60	60/400
SIZE: TQG (l x w x h")	50-32-36		62-32-36		69-36-54		80-36-54		87-36-58	
SIZE: AMMPS	45-32-36		55-32-36		65-36-53		75-36-53		82-36-53	
WEIGHT: TQG (lbs)	888	911	1182	1220	2124	2238	3006	3015	4063	4153
WEIGHT: AMMPS	784	787	1085	1100	1492	1513	2068	2174	2932	3112
FUEL: TQG @ prof. (60 Hz, DL-2, gal/hr)	.46		.74		1.22		1.83		3.28	
FUEL: AMMPS (60 Hz, DL-2, gal/hr)	.34		.55		.77		1.59		3.01	

Table 3.1: Advanced Medium Mobile Power Sources performance data, from [61].

More significant power requirements are currently met by the 100 kW and 200 kW TQGs, illustrated in Figure 3.7, pending fielding of the Large Advanced Mobile Power Sources (LAMPS) under a design and build contract awarded in 2012 [58].

Figure 3.7: Tactical Quiet Generators, 100 kW (left) and 200 kW (right), from [58].

3.2.2 Photovoltaic Solar

PV solar panels convert solar energy into regulated direct current (DC) power that can be used for charging batteries and operating other DC devices. Power for AC loads can be supplied by routing panel output through an inverter that converts DC to AC. Figure 3.8 displays one example of a fielded tactical PV system.

Figure 3.8: Solar array component of the USMC Ground Renewable Expeditionary Energy Network System (GREENS), from [62].

Advantages of solar include:

- Panels are lightweight and easily deployable
- Solar energy is a readily available, renewable power source
- Panels and associated controllers are solid state, with no moving parts to wear out

Factors that may limit the utility or effectiveness of PV solar include:

- Solar panel output has substantial daily and seasonal variation; see Figure 3.9. An effective system requires complementary energy storage to manage these variations
- Site conditions—overhead growth or concealment, surrounding terrain, and placement or orientation restrictions—may limit effectiveness of the panels
- Panels require frequent cleaning to maintain maximum power output, particularly in dusty environments

3.2.3 Other Sources

Wind turbines and waste-to-energy (WTE) plants have been prototyped, field tested, and commercially developed as proposed supplements to meeting tactical power demands [54], [64]. To date, none have been adopted as systems of record within DOD or fielded in significant quantities.

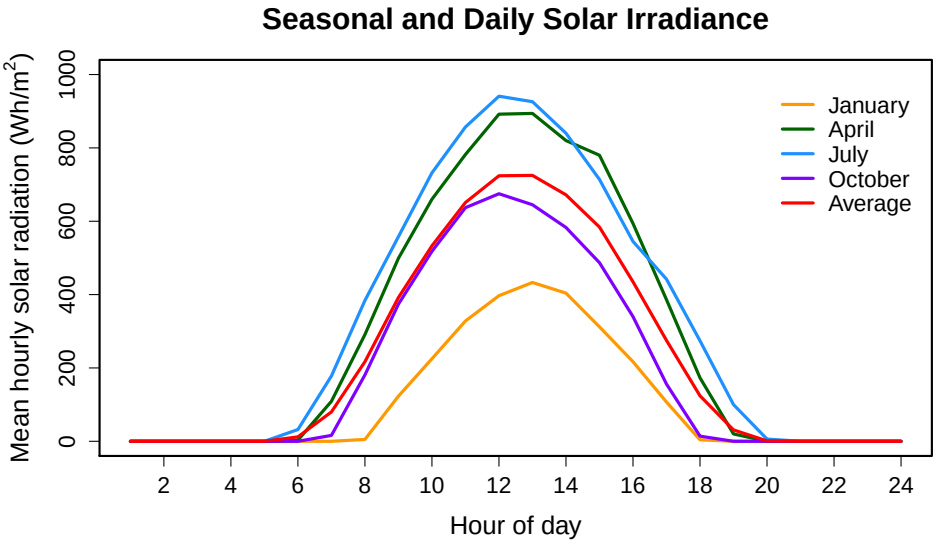

Figure 3.9: Variation in solar irradiance at 37 degrees north latitude. Chart by author using 2010 Four Corners, NM data from [63].

3.3 Energy Storage

Intermittent sources such as wind and solar require an energy storage device to bridge periods of low production. Diesel generator systems, with or without the inclusion of renewable production, also exhibit increased efficiency when energy storage capabilities are present and intelligently managed. Storage mechanism in the power industry include the following items:

- Chemical batteries
- Capacitors
- Pumped hydroelectric
- Thermal mass
- Compressed air
- Flywheels
- Hydrogen conversion [65]

Complexity, size, weight, initial investment, or specialized site requirements render all but batteries unsuitable for the tactical environment [29]. Lithium-ion is presently the most common chemistry due to its high power capability, high power to weight and volume ratios, and reasonable lifecycle [29].

Batteries are DC devices; interfacing with AC generators requires an appropriate conversion. On charging, a rectifier converts the AC output of the generator into a DC source that can charge the battery. On discharge, an inverter converts DC energy from the battery into AC power to supplant or assist the generator in powering AC loads. This rectification/inversion process, combined with losses in charging circuitry and battery chemistry, result in round-trip energy efficiencies well below 100%. In practice, only about 80% of the energy devoted to charging a battery will be recovered when subsequently discharging [18].

3.4 Electrical Loads

We broadly characterize expeditionary power loads as *stable* or *transient* based upon the fluctuations that they create in the grid. Stable loads are relatively small or exhibit little short-term variation. Examples are lighting, communication systems, computer networks, and aggregated minor plug loads. Transient loads are cyclical and large in proportion to overall demand. They may operate either semi-autonomously, such as HVAC, refrigeration, and water heating, or under the control of a user, such as kitchen, laundry, or water purification equipment.

3.4.1 Environmental Control Units

ECUs are electrically powered, thermostatically controlled devices employed to heat, cool, dehumidify, filter, and circulate air in expeditionary shelters [66]. In cooling mode, they utilize a forced air refrigeration system, while in heating mode they distribute forced air warmed by resistive heating elements. Some ECUs are designed for placement within a shelter with their exhaust ducted through the shelter walls to the external environment. Others are intended for external placement, with conditioned air provided to a shelter via flexible ducting. Figure 3.10 contains examples of two ECU models.

Figure 3.10: 36,000 BTU/hr environmental control unit (left). ECUs externally installed in support of insulated fabric tents (right), from [67] and [68].

ECUs are rated by their capacity, measured in BTU/hr, to add (heating mode) or remove (cooling mode) thermal energy from a shelter. Other relevant characteristics are the volume of air moved per unit time, measured in cubic feet per minute (CFM), and the electrical power required for operation, measured in kW. Technical data for several ECUs models appears in [66], [67], and [69].

Higher thermal capacity units require greater amounts of electrical power. Some ECU models offer low and high heat settings, and all provide fan-only setting. During cooling mode, however, it is significant to note that an ECU is not capable of variable output. It either operates at full capacity—and full power—or it provides no cooling at all.[11]

3.4.2 Expeditionary Shelters

Expeditionary shelters accommodate operations centers, billeting, medical suites, dining and recreation facilities, aircraft and vehicle maintenance, communication centers, and other functions. Desirable characteristics of a shelter include speed and ease of erection, durability in adverse environments, and low weight and volume for portability. Many shelters in the DOD inventory are soft-wall, consisting of fabric walls, floor, and roof supported

[11] Temperature control on many ECUs is managed by using a refrigerant bypass valve to unload, rather than stop, the compressor once the low temperature setpoint is reached. The compressor and fan continue to run during this "off" cycle but consume far less power.

by a metal or airbeam frame [66], [69], [70], [71], . These shelters are shipped unassembled and erected on site. Figure 3.11 and Figure 3.12 contain examples of small and large expeditionary shelters.

Figure 3.11: Small expeditionary shelters. Alaska Small Shelter System (AKSSS) (left) and Tent Extendable Modular Personnel (TEMPER) (right) shelters, from [66].

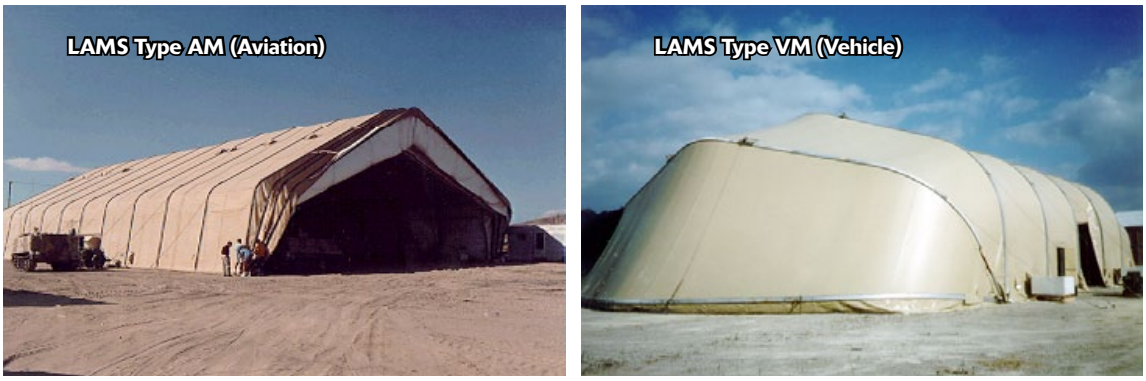

Figure 3.12: Large expeditionary shelters. The Large Area Maintenance Shelter (LAMS), for aviation (left) and vehicles (right), from [69].

Standard fabric shelters are poorly insulated, necessitating substantial HVAC capacity to maintain desired internal temperature in extreme climates. Modifications to improve insulative value and reduce HVAC demands include solar shades, insulating liners, and spray-on foam insulation [48], [72].

Other factors influencing heating and cooling requirements for each shelter include the contents, location, and physical characteristics of the shelter. These will be further discussed in Section 4.2.

3.5 Distribution

Distribution equipment includes power distribution panels and cabling required for assembly of a grid that can safely and reliably deliver power from the point of production to the point of consumption.

The tactical power distribution system of record within the USMC is titled the Mobile Electric Power Distribution-Replacement (MEPDIS-R), while the USA and United States Air Force (USAF) family of equipment is named the Power Distribution Illumination System, Electrical (PDISE) [73], [74]. Both systems incorporate protective devices and provide the ability to connect multiple generators. Figure 3.13 illustrates the sources and loads of a small camp connected using distribution equipment.

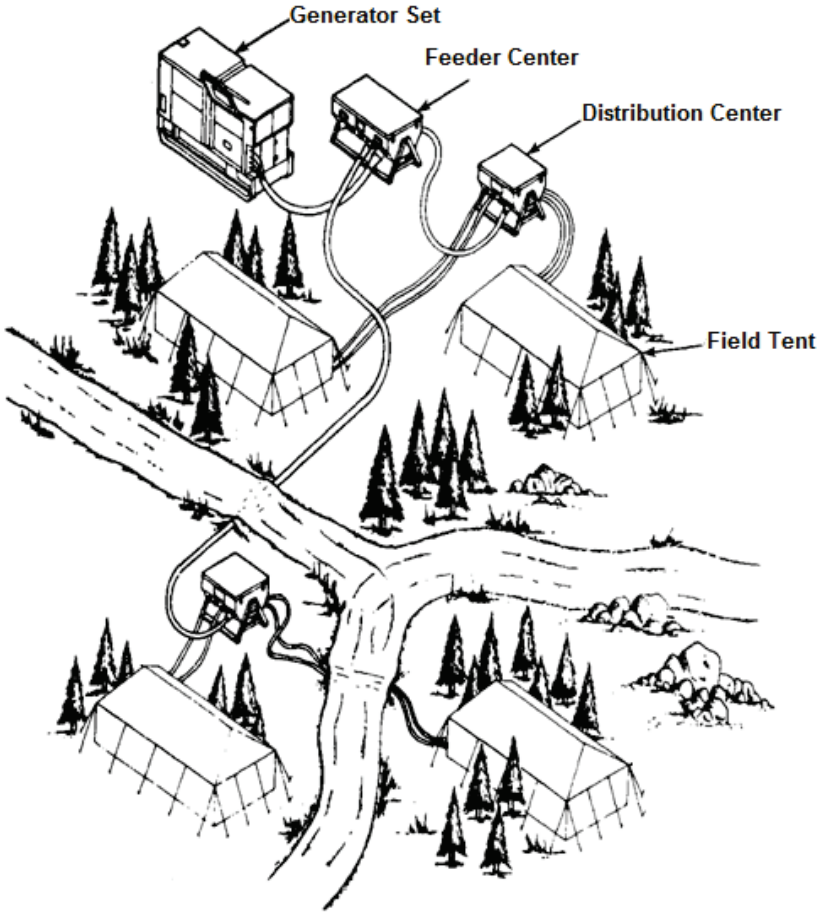

Figure 3.13: Tactical power distribution network, from [74].

3.6 Summary

Having established the foundational understanding of expeditionary energy systems, we continue with a discussion of our model limitations, assumptions, and mathematical formulation in Chapter 4.

CHAPTER 4:
Model

Our model minimizes fuel consumption by defining an optimal schedule for generator operation, ECU utilization, and energy storage management. The principle constraint we must observe is maintaining internal structure temperature within acceptable upper and lower bounds. We first develop a thermal sub-model to simulate temperature changes within a structure and then proceed to formulate the optimization model.

4.1 Model Simplifications and Assumptions

We adopt various simplifications and assumptions to maintain computational tractability, overcome shortfalls in available data, and maintain focus on our primary research questions.

Loads are balanced. Total load in each period is split among all operating generators proportional to their nameplate rated capacity. Single phase loads are connected and operated such that all phases are adequately balanced. We presume that an architecture capable of achieving the optimal control we describe is also capable of balancing loads and phases, therefore we conclude that this simplification does not diminish the validity of our conclusions.

Energy storage. Charge and discharge rate limits are constant over the entire range of battery level, and battery level varies linearly with chosen charge and discharge rates. The complex, rapidly changing field of optimized battery management is beyond the scope of the present work.

Power distribution. We do not model limitations and constraints of specific distribution systems. All power production in each period is aggregated and available to any load.

Thermal behavior. Shelter and ECU performance under varying environmental conditions was estimated using software tools and was not able to be independently validated using field or test data.

Generator fuel consumption curve. Generator fuel consumption is modeled as piecewise linear using six points from 0 to 110% of rated power. This reflects a limitation in

source data gathered under testing protocols that required evaluation only at these discrete power levels [75].

4.2 Thermal Model

The temperature within each structure is a function of external environmental conditions, structural characteristics, and ECU output. Principal components of these factors are:

Environmental

- Solar radiation intensity and angle
- Wind
- Relative humidity
- Air temperature
- Ground temperature
- Ground surface type

Structural

- Surface area
- Volume
- Shape
- Insulation
- Number of personnel inside
- Personnel activity level
- Type and quantity of equipment in use
- Ventilation and infiltration

ECU Output

- Operational status (on / off)
- Cooling capacity [76]

4.2.1 Model Development

Though our model is indifferent between electrically-powered heating and cooling, for clarity we discuss only the case of cooling shelters in a hot environment. We adopt a convention that heat added to a structure by the environment, personnel, or equipment is positive with rate $\dot{Q}^+$, while an operational ECU removes heat at rate $\dot{Q}^-$. Internal temperature, τ_{int}, rises when $\dot{Q}^+ > \dot{Q}^-$, lowers when $\dot{Q}^+ < \dot{Q}^-$, and remains constant when $\dot{Q}^+ = \dot{Q}^-$. Thus,

$$\frac{d\tau_{int}}{dt} \propto \dot{Q}^+ - \dot{Q}^- \tag{4.1}$$

Included within $\dot{Q}^+$ are terms for heat transfer via conduction through the floor and walls of the structure. Conduction is described by

$$\dot{Q}_{cond} = \frac{\kappa A(\tau_{ext} - \tau_{int})}{l} \tag{4.2}$$

where κ is thermal conductivity, A is area, τ_{ext} is the exterior temperature, and l is thickness [65]. We assume a constant τ_{ext} for small time intervals and modify (4.1) to reflect that Q^+ is a function of internal temperature:

$$\frac{d\tau_{int}}{dt} \propto \dot{Q}^+(\tau_{int}) - \dot{Q}^- \tag{4.3}$$

We use the HVAC Requirements Calculator of the Automatic Distribution Illumination System, Electrical (AutoDISE) software [77], shown in Figure 4.1, to estimate $\dot{Q}^+(\tau_{int})$. Parameters for construction materials, site conditions, and external environmental factors are provided to the software, which returns the steady-state cooling or heating capacity necessary to maintain the desired internal temperature and humidity [76]. Figure 4.1 illustrates this interface.

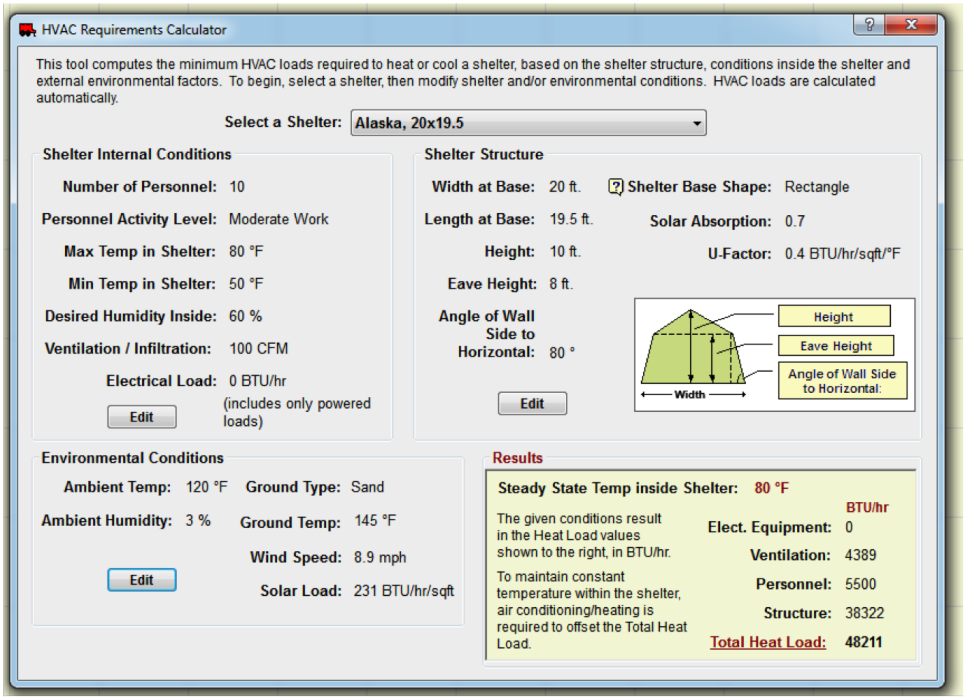

Figure 4.1: AutoDISE HVAC requirements calculator, from [77].

AutoDISE steady-state conditions correspond to $d\tau_{int}/dt = 0$, or $\dot{Q}^{+}(\tau_{int}) = \dot{Q}^{-}$, where $\dot{Q}^{-}$ is the result provided by AutoDISE. By varying τ_{int} over our range of interest while holding all other inputs constant we observe the behavior of $\dot{Q}^{+}(\tau_{int})$ and are able to develop linear approximations.

The final component in our framework is specifying the relationship of Equation (4.3). The portion of heat flow that manifests as a change in air temperature depends upon the mass and heat capacity of the air in the shelter relative to the mass and heat capacity of other shelter contents [78]. We represent this with ϕ and select a value of 0.10 as our approximation.

Air density (ρ) and heat capacity (cp) vary less than 4% within the temperature range considered by this model. We treat these as constants with the specified values.

4.2.2 Thermal Model Formulation

4.2.3 Sets and Indices

$s \in S$	Set of all structures and associated ECUs
$t \in T$	Set of time intervals

Parameters

cp	Heat capacity of air [0.9526 $BTU/kg \cdot^\circ C$]
ρ	Density of air [1.1894 kg/m^3]
w	Time interval width [minutes]
ϕ	Proportion of heat flow that manifests as a change in air temperature

Shelter and Environmental Characteristics

v_s	Internal volume of structure s [m^3]
β_s	Equilibrium heat transfer rate intercept for structure s [BTU/hr]
m_s	Equilibrium heat transfer rate slope for structure s [$BTU/hr \cdot^\circ C$]
$\dot{Q}_s^-$	Heat removal capacity of ECU for structure s [BTU/hr]

Variables

$\tau_{s,t}$	Shelter s internal temperature at end of interval t [$^\circ C$]
$\dot{Q}_{s,t}^+(\tau_{s,t-1})$	Rate that heat is added to structure s in period t [BTU/hr]

Heat Transfer Equations

$$\dot{Q}^{+}_{s,t}(\tau_{s,t-1}) = m_s \cdot \tau_{s,t-1} + \beta_s \tag{4.4}$$

$$\tau_{s,t} = \tau_{s,t-1} + \frac{w}{60} \cdot \frac{\phi}{\rho \cdot v_s \cdot cp} \left(\dot{Q}^{+}_{s,t}(\tau_{s,t-1}) - \dot{Q}^{-}_{s} \right) \tag{4.5}$$

4.3 Optimization Formulation

We employ a discrete-time mixed integer linear program to minimize generator fuel consumption by prescribing periods of ECU operation subject to specified internal temperature requirements and equipment operating limitations.

4.3.1 Sets and Indices

$s \in S$	Set of all structures and associated ECUs
$g \in G$	Set of generators
$t \in T$	Set of time intervals
$c \in C$	Set of fuel curve linearization points
$b \in B$	Set of storage batteries

Parameters

cp	Heat capacity of air [0.9526 $BTU/kg \cdot C$]
ρ	Density of air [1.1894 kg/m^3]
w	Time interval width [minutes]
ϕ	Proportion of heat flow that manifests as a change in air temperature
v_s	Internal volume of structure s [m^3]
$\beta_{s,t}$	Equilibrium heat transfer rate intercept for structure s in interval t [BTU/hr]
$m_{s,t}$	Equilibrium heat transfer rate slope for structure s in interval t [$BTU/hr \cdot ^\circ C$]
$\dot{Q}^{-}_{s}$	Heat removal capacity of ECU for structure s [BTU/hr]
r_s	Power required by ECU s in operation [kW]
k_g	Maximum rated power of generator g [kW]

$hi_{s,t}$ High temperature limit for structure s in interval t [$^{\circ}C$]

$lo_{s,t}$ Low temperature limit for structure s in interval t [$^{\circ}C$]

$erun_s$ Minimum run time for ECU s [minutes]

$grun_g$ Minimum run time for generator g [minutes]

$erest_s$ Minimum rest time for ECU s [minutes]

$grest_g$ Minimum rest time for generator g [minutes]

w Time interval width [minutes]

u_t Unmanaged load requirements in time interval t [kW]

a_t Unmanaged power production in time interval t [kW]

$fint_g$ Y-intercept of fuel curve for generator g [galllons/hr]

$fx_{g,c}$ Fuel curve x-axis linearization points [% of full power]

$fy_{g,c}$ Fuel curve y-axis linearization points [gallons/hr]

cap_b Capacity of battery b [kWh]

$charg_b$ Maximum charge rate of battery b [kW]

$disch_b$ Maximum discharge rate of battery b [kW]

η_b Efficiency of battery b [%]

4.3.2 Continuous Variables

$\tau_{s,t}$ Shelter s internal temperature at end of interval t [$^{\circ}C$]

$f_{g,t}$ Total fuel consumed by generator g during interval t [gallons]

$vf_{g,t}$ Power-dependent fuel consumption rate by generator g during interval t [gallons/hr]

$blvl_{b,t}$ Level of battery b at end of interval t [kWh]

P_t^* Power level of running generators in interval t [% of full power]

$P_{g,t}$ Power level of generator g in interval t [% of full power]

$$= \begin{cases} P_t^* & \text{if generator } g \text{ is running in interval } t \\ 0 & \text{otherwise} \end{cases}$$

$in_{b,t}$ Power directed to battery b in interval t [kW]

$out_{b,t}$ Power supplied by battery b in interval t [kW]

4.3.3 Binary Variables

$$Genon_{g,t} = \begin{cases} 1 & \text{if generator } g \text{ is running during interval } t \\ 0 & \text{otherwise} \end{cases}$$

$$Genstart_{g,t} = \begin{cases} 1 & \text{if generator } g \text{ is started at beginning of interval } t \\ 0 & \text{otherwise} \end{cases}$$

$$Genstop_{g,t} = \begin{cases} 1 & \text{if generator } g \text{ is stopped at beginning of interval } t \\ 0 & \text{otherwise} \end{cases}$$

$$Y_{s,t} = \begin{cases} 1 & \text{if ECU for shelter } s \text{ is operated in time interval } t \\ 0 & \text{otherwise} \end{cases}$$

$$Thermstart_{s,t} = \begin{cases} 1 & \text{if ECU for shelter } s \text{ is started at beginning of interval } t \\ 0 & \text{otherwise} \end{cases}$$

$$Thermstop_{s,t} = \begin{cases} 1 & \text{if ECU for shelter } s \text{ is stopped at beginning of interval } t \\ 0 & \text{otherwise} \end{cases}$$

4.3.4 Specially Ordered Set Type 2 (SOS2) Variables

$\lambda_{g,t,c}$ c^{th} fuel curve linearization inflection point for generator g in interval t

Linear interpolation of fuel consumption is performed by employing specially ordered set, type 2 (SOS2) variables in the General Algebraic Modeling System (GAMS) optimization software. SOS2 variable sets can be of any length, however the values assigned to members of the set must obey two rules: (1) at most two members of the set may have non-zero values, and (2) any non-zero values must be adjacent members of the set.

As an example, if the parameter for generator g's power level linearization points is $fx_{g,c} = [0,20,40,60,80,100]$ and the linearization SOS2 variable is $\lambda_{g,c} = [0,0,0.4,0.6,0,0]$, then the interpolated value is $40 \times 0.4 + 60 \times 0.6 = 52$. An additional constraint ensures that the members of the SOS2 variable set sum to one.

4.3.5 Objective

$$minimize \sum_{t \in T} \sum_{g \in G} f_{g,t} \tag{4.6}$$

Our formulation minimizes total fuel consumption subject to the following:

4.3.6 Constraints

$$\sum_{s \in S} Y_{s,t} r_s + u_t + \sum_{b \in B} in_{b,t} \leq \sum_{g \in G} P_{g,t} k_g + \sum_{b \in B} \eta_b out_{b,t} + a_t \qquad \forall t \in T \tag{4.7}$$

$$P_{g,t} \leq Genon_{g,t} \qquad \forall g \in G, t \in T \tag{4.8}$$

$$P_{g,t} \geq P_t^* - (1 - Genon_{g,t}) \qquad \forall g \in G, t \in T \tag{4.9}$$

$$P_{g,t} \leq P_t^* \qquad \forall g \in G, t \in T \tag{4.10}$$

$$P_{g,t} = \sum_{c \in C} \lambda_{g,t,c} fx_{g,c} \qquad \forall g \in G, t \in T \tag{4.11}$$

$$vf_{g,t} = \frac{w}{60} \sum_{c \in C} \lambda_{g,t,c} fy_{g,c} \qquad \forall g \in G, t \in T \tag{4.12}$$

$$\sum_{c \in C} \lambda_{g,t,c} = 1 \qquad \forall g \in G, t \in T \tag{4.13}$$

$$\lambda_{g,t,c} \geq 0 \qquad \forall c \in C, g \in G, t \in T \tag{4.14}$$

$$f_{g,t} = \frac{w}{60} (fint_g Genon_{g,t} + vf_{g,t}) \qquad \forall g \in G, t \in T \tag{4.15}$$

$$\tau_{s,t} \leq hi_{s,t} \qquad \forall s \in S, t \in T \qquad (4.16)$$

$$\tau_{s,t} \geq lo_{s,t} \qquad \forall s \in S, t \in T \qquad (4.17)$$

$$\tau_{s,t} = \tau_{s,t-1} + \frac{w}{60} \cdot \frac{\phi}{\rho \cdot v_s \cdot cp} \left(m_s \cdot \tau_{s,t-1} + \beta_s - \dot{Q}_s^- \right) \qquad \forall s \in S, t \in T \qquad (4.18)$$

$$Y_{s,t} = Y_{s,t-1} + Thermstart_{s,t} - Thermstop_{s,t} \qquad \forall s \in S, t \in T \qquad (4.19)$$

$$Y_{s,t'} \geq Thermstart_{s,t} \qquad \forall s \in S, t \leq t' < t + erun_s/w \qquad (4.20)$$

$$Y_{s,t'} \leq (1 - Thermstop_{g,t}) \qquad \forall s \in G, t \leq t' < t + erest_s/w \qquad (4.21)$$

$$Thermstart_{s,t} + Y_{s,t-1} \leq 1 \qquad \forall s \in S, t \in T \qquad (4.22)$$

$$Thermstop_{s,t} - Y_{s,t-1} \leq 0 \qquad \forall s \in S, t \in T \qquad (4.23)$$

$$Thermstart_{s,t} + Thermstop_{s,t} \leq 1 \qquad \forall s \in S, t \in T \qquad (4.24)$$

$$Genon_{g,t} = Genon_{g,t-1} + Genstart_{g,t} - Genstop_{g,t} \qquad \forall g \in G, t \in T \qquad (4.25)$$

$$Genon_{g,t'} \geq Genstart_{g,t} \qquad \forall g \in G, t \leq t' < t + grun_g/w \qquad (4.26)$$

$$Genon_{g,t'} \leq (1 - Genstop_{g,t}) \qquad \forall g \in G, t \leq t' < t + grest_g/w \qquad (4.27)$$

$$Genstart_{g,t} + Genon_{g,t-1} \leq 1 \qquad \forall g \in G, t \in T \qquad (4.28)$$

$$Genstop_{g,t} - Genon_{g,t-1} \leq 0 \qquad \forall g \in G, t \in T \qquad (4.29)$$

$$Genstart_{g,t} + Genstop_{g,t} \leq 1 \qquad \forall g \in G, t \in T \qquad (4.30)$$

$$in_{b,t} \leq charg_b \qquad \forall b \in B, t \in T \qquad (4.31)$$

$$out_{b,t} \leq disch_b \qquad \forall b \in B, t \in T \qquad (4.32)$$

$$blvl_{b,t} = blvl_{b,t-1} + \frac{w}{60}(in_{b,t} - out_{b,t}) \qquad \forall b \in B, t \in T \qquad (4.33)$$

$$0 \leq blvl_{b,t} \leq cap_b \qquad \forall b \in B, t \in T \qquad (4.34)$$

$$P_t^* \geq 0 \qquad \forall t \in T \qquad (4.35)$$

$$P_{g,t} \geq 0 \qquad \forall g \in G, t \in T \qquad (4.36)$$

$$vf_{g,t} \geq 0 \qquad \forall g \in G, t \in T \qquad (4.37)$$

$$Genstart_{g,t} \in \{0,1\} \qquad \forall g \in G, t \in T \qquad (4.38)$$

$$Genstop_{g,t} \in \{0,1\} \qquad \forall g \in G, t \in T \qquad (4.39)$$

$$Genon_{g,t} \in \{0,1\} \qquad \forall g \in G, t \in T \qquad (4.40)$$

$$Thermstart_{s,t} \in \{0,1\} \qquad \forall s \in S, t \in T \qquad (4.41)$$

$$Thermstop_{s,t} \in \{0,1\} \qquad \forall s \in S, t \in T \qquad (4.42)$$

$$Y_{s,t} \in \{0,1\} \qquad \forall g \in G, t \in T \qquad (4.43)$$

Equation (4.6) seeks to minimize fuel consumption. Equation (4.7) ensures that power supplied by all sources in each period is sufficient for all running loads.

Equations (4.8) through (4.10) require all parallelled generators to operate at the same percentage of full load.

Equations (4.11) through (4.14) calculate variable fuel consumption by each generator as a piecewise linear function of operating state and power level. Equation (4.15) determines total fuel consumed in each time period.

Equations (4.16) and (4.17) maintain temperature of each structure within the specified range.

Equations (4.18) through (4.24) establish ECU and shelter thermal continuity in successive periods and enforce minimum run and rest times for each ECU.

Equations (4.25) through (4.30) establish generator continuity in successive periods and enforce minimum run and rest times for each generator.

Equations (4.31) through (4.34) maintain battery charge level continuity and enforce battery charge and discharge limitations.

Equations (4.35) through (4.43) enforce binary and non-negativity constraints.

4.4 Summary

The thermal and optimization models presented in this chapter establish a mechanism for evaluating the potential benefits of optimal time-shiftable load scheduling. In the next chapter we apply these models to a representative grid configuration and analyze the results.

CHAPTER 5:
Application and Baseline Analysis

We apply the model developed in Chapter 4 by creating six variants that explore optimality and computational performance tradeoffs. Using field data from Afghanistan, we approximate a tactical power grid and apply our six model variants to establish analytical baseline levels of fuel consumption, thermal conditions, storage performance, and generator operation.

5.1 Model Variants

The thermal and optimization models are combined with a discrete-time simulation to develop an ensemble framework that accepts equipment characteristics, environmental factors, projected unmanaged demand, and anticipated renewable production as inputs and returns operating schedules for ECUs, generators, and storage as outputs. Figure 5.1 depicts this relationship.

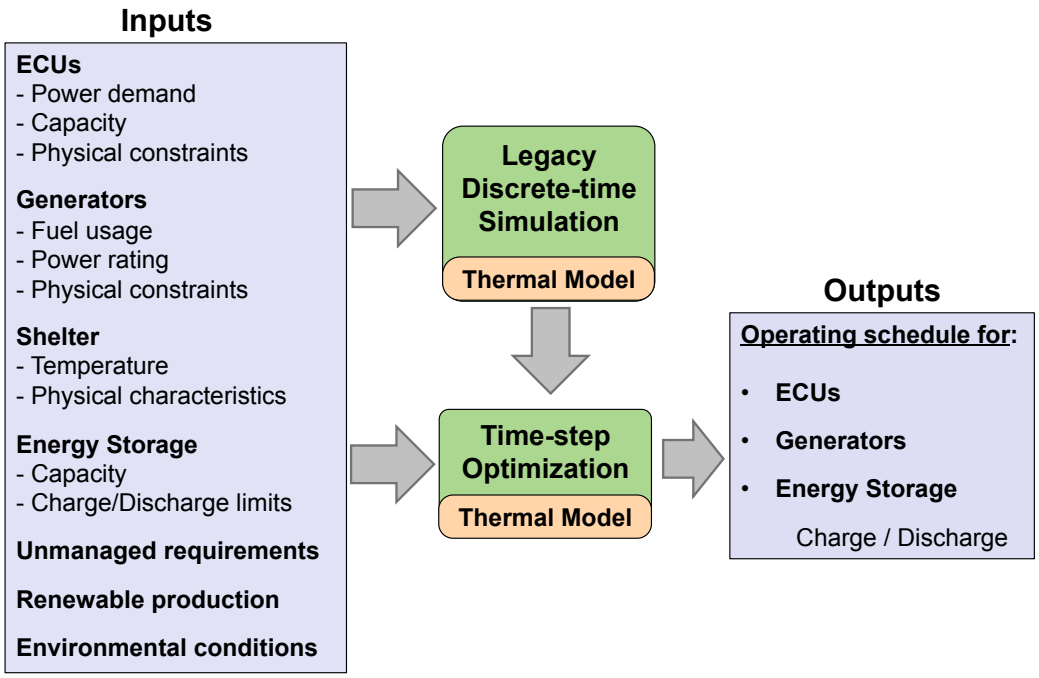

Figure 5.1: Ensemble simulation and optimization model framework.

5.1.1 Model Variants

We develop six variants of the model to evaluate the potential impact of optimal load management. The first implementation performs only discrete-time simulation of a legacy unmanaged grid to establish a minimum fuel efficiency benchmark. Another model, granted complete visibility on upcoming conditions and permitted to optimize all decisions, establishes a theoretical upper bound on fuel efficiency under ideal circumstances. Four intermediate variants aid in isolating the contribution of load management and evaluating potential system performance under imperfect knowledge. The six variants are:

Legacy unmanaged (LGCY). We stipulate that all generators run continuously to ensure sufficient power is available to supply all connected loads and perform time-step simulation using the thermal model of Section 4.2 to establish thermostatically-determined ECU start and stop times. The model sums total ECU and unmanaged loads in each period to determine total demand, and supplies this demand first with perishable renewable production and then with generator output to fulfill any remaining balance. Equations (4.11) through (4.15) determine generator fuel consumption based on load in each period.

Perfect future knowledge, storage only management (PFK-SOM). A hybrid policy in which ECUs are unmanaged and thermostatically controlled as in the legacy unmanaged arrangement and generators run continuously. We optimize storage charge and discharge using full visibility over the entire planning period.

Perfect future knowledge, generator and storage management (PFK-GSM). ECUs remain unmanaged and thermostatically controlled as in PFK-SOM. We optimize generators operation *and* energy storage using full horizon visibility.

Perfect future knowledge, full management (PFK-FM). We provide the optimization model of Section 4.3 visibility on all parameters in every period throughout the planning horizon, allowing it to return globally optimal decisions for ECU operation, generator control, and storage management. To maintain computational tractability we use the linear relaxation of this integer model unless otherwise specified.

Rolling horizon, perfect future knowledge (RH-PFK). We divide the entire planning horizon into multiple increments and iterate through them sequentially. At the beginning of iteration n the model receives perfect knowledge of conditions upcoming in increments n and $n+1$ and develops an optimal schedule for these two increments. Increment n decision variables for generators ($Genon_{g,t}, Genstart_{g,t}, Genstop_{g,t}$) and ECUs ($Y_{s,t}$) are fixed to the value determined by the schedule, and the model finishes by executing increment n to determine optimal levels for the variables that were not fixed. This cycle of two-increment visibility/optimization and one-increment execution continues until the end of the planning horizon. Figure 5.2 illustrates this approach.

Rolling horizon with uncertainty (RH-U). Similar to RH-LPK, however at the beginning of increment n we supply the model with *forecasted* demand and environmental parameters for increments n and $n+1$ and receive an optimal ECU, generator, and storage management schedule for these increments based on our forecasts. In the execution phase we replace the increment n forecasted planning parameters with "actual" values drawn from specified random distributions and optimize for this single increment.

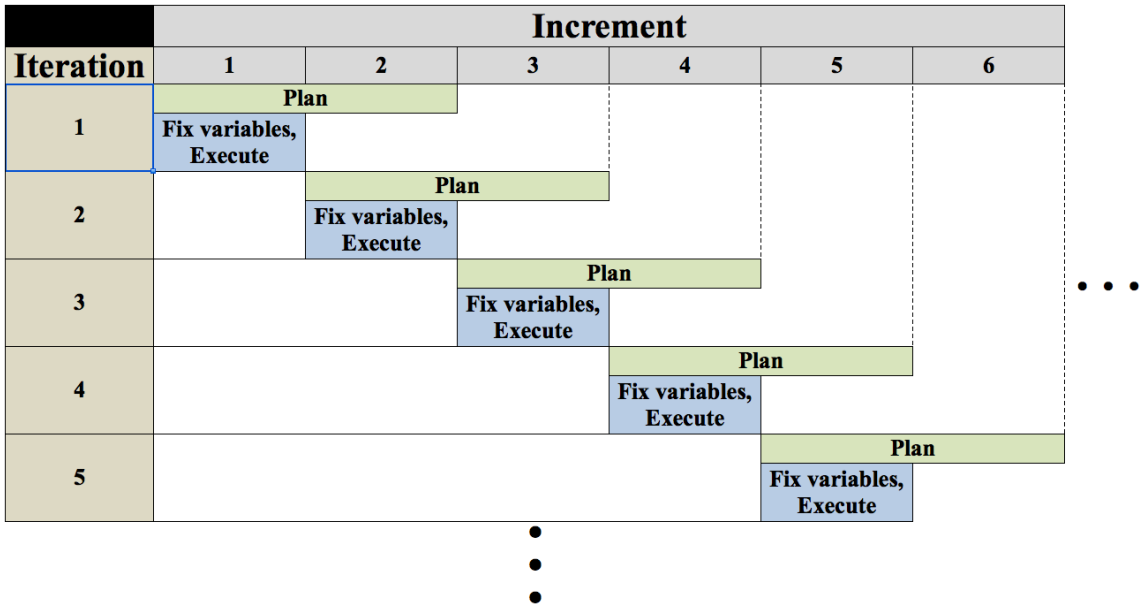

Figure 5.2: Rolling horizon optimization.

The first four variants demonstrate the effect of increasing optimization opportunities over the full horizon. The final two variants evaluate rolling horizon performance under both perfect and imperfect knowledge conditions. Table 5.1 provides a summary of all six model variants.

Variant		ECUs	Storage	Generators
Legacy	LGCY	Fixed to simulation results		Fixed ON
Storage optimized with perfect future knowledge	PFK-SOM	Fixed to simulation results	Optimized	Fixed ON
Generator and storage optimized with perfect future knowledge	PFK-GSM	Fixed to simulation results	Optimized	Optimized
Perfect future knowledge, full management	PFK-FM	Optimized	Optimized	Optimized
Rolling horizon with perfect future knowledge	RH-PFK	Optimized	Optimized	Optimized
Rolling horizon with uncertainty	RH-U	Optimized	Optimized	Optimized

Table 5.1: Summary of model variations.

5.1.2 Uncertainty Implementation

The two-step rolling horizon variants require *forecasted* demand and environmental conditions for the planning phase, and specification of *actual* demand and environmental conditions for the execution phase. We define these parameters as follows:

$a_t^{forecast}$ Forecasted renewable production in period t

a_t^{actual} Actual renewable production in period t

$u_t^{forecast}$	Forecasted unmanaged demand production in period t
u_t^{actual}	Actual unmanaged demand in period t
$\beta_{s,t}^{forecast}$	Forecasted thermal intercept for shelter s in period t
$\beta_{s,t}^{actual}$	Actual thermal intercept for shelter s in period t

For the rolling horizon with perfect future knowledge (RH-PFK) variant, all actual values equal their respective forecasted values.

For rolling horizon with uncertainty (RH-U), actual values for the execution phase are random uniform values, $U[min, max]$, centered around forecasted values with a floor of zero to prevent negative results. We introduce three parameters to specify the maximum absolute difference between forecasted and actual values:

var_a	Renewable production variability
var_u	Unmanaged demand variability
var_β	Thermal intercept variability

$$a_t^{actual} = max\left(0, U\left[\left(a_t^{forecast} - var_a \cdot a_t^{forecast}\right), \left(a_t^{forecast} + var_a \cdot a_t^{forecast}\right)\right]\right) \quad (5.1)$$

$$u_t^{actual} = max\left(0, U\left[\left(u_t^{forecast} - var_u \cdot u_t^{forecast}\right), \left(u_t^{forecast} + var_u \cdot u_t^{forecast}\right)\right]\right) \quad (5.2)$$

$$\beta_{s,t}^{actual} = max\left(0, U\left[\left(\beta_{s,t}^{forecast} - var_\beta \cdot \beta_{s,t}^{forecast}\right), \left(\beta_{s,t}^{forecast} + var_\beta \cdot \beta_{s,t}^{forecast}\right)\right]\right) \quad (5.3)$$

Conditions may exist where actual unmanaged demand in a period is higher than forecasted, while actual renewable production is simultaneously lower than forecasted, leading to infeasibilities from Equation (4.7). We prevent this by requiring the RH-U model to provision sufficient power generation capacity in the planning stage to accommodate demand and renewable variability.

Additionally, actual environmental conditions may differ from forecasted values, causing shelter temperatures to exceed our upper or lower bounds during the execution phase. Rather than enforcing Equations (4.16) and (4.17) in the RH-U model, we include the extent and frequency of temperature violations with fuel consumption as our measures of effectiveness.

5.2 Baseline Grid Configuration

Our initial configuration is based on a tactical power system surveyed by Shields and Newell [79] in September and October 2011. Located in southwest Afghanistan, at the time of the survey this power system supplied a patrol base that housed 45 Marines sheltered in eight structures served by ten ECUs, three conventional generators, and two hybridized generators with battery storage. Figure 5.3 outlines the patrol base equipment inventory and configuration.

The hybrid components of the system include a 84 kWh storage battery de-rated to 42 kWh and a 4.8 kW PV system that harvested approximately 25 kWh of solar energy per day [80]. COC and billeting plug loads averaged 68.5 kWh per day, and two 2.5 kW B0075 refrigerated storage units (reefers) and a Ground Based Operation Surveillance System (GBOSS) consumed another 61.7 kWh per day [79].

5.2.1 Equipment Manifest

Our baseline configuration approximates the grid assessed by Shields and Newell with the following exceptions:

- Wooden buildings are modeled as Base-X 307 fabric structures to take advantage of thermal performance data available in AutoDISE.
- The B0014 and B0018 ECUs serving the COC are aggregated into a single ECU due to limitations of our present model which require a one-to-one correspondence between shelters and ECUs.
- The 500 watt (W) GBOSS tower and its dedicated 5 kW generator are not included in the model.
- Though the direct current air conditioners (DCACs) are capable of variable speed operation, they are modeled as conventional ECUs with on/off operation due to limitations of the present model which do not permit continuously variable ECU output.
- The two B0075 reefer units and all COC and billeting plug loads are treated as unmanaged demand.

- The patrol base was outfitted with TQGs while the model uses AMMPS generators. AMMPS is the program of record replacement for the TQGs and is a more relevant modeling selection.

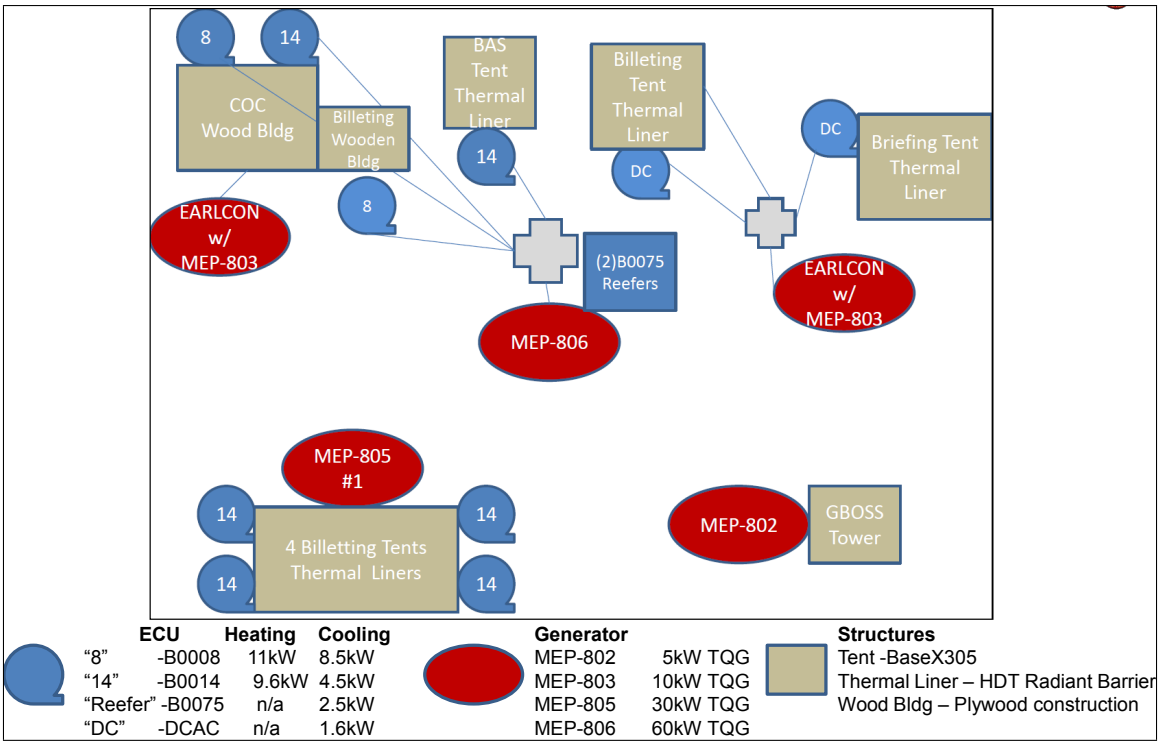

Figure 5.3: Southwest Afghanistan USMC patrol base showing structures, ECUs, and generators, from [79].

Tables 5.2 through 5.4 provide parameters for the shelters and generators included in the baseline model configuration. Additional information on thermal model slope and intercept calculations are in Appendix A.

Baseline Shelter Configurations				
Parameter	**Shelters 1-5**	**Shelters 6, 7**	**Shelter 8**	**Shelter 9**
Usage	Billeting	Billeting	Billeting	COC
Type	Base-X 305	Base-X 305	Base-X 307	Base-X 307
Min. internal temp. [$^{\circ}F$]	70	70	70	70
Max. internal temp. [$^{\circ}F$]	80	80	80	80
ECU capacity [BTU/hr]	36,000	20,000	60,000	96,000
ECU power [kW]	4.5	1.6	8.5	13.0
Thermal slope [$BTU/(hr\cdot^{\circ}C)$]	-931	-931	-1,226	-1,254
Thermal intercept [BTU/hr]	37,790	37,790	48,794	60,456
ECU run / rest time [$minutes$]	2 / 2	2 / 2	2 / 2	2 / 2

Table 5.2: Shelter configuration for baseline model.

Baseline Generator Configurations				
Parameter	**Generator 1**	**Generator 2**	**Generator 3**	**Generator 4**
Type	AMMPS	AMMPS	AMMPS	AMMPS
Frequency [$Hertz$]	60	60	60	60
Rating [kW]	10	10	30	60
Gen. run / rest time [$minutes$]	5 / 5	5 / 5	5 / 5	5 / 5

Table 5.3: Generator configuration for baseline model.

FUEL CONSUMPTION USING AVL					
Power Percent	Generator Model				
	5-kW	10-kW	15-kW	30-kW	60-kW
	gal/hr	gal/hr	gal/hr	gal/hr	gal/hr
110%	0.55	0.98	1.39	3.11	5.33
100%	0.51	0.88	1.24	2.79	4.92
75%	0.42	0.70	0.95	2.00	3.96
50%	0.34	0.53	0.73	1.39	2.74
25%	0.27	0.38	0.49	0.92	1.66
10%	0.23	0.29	0.38	0.65	1.08
0%	0.20	0.24	0.31	0.59	0.74

Table 5.4: Fuel consumption of AMMPS generator sets, from [75].

5.2.2 Storage, Renewables, Unmanaged Demand, and Uncertainty

We establish the following parameters for the baseline configuration:

Storage. We aggregate all storage into a single battery and set the following values:

$$charg_b = disch_b = \frac{0.2 \cdot cap_b}{hr} = 8.4 \text{ kW} \qquad \forall b \in B$$
$$\eta_b = 75\% \qquad \forall b \in B$$

Renewables. Renewable production of 25 kWh per day is evenly distributed for a baseline forecasted renewable contribution of 1.04 kW in each period.

$$a_t = a_t^{forecast} = 1.04 \text{ kW} \qquad \forall t \in T$$

Unmanaged demand. We treat COC and billeting plug loads of 68.5 kWh per day as evenly distributed, resulting in demand of 2.85 kW during each period. The potential demand of two 2.5 kW reefers are added to establish a forecasted unmanaged demand level of 7.85 kW in each period.

$$u_t = u_t^{forecast} = 7.85 \text{ kW} \qquad \forall t \in T$$

Uncertainty. We specify maximum renewable and thermal intercept variability for Equations (5.1) through (5.3) as:

$$var_a = var_u = 0.15$$
$$var_\beta = 0.05$$

To accommodate this uncertainty we require that the RH-U variant provision generator capacity that is at least 120% of forecasted demand for each period.

5.3 Baseline Configuration Results

We present the results obtained from running all six model variants on the baseline configuration over a ten-hour optimization horizon with two-minute time steps ($w = 2$). Rolling horizon variants (RH-PFK and RH-U) employed 20 iterations, planning for 60 minutes and executing 30 minutes in each iteration. Optimization dimensions and computational performance data are contained in Appendix B.

5.3.1 Fuel Consumption

Cumulative fuel consumption for each model variant over the ten-hour optimization horizon is tabulated in Table 5.5.

Baseline Cumulative Fuel Consumption			
Variant	**Best Solution [gallons]**	**Best Possible [gallons]**	**Reduction vs. LGCY [%]**
PFK-GSM	23.5	23.1	28.6
PFK-SOM	33.0	32.8	NA
LGCY	32.9	32.9	NA
PFK-FM (RMIP)	15.9	NA	51.7
PFK-FM (integer)	22.3	19.7	32.2
RH-PFK	22.9	22.9	30.4
RH-U	23.7	23.5	28.0

Table 5.5: Cumulative fuel consumption for baseline configuration after 10 hours.

For the baseline configuration we include both integer and relaxed mixed integer program (RMIP) linear solutions for the perfect future knowledge, full management (PFK-FM) model. The integer solution required 22 hours to close within 12% of optimality.

Unsurprisingly, the legacy unmanaged (LGCY) mode is at the upper end of fuel consumption. Though we expect the performance of perfect future knowledge, storage-only management (PFK-SOM) to be at least equal to that of LGCY, our results indicate that the best integer solution for PFK-SOM uses slightly more fuel. This is attributable to our stopping conditions that include a relative optimality gap of 4%. If we permit the model to continue optimizing we would see PFK-SOM improve to at least the LGCY value, but in no case would it go below the best possible solution of 32.8 gallons. We conclude that a PFK-SOM scheme in which generators are always running offers no significant advantage over existing LGCY methods for the modeled grid conditions.

The perfect future knowledge, generator and storage management (PFK-GSM) performance shows a considerable reduction in fuel consumption relative to LGCY values. Recall that in PFK-GSM the generators and storage are optimized and ECU operation is fixed beforehand to the behavior that would occur if they were under thermostatic control. These results indicate that under some conditions we may see considerable improvements to fuel efficiency by merely predicting—and subsequently constraining—upcoming ECU behavior and then optimizing generator operation to match the defined load schedule.

The RH-U model, burdened with our requirement to provision sufficient capacity to meet 120% of predicted load in each period, nevertheless consumes only 3.5% more fuel than

its perfect knowledge counterpart, RH-PFK. This is explained by the high system load factor for both variants, illustrated in Figure 5.4. We showed in Figure 1.6 that generator efficiency "flattens" as load factor increases, resulting in only modest changes to fuel efficiency as we move between load factors above 50%.

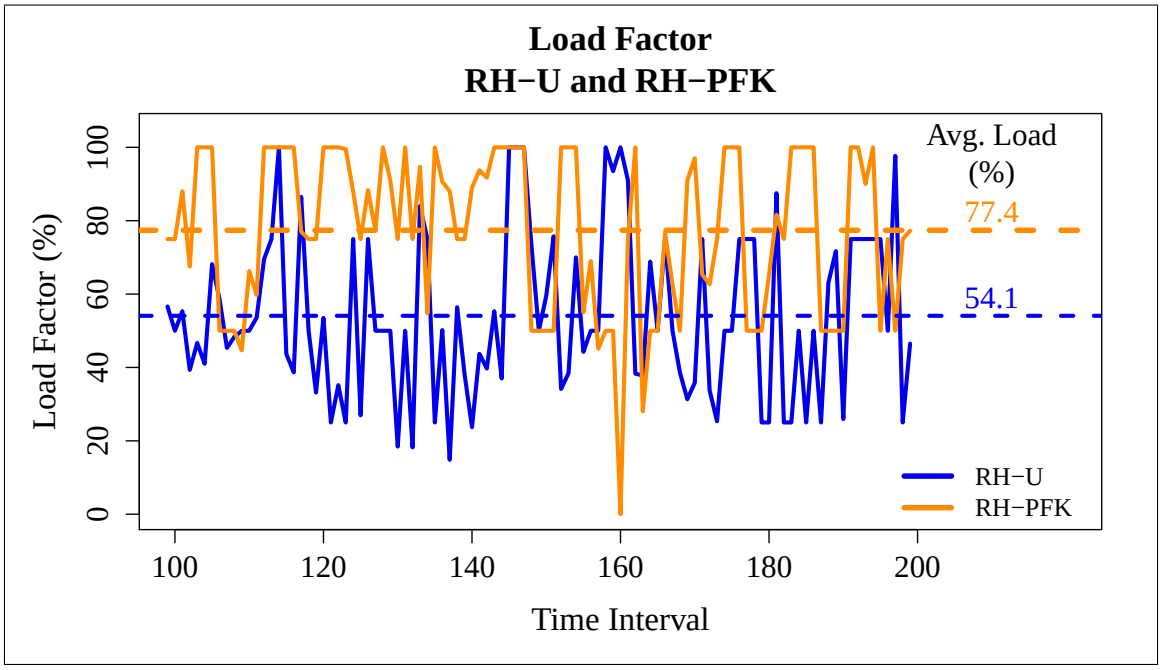

Figure 5.4: Baseline configuration generator loading for RH-U and RH-PFK.

5.3.2 Thermal Observations

Figure 5.5 displays the interior temperature of Base-X 305 shelter equipped with a B0014 ECU over the ten-hour horizon for LGCY and RH-U variants. The sawtooth pattern shown by LGCY is characteristic of a thermostatically controlled load that switches modes only when reaching a high or low limit. PFK-SOM and PFK-GSM fix ECU operation to the same thermostatically determined cycles and exhibit the exact same behavior.

The optimal ECU scheduling of RH-U results in temperature variations driven by globally optimal fuel efficiency considerations. RH-PFK presents similar results to RH-U; Figure 5.6 displays both over a subset of the optimization period for comparison.

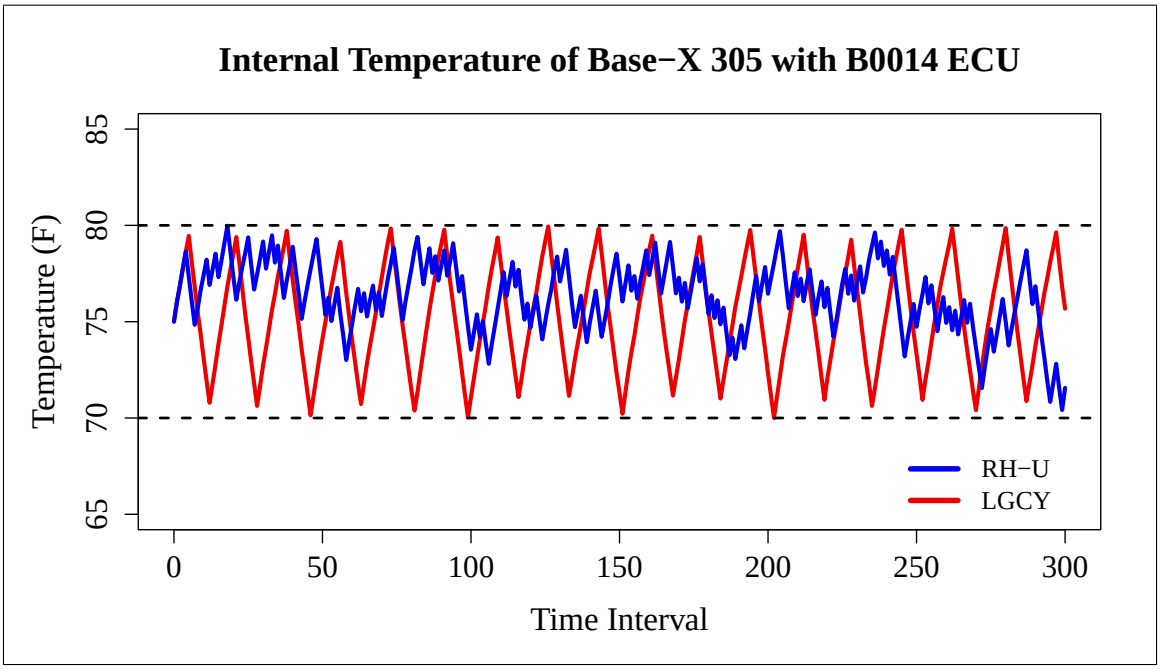

Figure 5.5: Baseline thermal behavior of a Base-X 305 shelter equipped with B0014 ECU under LGCY and RH-U variants.

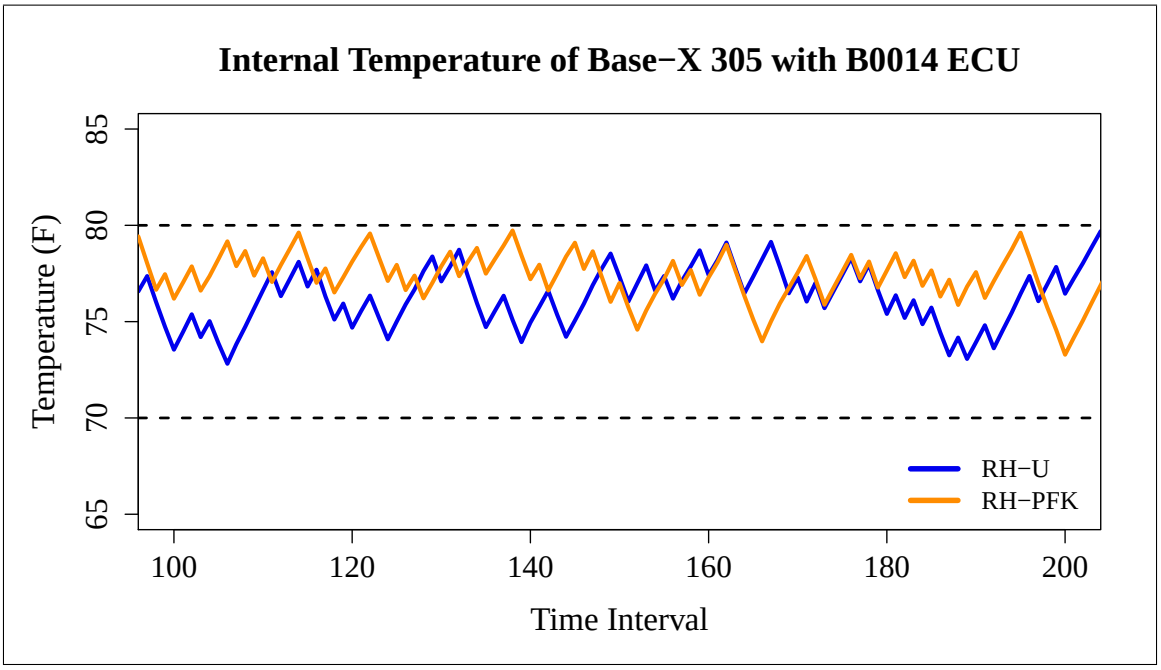

Figure 5.6: Comparison of interior temperatures for Base-X 305 shelter with B0014 ECUs under RH-U and RH-PFK.

The DCAC units have far less cooling capacity than the B0014 ECU, resulting in slower cooling and higher duty cycle for the same environmental and shelter conditions. Figure 5.7 shows LGCY and RH-U results for interior temperature in a Base-X 305 equipped with a DCAC. With the exception of two brief periods the DCAC is always running in the LGCY variant.

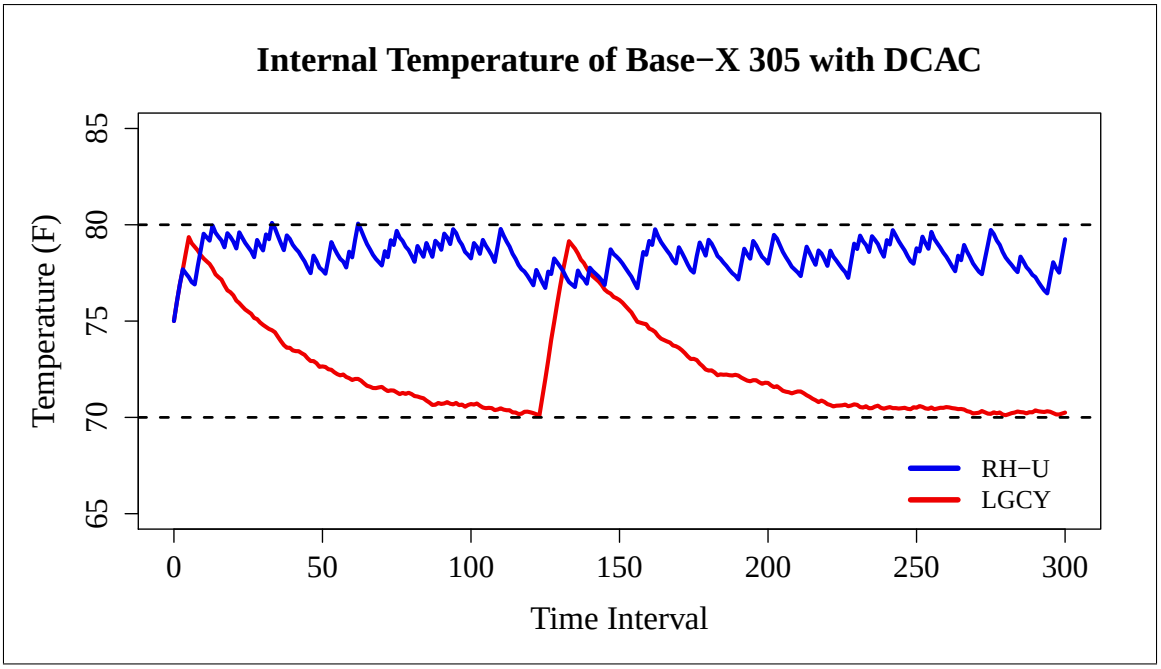

Figure 5.7: Baseline thermal behavior of a Base-X 305 shelter equipped with DCAC under LGCY and RH-U variants.

We point out two observations from these results. The first is the overall upward temperature bias in RH-U relative to LGCY. In the Base-X 305 with B0014 ECU shown in Figure 5.5, the mean RH-U temperature is 1.2 F higher than the mean LGCY temperature. This difference rises to 5.8 F in the Base-X 305 with DCAC shown in Figure 5.7. This is consistent with our thermal model, which recognizes that more energy—and more fuel—are required to maintain lower shelter interior temperatures.

The second, seemingly contrary, observation is that an optimally scheduled ECU will often initiate cooling well before approaching the high temperature limit. An example of this phenomenon are highlighted in Figure 5.8. We draw two conclusions from this observation. First, the model elects to use currently available energy to do work now rather than store the energy in the battery to do work later. We discuss storage utilization further in Section 5.3.4 and Section 6.3. Finally, we conclude that the RH-U model validates our premise that time-shifting ECU operation can be employed to shape demand and lower overall overall fuel consumption.

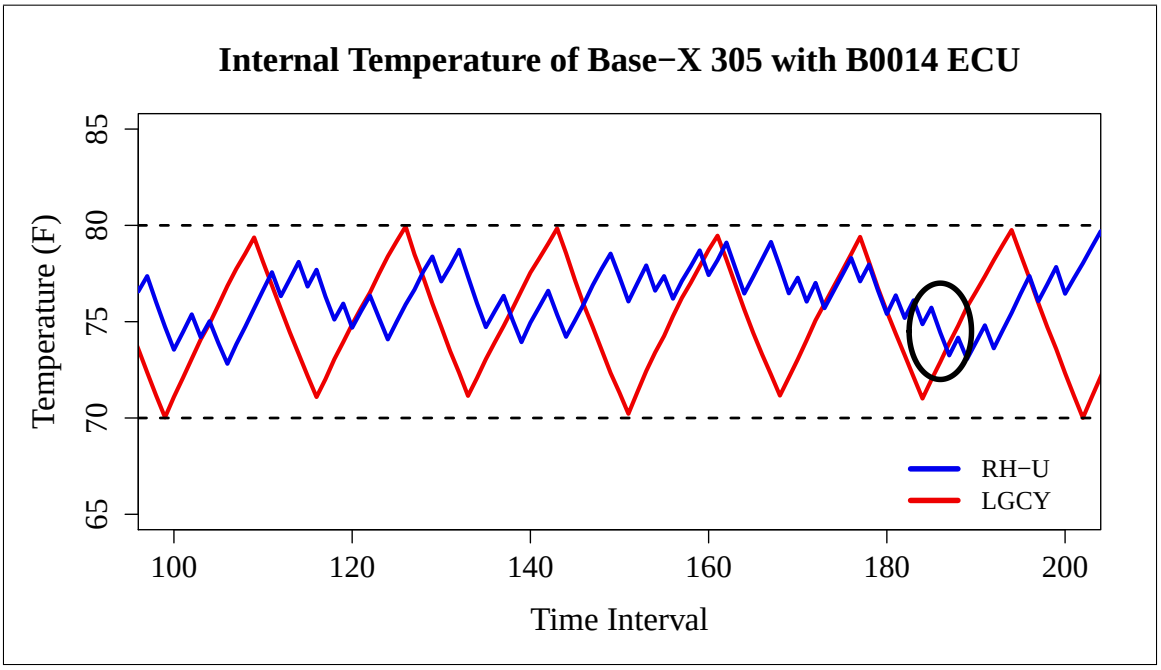

Figure 5.8: Behavior of optimally scheduled ECUs with one example of time-shifted load management highlighted. Many other instances of time-shifting can be seen in the figure.

As discussed in Section 5.1.2, evaluation of RH-U requires an assessment of the frequency and magnitude of temperature violations that occur due to differences between forecasted and actual environmental conditions. Table 5.6 provides this data for all nine shelters over the entire ten-hour time horizon. We determine that 20 minutes of temperature violation over the 90 shelter-hours modeled in the baseline configuration are not significant. We give further attention to the effects of environmental uncertainty in Section 6.2.1.

RH-U Temperature Violations for All Shelters in All Periods				
Min. Temp. [F]	**Low Limit Violations**	**Max. Temp. [F]**	**High Limit Violations**	**Cumulative Violation Time [minutes]**
70.6	0	80.25	10	20

Table 5.6: Temperature violations for nine shelters over ten hours using RH-U model in the baseline configuration.

5.3.3 Generator Operation

Analysis of generator operation provides deeper insights on the origin of fuel savings achieved through optimal ECU management. Figure 5.9 displays the number of running generators in each period for the LGCY and RH-U models. Permitting optimal scheduling of both ECUs and generators provides our RH-U model the freedom to provision the most efficient generator mix capable of fulfilling demand. Table 5.7 lists the number of periods that each generator is running under baseline conditions in the RH-U model.

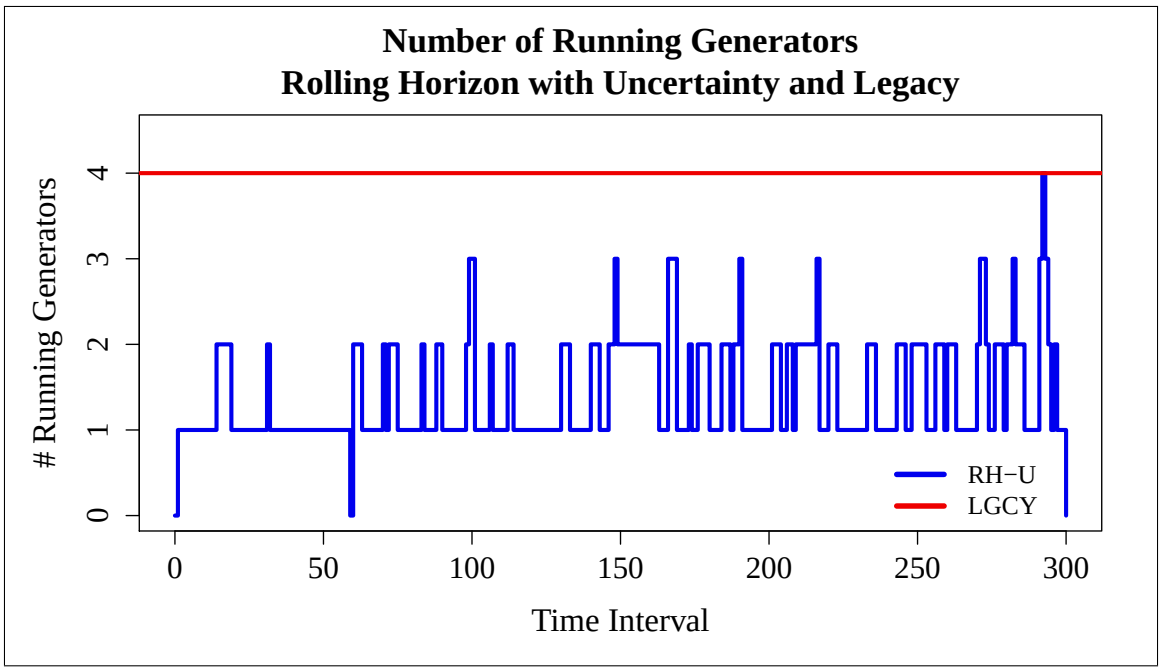

Figure 5.9: Number of running generators in each period of baseline configuration for RH-U and LGCY.

Baseline Configuration Running Time under RH-U				
Parameter	**Generator 1**	**Generator 2**	**Generator 3**	**Generator 4**
Capacity [kW]	10	30	60	10
Operational periods (out of 300)	71	82	172	98
Running time [%]	23.6	27.3	57.3	32.7

Table 5.7: Generator utilization in the baseline configuration for RH-U model.

Each model is encumbered with specific limitations, granted various optimization freedoms, and permitted horizon visibility that affect *how* it generates, stores, and utilizes power for temperature control. Because every model must achieve the same result of removing sufficient thermal energy from all shelters to maintain the desired temperature,

however, the total amount of energy delivered to the loads, shown in Table 5.8, is approximately equal for all variants.

RH-U and RH-PFK first reduce fuel consumption by provisioning fewer generators to deliver the total required energy over the course of our optimization trial. The fuel savings from fewer running generators are compounded by the fact that each running generator must operate at higher—and more fuel efficient—load factors to deliver the same total energy. Figure 5.10 shows generator load and average utilization for 100 time intervals (200 minutes) of our optimization trial.

We will examine the effect of changes to our generator mix and characteristics in Section 6.1.

Baseline Configuration Delivered Energy					
	LGCY	**RH-U**	**RH-PFK**	**PFK-SOM**	**PFK-GSM**
Delivered energy [kWh]	261.9	252.8	254.2	263.9	265.6

Table 5.8: Total energy delivered over 10 hours in the baseline configuration.

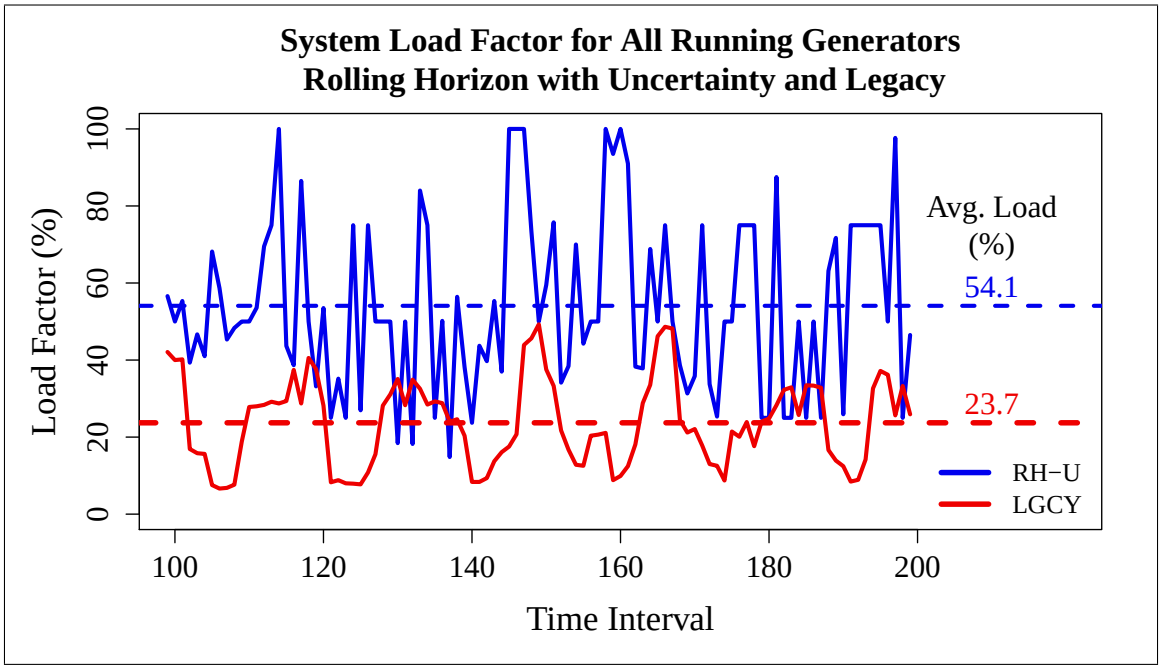

Figure 5.10: Baseline configuration generator loading for RH-U and LGCY.

5.3.4 Energy Storage

Battery level in the baseline configuration for each storage-capable model is shown in Figure 5.11, and total the energy placed in the battery over the duration of the ten-hour horizon is listed in Table 5.9. We make two observations from this information. First, battery utilization is low for all variants despite our generously simplified battery model. At no time is more than 10% of our total 42 kWh battery capacity employed by any model variant. This is consistent with Van Broekhoven *et al.* [18], who find diminishing returns from energy storage as grid design progresses from spot generation to a microgrid.

Our second observation is that the PFK-SOM model, despite having battery storage as its only avenue for optimization, makes the least use of available storage capability. This indicates that energy storage alone, without a concurrent ability to control electrical production or loads, offers limited benefit in our baseline grid.

Additional discussion on the impact of variations to storage capabilities and capacities is contained in Section 6.3.

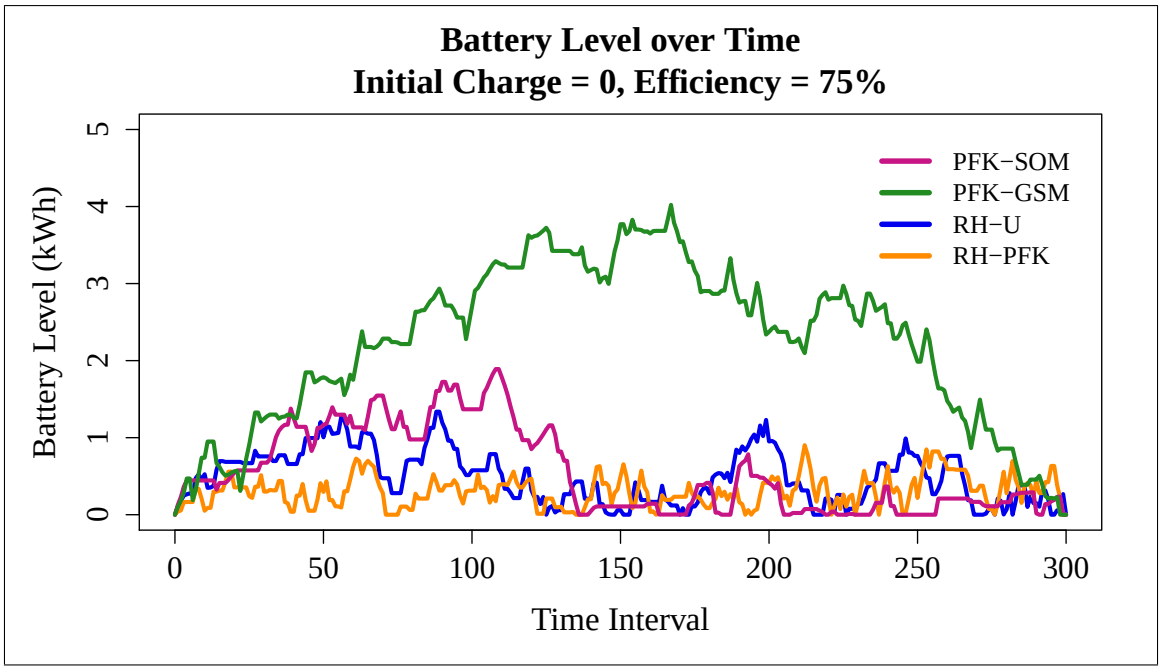

Figure 5.11: Baseline configuration battery level.

Baseline Configuration Battery Utilization				
	RH-U	**RH-PFK**	**PFK-SOM**	**PFK-GSM**
Total energy placed in battery [kWh]	15.19	19.12	9.37	16.11
Percentage of total production	6.0	7.5	3.5	6.1

Table 5.9: Battery utilization in the baseline configuration for storage-capable models.

5.4 Baseline Configuration Summary

Our suite of model variants evaluates baseline grid performance by using LGCY operation as an upper bound and PFK-FM as a theoretical lower bound on fuel consumption. Intermediate variants offer insight on efficiency gains that may be achieved under various optimization opportunities and limitations on knowledge of future conditions.

In particular, the results for RH-U suggest the potential for computationally feasible optimal scheduling of ECUs, generators, and storage devices to reduce fuel consumption relative to existing "always on" spot generation arrangements by as much as 28% while maintaining temperatures within specification and remaining tolerant of uncertainty in any remaining unmanaged loads.

CHAPTER 6:
Sensitivity Analysis

We continue our analysis of the baseline configuration presented in Chapter 5 by conducting sensitivity analysis to evaluate the effect that changes to generator configuration, thermal and environmental parameters, storage characteristics, and unmanaged demand have on fuel consumption.

6.1 Generator Configuration

6.1.1 Generator Mix

Our baseline grid parameters dictate that the maximum electrical output demanded of the generators in any period is 56.23 kW[12], well below our total generation capacity of 110 kW. Figure 6.1 shows the impact on fuel efficiency as we change the mix of generators available to our models.

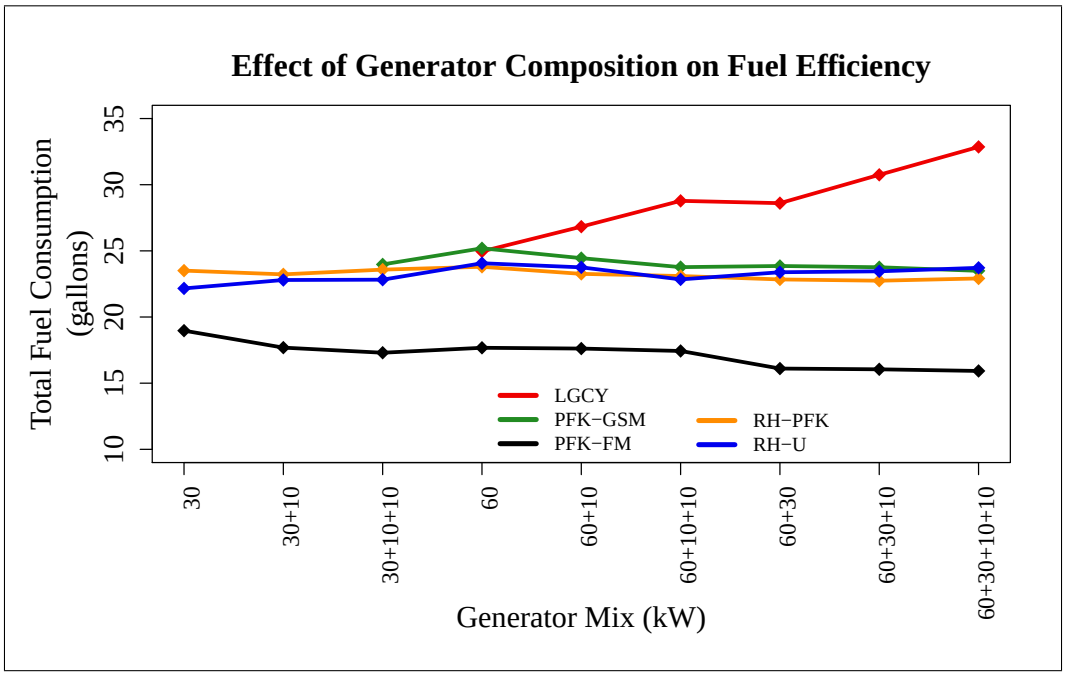

Figure 6.1: Effect of generator composition on fuel efficiency.

[12] 1 × 13 kW ECU + 5 × 4.5 kW ECU + 2 × 1.6 kW ECU + 1 × 8.5 kW ECU + 115% × 7.85kW unmanaged demand − 0 kW renewables

We draw attention to three features of Figure 6.1:

1. LGCY fuel consumption converges to our optimized fuel consumption as generation capacity approaches 60 kW, the minimum required to simultaneously supply all loads. By this point all running generators are at high load factors and within the upper portion of the generator fuel efficiency curve.
2. Below 60 kW generation capacity, unmanaged load may exceed production and LGCY becomes infeasible. Through optimal management of storage and remaining generators, PFK-GSM remains feasible down to 50 kW of total generation capacity. By optimally managing generators, storage, **and** loads, RH-PFK and RH-U remain feasible and capable of supporting the grid *under these particular environmental conditions* with only 30 kW of total electrical production.
3. A single 60 kW generator uses slightly more fuel than its optimized 30+10+10 kW neighbor. While a 60 kW generator is the most efficient means of fulfilling the 56 kW peak demand, in practice a cluster of smaller generators may offer better aggregate efficiency for actual grid demand profiles.

We see that optimal scheduling provides the greatest improvements to fuel efficiency when the existing grid suffers from overgeneration, and diminishes to near-zero as the grid becomes ideally sized for the expected load. Our chosen baseline parameters serendipitously result in a maximum possible load that lies just within the capacity of the 60 kW generator, providing the LGCY model a better representation here than we would, on average, expect to see under a wider range of circumstances.

Further investigation into the ability of optimal scheduling to extend grid capability by multiplexing, or time-sharing generator output to serve collective loads in excess of net production capacity, is deferred to future studies.

6.1.2 Generator Agility

Once started, generators require a warm-up period before they are ready to synchronize phase with previously running generators and assume their share of electrical load. Likewise, when a generator is to be secured it must be electrically unloaded and permitted to cool before shutting down.

We enforce these physical constraints as generator run and rest times, which specify the amount of time that a generator, once added to the grid, must remain connected before removal and, conversely, the amount of time that a generator, once removed from the grid, must remain disconnected before it may be reconnected and again contribute to power production.

More agile generators—those with shorter run and rest times—reduce optimization constraints and presumably offer the potential for greater fuel efficiency. Our baseline configuration sets run and rest times to five minutes, and Figure 6.2 reveals no significant changes to fuel efficiency as we run four of our model variants with run / rest times varying from 0 to 20 minutes.

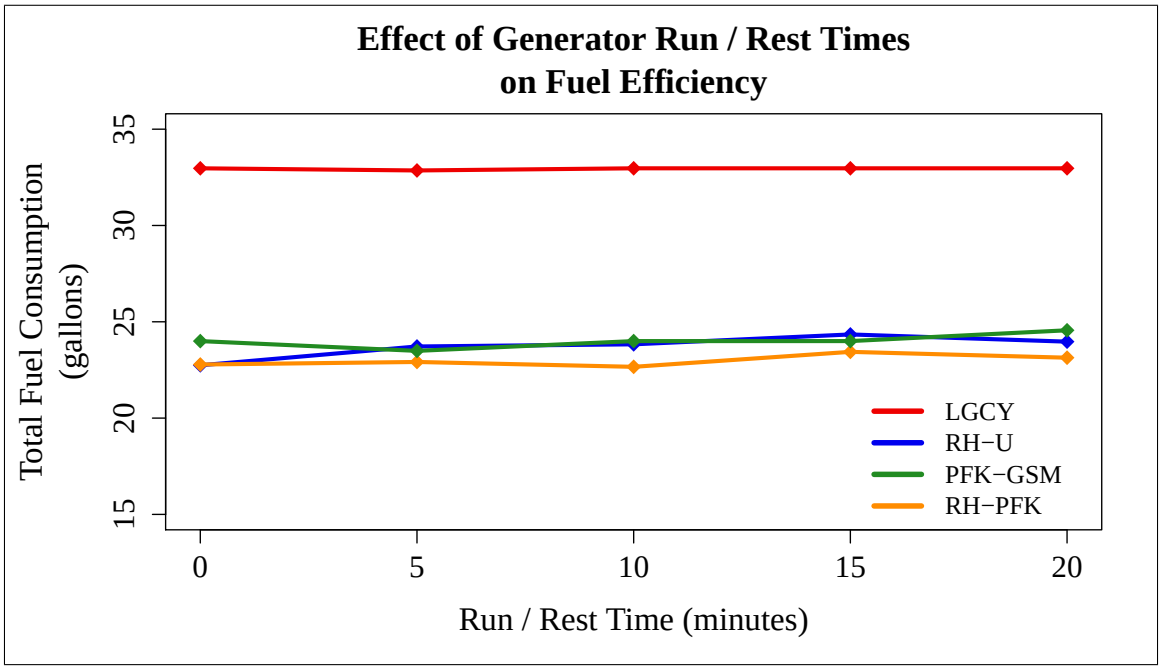

Figure 6.2: Impact of generator agility on fuel efficiency.

Though total fuel consumption is largely unaffected by variations to run and rest times, the actual mix of generators selected by RH-U to achieve these results varies as shown in Figure 6.3.

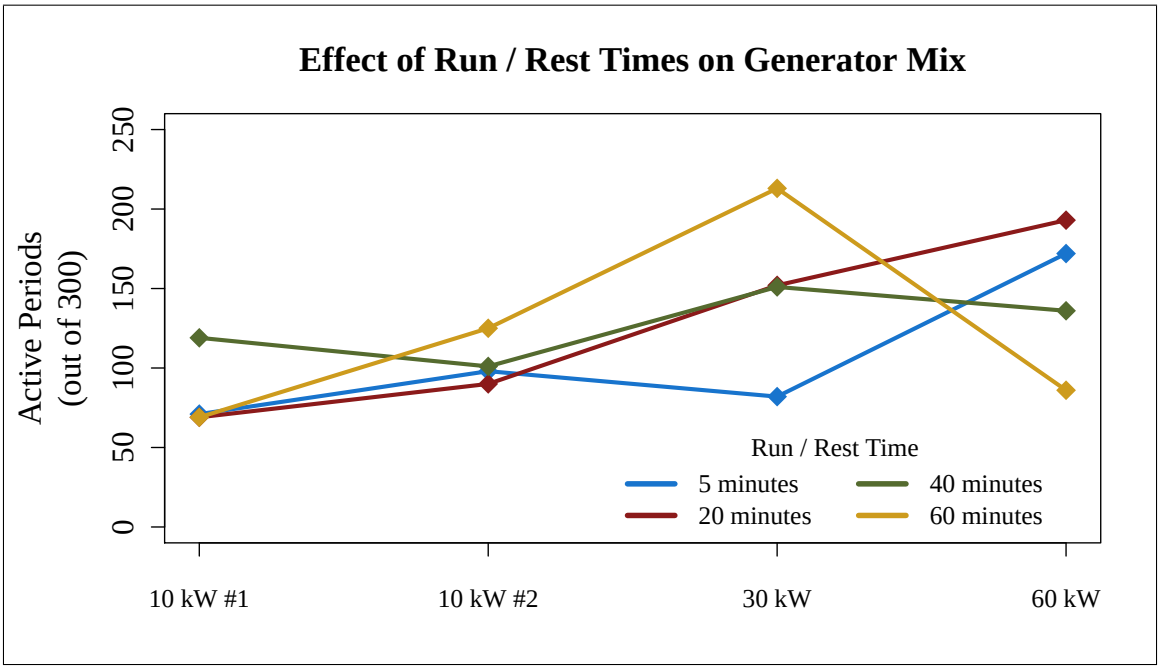

Figure 6.3: Effect of various run / rest times on RH-U generator mix.

We recommend additional investigation to consider:

- Multi-factor analysis of potential interactions between run / rest times and the various generator configurations described in Section 6.1.1.
- Imposing a penalty for each generator start to balance optimal fuel efficiency with equipment wear.

6.2 Thermal Conditions

6.2.1 Environmental Influence

We implement changes in environmental conditions by adjusting the intercept value of our thermal model, with larger values corresponding to warmer exterior conditions and greater cooling requirements. Figure 6.4 displays the results of running our baseline configuration with thermal intercept for each shelter scaled between 60% and 110% of its baseline values.

At scaling factors below 0.6 the Base-X 305 billeting shelters require heating and become infeasible in our current cooling-only model. At factors above 1.1 thermal burden exceeds the capacity of the DCACs and none of the variants are able to maintain the temperature of these shelters below the high limit.

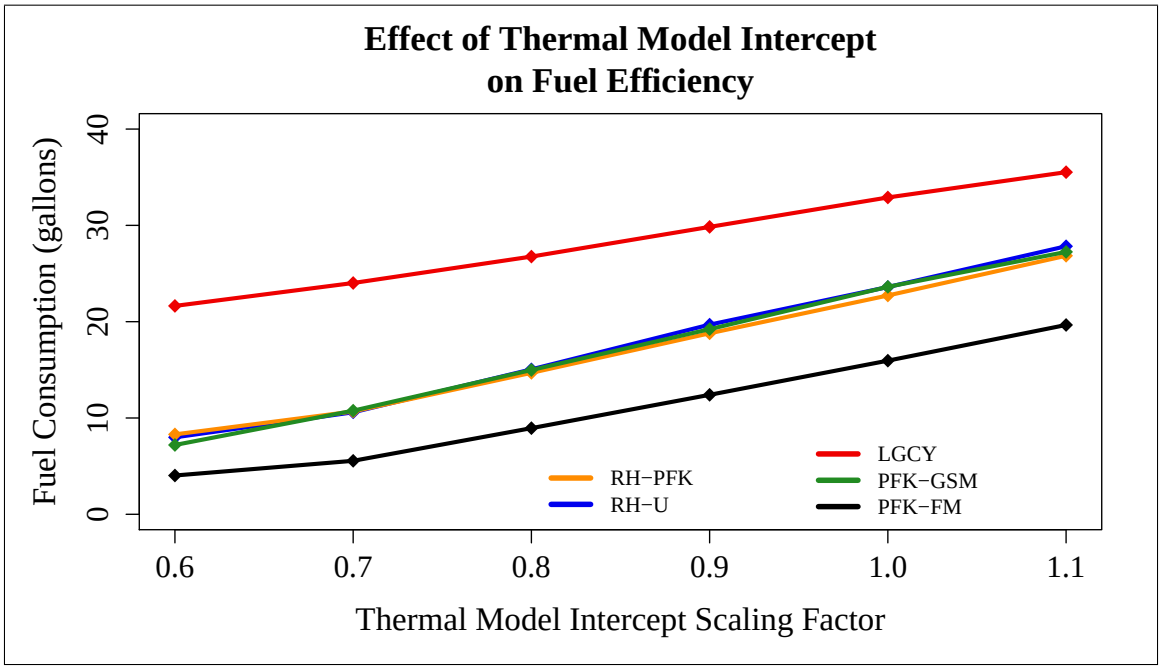

Figure 6.4: Effect of thermal model intercept on fuel efficiency.

Between these two levels we can see in Figure 6.4 that differences in fuel consumption between LGCY and our optimized variants narrow as thermal burden increases. Table 6.1 details this relationship between LGCY and RH-U fuel consumption.

Effect of Changing Environment on Fuel Consumption			
Thermal Intercept Scaling Factor	**LGCY Fuel Consumption [gallons]**	**RH-U Fuel Consumption [gallons]**	**RH-U Reduction vs. LGCY [%]**
0.6	21.64	7.99	63.1
0.7	24.02	10.59	55.9
0.8	26.76	15.05	43.8
0.9	29.84	19.69	34.0
1.0	32.90	23.60	28.3
1.1	35.52	27.83	21.7

Table 6.1: Comparison of LGCY and RH-U fuel consumption with changing environmental conditions.

Increased thermal burden imposes two constraints upon ECUs. First, they must operate more *on average* to remove heat added throughout the optimization horizon and maintain shelter temperature within specifications. Second, interior temperatures rise faster and limit

the length of time that an ECU may remain idle before a temperature limit is reached. These influences serve to limit time-shifting freedom and result in diminishing optimization advantages as load duty cycle increases.

6.2.2 Shelter Thermal Limits

Interior temperature limits are selected for personnel comfort and equipment safety and reliability. We evaluate the effect that changes to these limits have on fuel efficiency by maintaining a low limit of 70 F and varying our high limit from 75 F to 85 F. Results are displayed in Figure 6.5, where we see fuel consumption declining as the distance between low and high temperature limits increases.

We find that these improvements are attributable to the increasing upper limit of our temperature band rather than the distance between high and low limits. Our optimization models require a sufficiently large temperature band to prevent infeasibilities in successive periods, but we find that beyond this threshold there is no significant effect from a larger band. As seen in Figures 6.6 and 6.7, when provided the freedom to operate in a wide band the optimally scheduled ECUs elects to operate exclusively near the upper, more fuel efficient, limit.

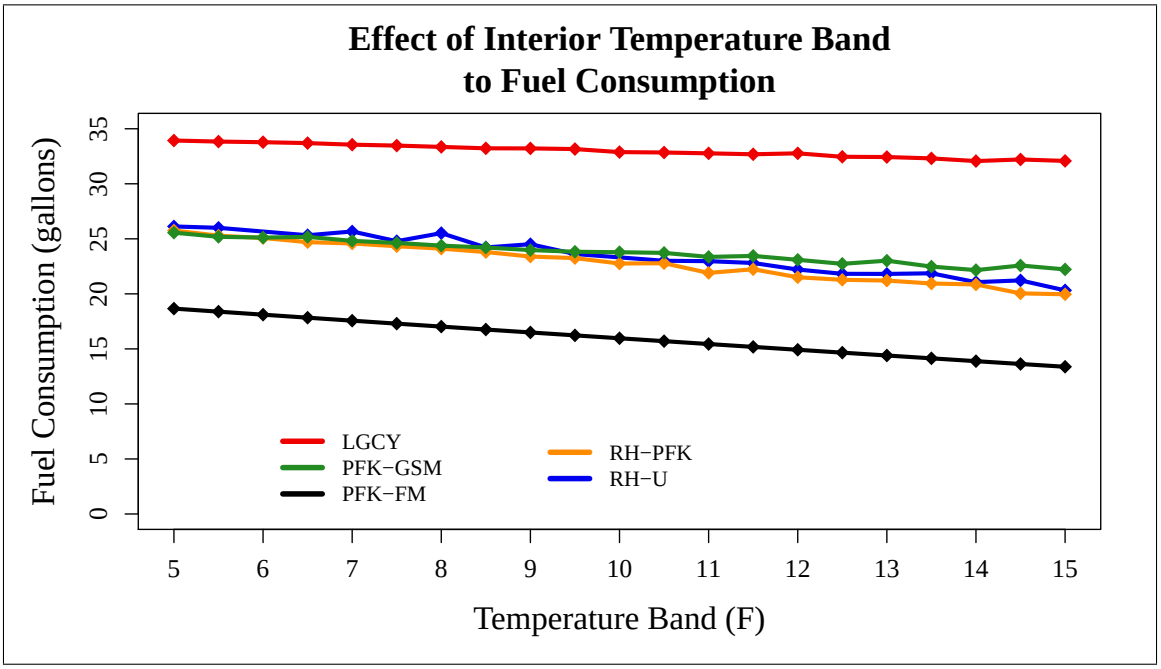

Figure 6.5: Effect of interior temperature band on fuel efficiency. Minimum interior temperature is held at 70 F while maximum interior temperature varies from 75 F to 85 F.

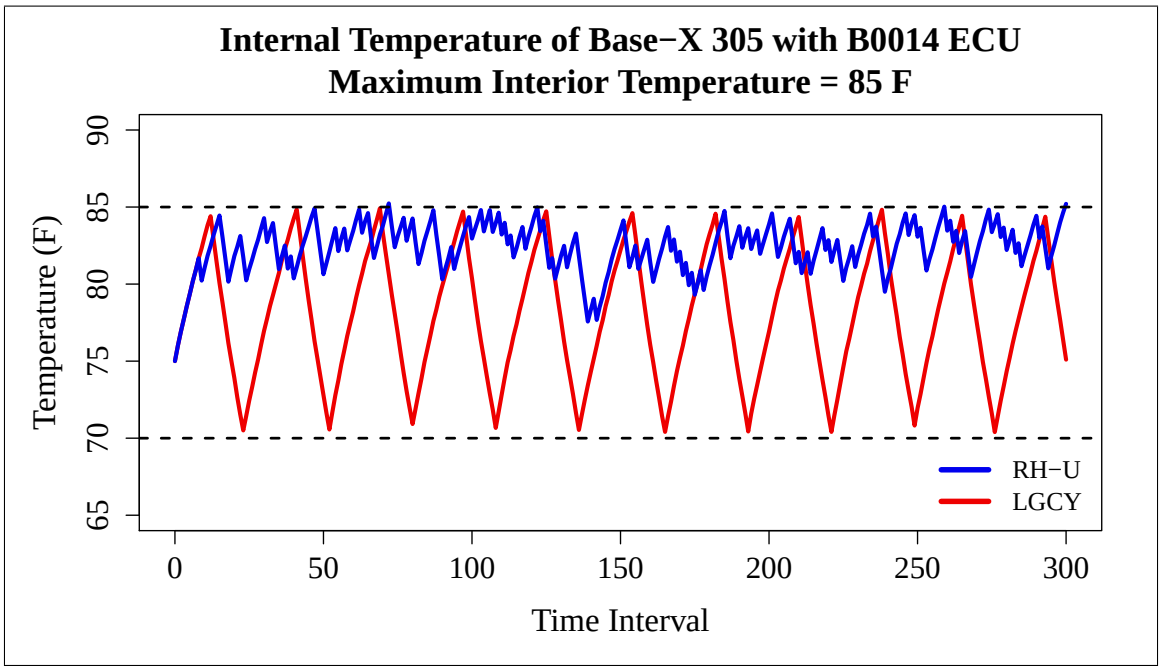

Figure 6.6: Interior temperature of a Base-X 305 shelter served by B0014 ECU with 70 F to 85 F temperature limits.

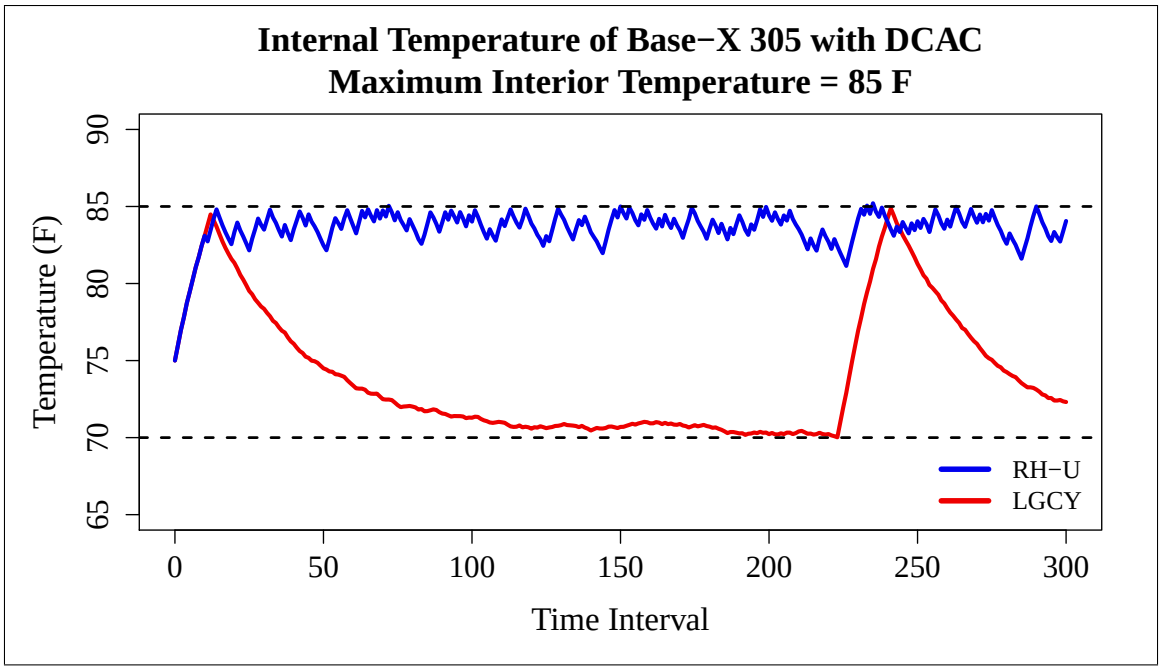

Figure 6.7: Interior temperature of a Base-X 305 shelter served by DCAC with 70 F to 85 F temperature limits.

6.3 Storage Utilization

Storage utilization for our model variants using the baseline 42 kWh battery with 75% efficiency were shown in Section 5.3.4. We conduct additional exploration to determine the effect that changes of battery efficiency and capacity have on fuel consumption.

6.3.1 Battery Efficiency

We run the model with battery efficiency varying from 75% to 100% and show the results for multiple variants in Figure 6.8. The LGCY variant does not have storage enabled but is included for reference. The optimally scheduled variants exhibit minor reductions as battery efficiency improves. Table 6.2 details the results for RH-U, and we see that the best integer solution for higher efficiencies improves upon the best theoretically possible solution of lower efficiencies, confirming a relationship between efficiency and fuel consumption. The practical impact is small in the configuration considered, suggesting that we would see, at most, a 3.6% reduction in fuel use if technological advances placed lossless storage options at our disposal.

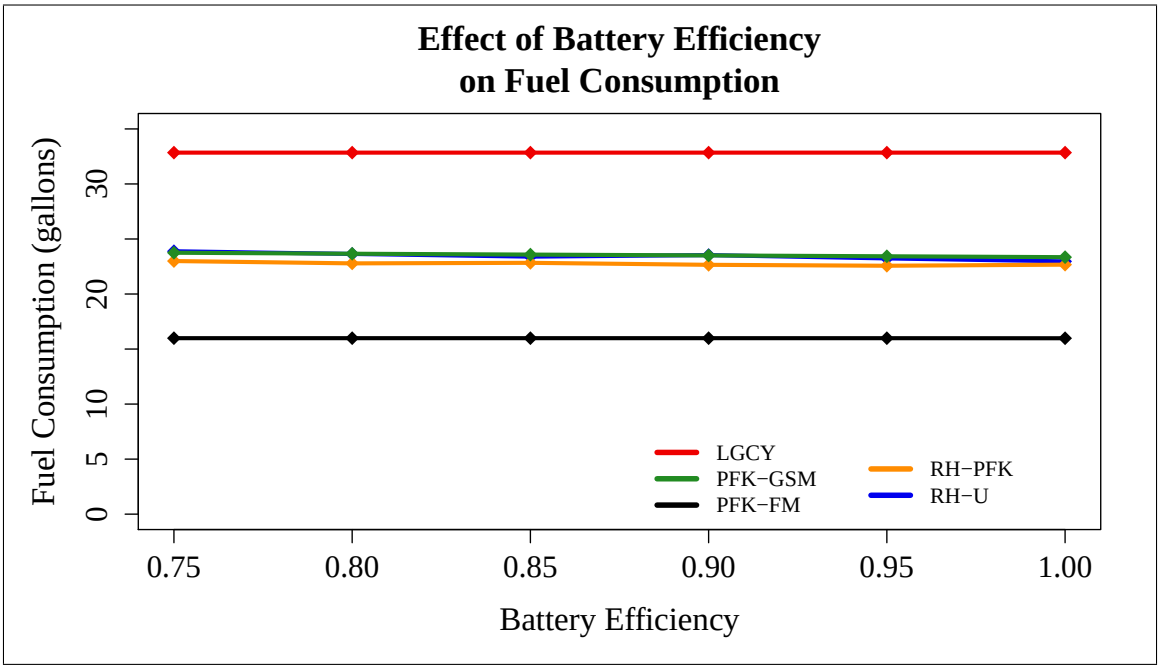

Figure 6.8: Effect of battery efficiency on fuel consumption.

Figures 6.9 through 6.11 illustrate how the battery is used at 75% and 100% for the PFK-GSM, RH-PFK, and RH-U variants.

Effect of Battery Efficiency on RH-U Fuel Consumption		
Battery Efficiency [%]	**Best Integer [gallons]**	**Best Possible [gallons]**
75	23.89	23.76
80	23.64	23.49
85	23.40	23.25
90	23.54	23.28
95	23.23	23.20
100	22.97	22.91

Table 6.2: RH-U fuel consumption for battery efficiency values of 75% to 100%.

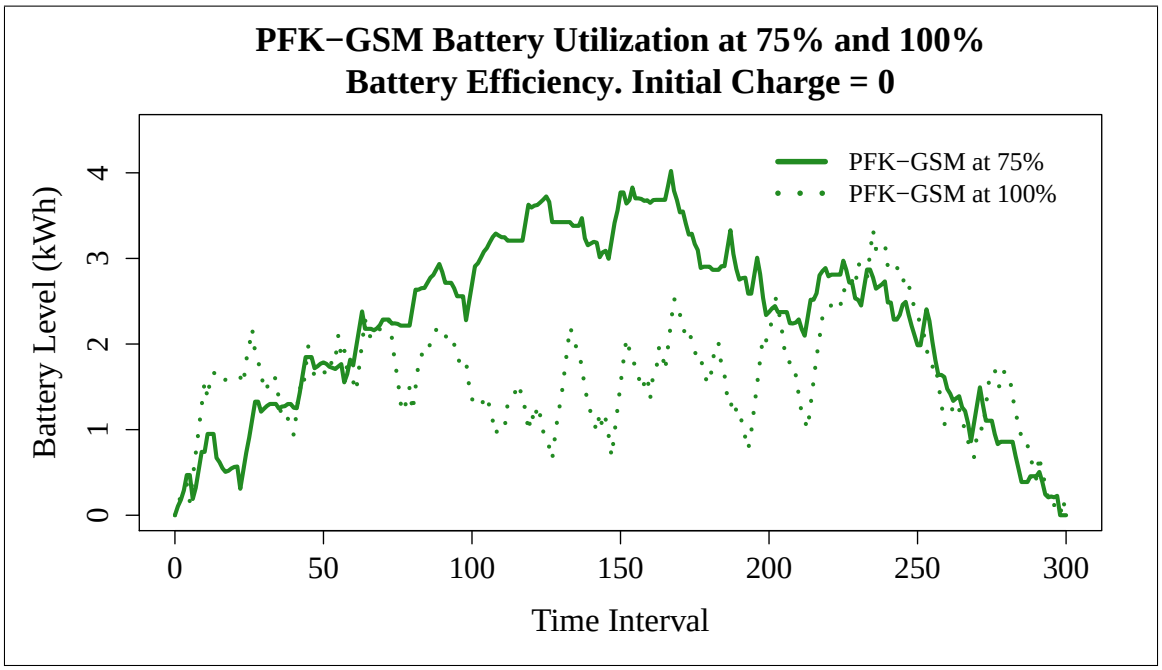

Figure 6.9: Battery utilization by PFK-GSM model at 75% and 100% battery efficiency.

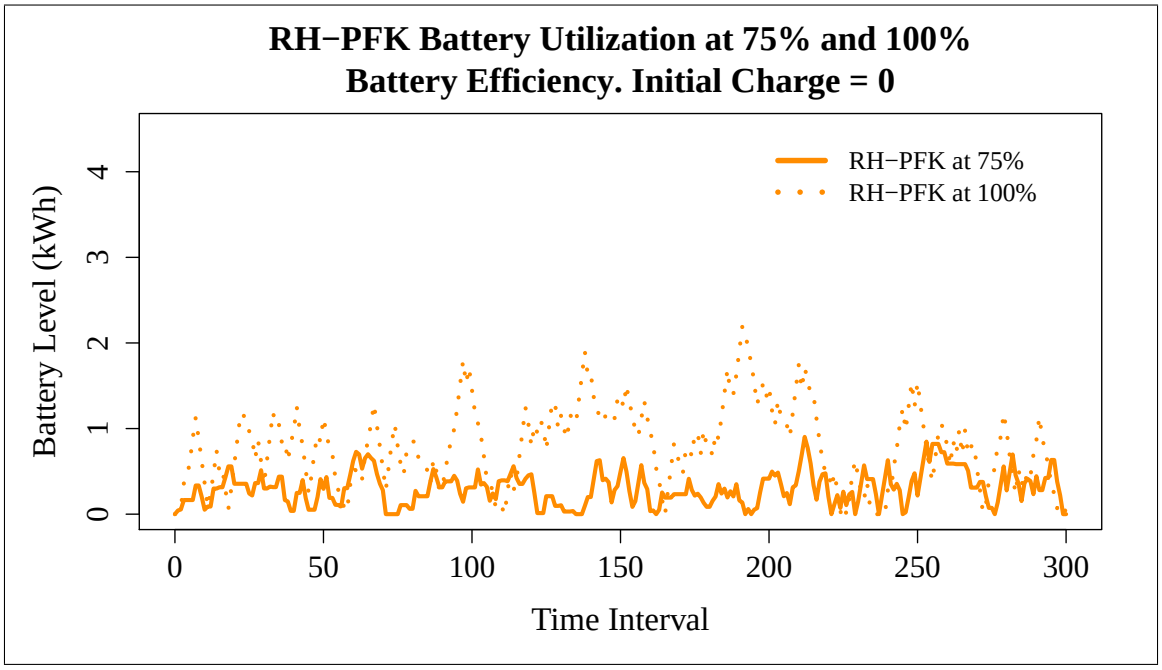

Figure 6.10: Battery utilization by RH-PFK model at 75% and 100% battery efficiency.

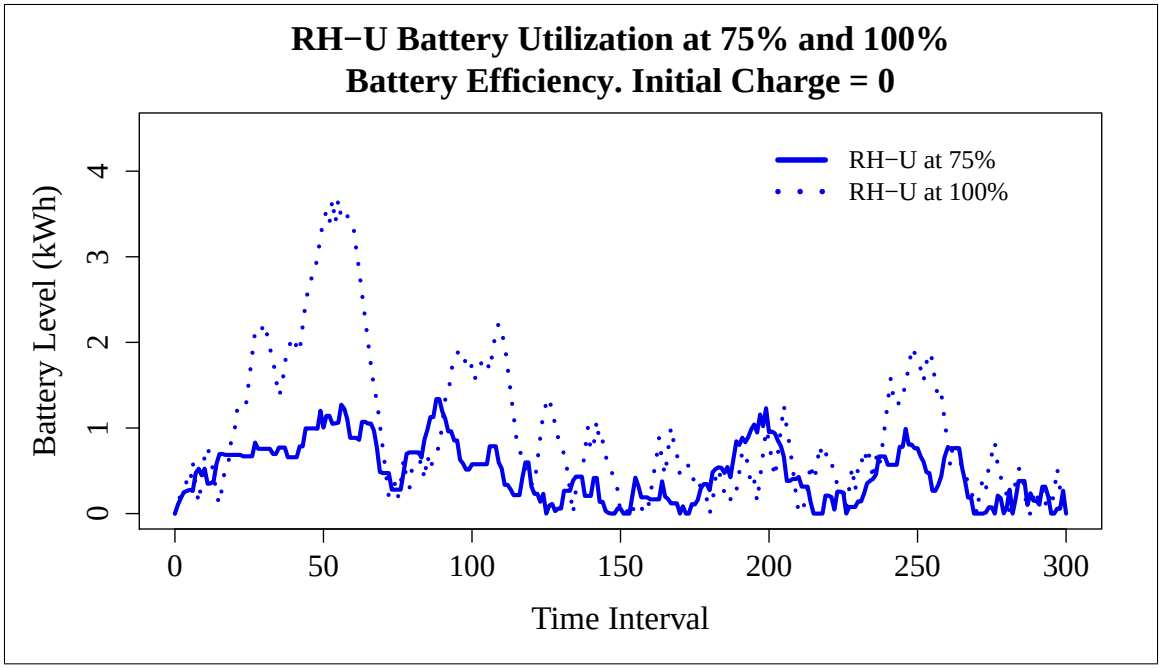

Figure 6.11: Battery utilization by RH-U model at 75% and 100% battery efficiency.

6.3.2 Battery Capacity

Changes to battery capacity affect our storage-enabled model variants in two ways. First, additional capacity permits a larger amount of energy to be stored for use in future periods. Additionally, our model computes maximum battery charge and discharge rates as linear functions of battery capacity. Doubling capacity also doubles the *rate* at which energy can be placed into or removed from the battery.

We determine the impact of these joint effects on fuel consumption by varying battery capacity from 0 to 80 kWh under the RH-U variant. These results are displayed in Table 6.3. We note that the best possible solution for some battery capacities is marginally worse than the best possible solution for a lower battery capacity. We attribute this to our choice of absolute and relative optimality gaps and to the rolling horizon methodology that makes early decisions before all information is known. We expect that any significant advantages of larger batteries would be evident, and we therefore conclude that having additional capacity and higher charge / discharge rates offers no discernible benefit to an optimally scheduled system in our modeled configuration.

Effect of Battery Capacity on RH-U Fuel Consumption		
Battery Capacity[kWh]	**Best Integer [gallons]**	**Best Possible [gallons]**
0	23.95	23.66
10	23.62	23.44
20	23.80	23.58
30	23.11	22.81
40	23.89	23.65
50	23.63	23.43
60	23.23	22.76
70	23.52	23.47
80	23.75	23.68

Table 6.3: RH-U fuel consumption for battery capacities values of 0 to 80 kWh.

Figure 6.12 depicts battery level over the course of a ten-hour optimization horizon under the RH-U variant with four battery sizes from 20 kWh to 80 kWh, while Table 6.4 lists the total amount of energy placed into storage.

We conclude that storage is a minor contributor to fuel efficiency under the conditions we have modeled. We encourage further research that extends this methodology to evaluation of additional grid configurations and performs multi-factor designed experiments to isolate the effects of battery capacity, efficiency, and charge / discharge rates on fuel efficiency.

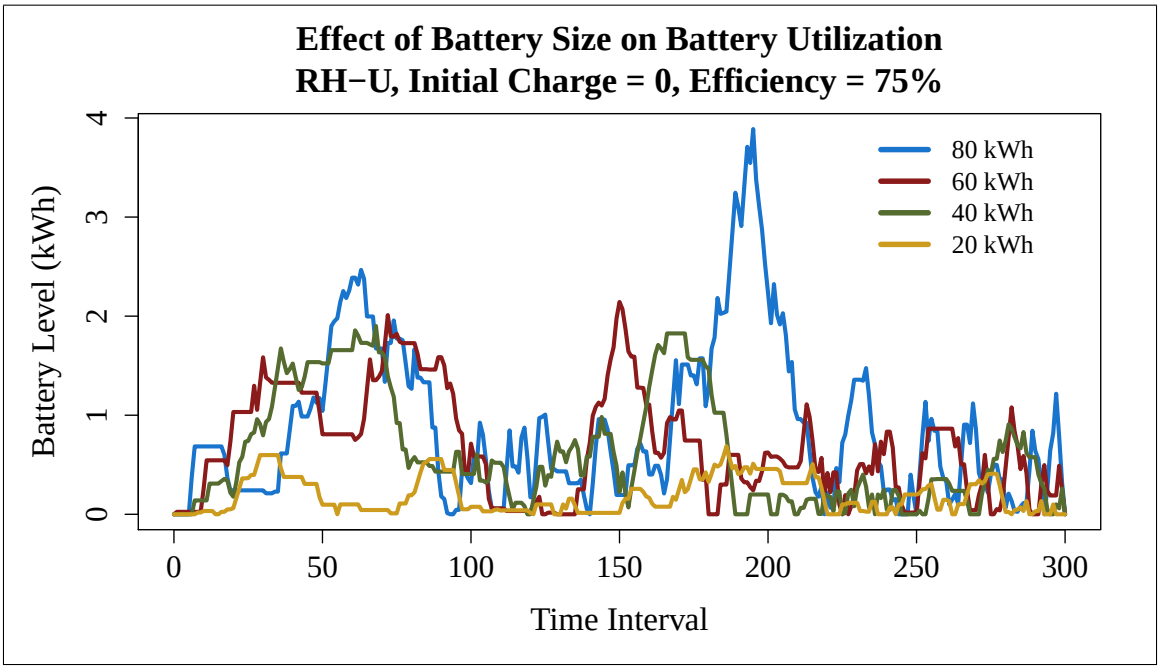

Figure 6.12: Battery utilization by RH-U for sizes from 20 kWh to 80 kWh.

Energy Placed in Battery by Battery Capacity for RH-U				
	20 kWh	**40 kWh**	**60 kWh**	**80 kWh**
Total energy placed in battery $[kWh]$	6.4	16.5	18.8	31.2

Table 6.4: Total energy placed in the battery by RH-U variant for battery sizes from 20 kWh to 80 kWh.

6.4 Variations in Unmanaged Demand and Renewable Production

Variations in unmanaged demand or renewable generation of up to 20% from forecasted levels ($var_a, var_u \leq 20\%$) do not have any significant effect on fuel consumption in the RH-U variant. At our forecasted value for unmanaged demand of 7.85 kW in each period, a 20% variation results in no more than ± 1.6 kW difference between forecasted planning and actual execution. This is small in relation to total load and sufficiently explains our observations.

We propose further research to evaluate environments with greater variations in unmanaged demand or unmanaged demand that is a larger proportion of overall demand. Additionally, we recommend consideration of robust demand handling mechanisms that would, for ex-

ample, perform priority-based cancellation and rescheduling of time-shiftable events to accommodate unmanaged demand variability without over-provisioning generators.

6.5 Summary

Analysis for our modeled configuration shows that the fuel efficiency of optimally scheduled systems relative to existing "always-on" systems is sensitive to (1) the excess generation capacity of the legacy system, (2) load duty cycles due to thermal burden on the shelter and ECU system, and (3) shelter interior temperature limits. Our results are not sensitive to storage capacity, storage efficiency, or generator run / rest times.

THIS PAGE INTENTIONALLY LEFT BLANK

CHAPTER 7:
Conclusions and Future Work

7.1 Conclusions

Optimal scheduling of time-shiftable loads has the potential to substantially reduce fuel consumption at the tactical edge, where energy costs and risks are the greatest. Intelligent management of generators, loads, and storage devices can minimize the number of running generators, improve average generator loading, and reduce peak-to-average power ratios while maintaining shelters within specified temperatures.

The benefits of optimal scheduling relative to unmanaged systems are most pronounced when loads operate at low duty cycles. This condition offers the greatest opportunity for load shifting to reduce peak demand and permit load satisfaction with smaller generators. As load duty cycle approaches 100% the benefits of optimal scheduling relative to a *properly sized* unmanaged microgrid diminish to zero. Because load duty cycle is itself cyclical, with patterns of high ECU duty cycles during the mid-day heat and low duty cycles in the cooler night hours, we expect any typical grid to operate well below 100% for a substantial portion of its periodic cycle and thus benefit from optimal scheduling.

Repeated assessments reveal that most expeditionary energy installations are **not** properly sized due to limitations on available generators and distribution equipment, risk attitudes that insist upon dedicated generators for critical loads, and expedient—rather than deliberate—system expansion and modification over time. Finally, even a well-designed system must "round up" cooling requirements to the nearest discretely-sized ECU and, once all electrical loads are summed, round up once again to the closest generator package capable of meeting the total load. Optimal scheduling offers a robust means to reduce the practical and systemic fuel consumption inefficiencies presented by the current architecture.

Our research suggests that optimally scheduled systems with energy storage will meet or exceed the performance of an unscheduled hybrid system by offering the choice to invest energy into current work instead of storing the energy, at a loss, to do work later. Optimal scheduling offers the potential to capture hybrid benefits while using a substantially smaller battery, reducing both deployment weight and battery lifecycle costs.

The enabling technologies necessary to implement optimal scheduling include appliance control, environmental monitoring and forecasting, and demand prediction. These technologies are already employed in the consumer, industrial, transportation, and commercial

utility sectors to manage energy demand and reduce costs. The DOD, as both the supplier and consumer of expeditionary energy, is uniquely positioned to adapt and vertically integrate these methods into its suite of tactical power and environmental control equipment.

These enabling technologies facilitate additional features that improve grid stability and performance. In the event of a partial outage, prioritized load-shedding can drop non-critical loads, such as billeting environmental control, in order to preserve continuity of power to critical loads such as perimeter security lighting, command and control equipment, and medical facilities. Multi-plexing, or time-sharing, of power production offers the potential to connect loads in excess of generation capacity without risk of overload, improving fuel efficiency in normal operations and enhancing grid resilience to generator casualties.

7.2 Future Work

We classify opportunities for future work into directions for additional analytical methods and directions for further research.

7.2.1 Analytical Methods

Our current model treats ECU operation as a binary on / off variable, consuming either zero or full rated power. This simplification ignores compressor unloading on current generation ECUs as well as the stepped or continuously variable cooling capacity and power demand of the DCAC and IECU. Higher-fidelity modeling of ECU operation will offer a more accurate and compelling analysis of potential fuel savings achieved through optimal scheduling.

We have limited our sensitivity analysis to variations of one parameter while all others are held constant. This single-factor analysis masks potentially confounding interactions between multiple parameters that may impact fuel efficiency. We recommend a multi-factor designed experiment to gain additional insight on the value of optimal scheduling under a broader range of conditions.

Our optimal scheduling model could be re-cast as a priority queueing model, viewing ECU demand or shelter thermal status as customers and electrical production as servers. This approach may reduce computational demand, provide greater ability for dynamic resource allocation and re-provisioning, and be more robust to uncertainty at the expense of global optimality. We propose additional investigation to determine the feasibility, advantages, and limitations of a tactical power queuing model relative to our optimal scheduling approach.

Machine learning and model predictive control present opportunities for enhanced uncertainty management. Our current rolling horizon with uncertainty model over-provisions generation capacity by a fixed percentage of forecast load in the planning phase to account for variations in actual conditions during the execution phase. Refining forecasts based upon historical conditions may reduce the amount of over-provisioning and the resulting generation-demand mismatch, leading to even greater fuel savings.

7.2.2 Further Research

Results from our PFK-GSM variant indicate that many of the fuel-efficiency benefits of optimally scheduled ECUs may be captured by determining, at the beginning of a planning period, what each thermostatically controlled ECU must do to maintain temperature, and then constraining their operation in an upcoming execution interval to that schedule while optimizing generator and storage operation to meet demand. We expect that this new variant, which we label rolling horizon, generator and storage management (RH-GSM), will sacrifice optimality but gain computational speed that could permit finer resolution modeling.

The telecommunication industry uses time-division multiplexing to serve the needs of multiple customers using resource levels that are incapable of meeting theoretical peak demand, but are sufficient to provide uninterrupted and transparent service for actual demand levels. Tactical power multiplexing offers the potential for fuel savings and grid resilience and warrants additional research on the risks, benefits, and sensitivities presented.

Our current research focuses on ECUs as the most egregious consumers of electricity on the battlefield. Capturing additional time-shiftable loads, both independent and user-controlled, may yield further opportunities for fuel conservation. Candidates for further study include water purification, water heating, refrigeration, laundry, mess operations, and manned and unmanned electrically-powered mobility platforms.

We recommend a comprehensive cost-benefit analysis that explores technology investment, deployment, and lifecycle costs against projected savings on the fully burdened cost of fuel to determine a net present value of implementing an optimally scheduled grid. We recommend field trials to validate the findings of our current research, and a systems engineering and cost-based analysis of alternatives for implementing optimal scheduling through retrofit of existing equipment or integration into succeeding generations of equipment.

THIS PAGE INTENTIONALLY LEFT BLANK

APPENDIX A:
Baseline Configuration Thermal Calculations

The heat transfer slope and intercept values for the thermal model of Section 4.2 are determined by shelter characteristics and environmental conditions. We provide the input parameter values, computational methodology, and results for the baseline scenario below.

Tables A.1 and A.2 contain the baseline AutoDISE and thermal model input values. We use these values to initialize the AutoDISE HVAC requirements calculator and then vary the "Max Temp in Shelter" parameter between 70 F and 90 F and record "Total Heat Load" results. Figures A.1 through A.3 show the HVAC requirements calculator interface for the three categories of shelters in the baseline configuration.

Tabulated results for internal shelter temperatures between 70 F and 90 F (21.1 C and 32.2 C) appear in Table A.3. Analysis reveals that the values are nearly linear over the range of temperatures we consider. Figure A.4 displays the plotted data and linear fit line, while Table A.4 contains the linear regression fit data that we use in the thermal model.

Environmental Conditions	
Parameter	**Value**
Ambient air temperature [$^{\circ}F$]	95
Ambient relative humidity [%]	15
Ground type	Grass/Dirt
Ground temperature [$^{\circ}F$]	105
Wind speed [$miles/hr$]	8.9
Solar load [$BTU/(hr \cdot sqft)$]	275

Table A.1: Baseline grid configuration environmental conditions.

Shelter Structural Characteristics and Internal Conditions			
	Shelters 1-7	**Shelter 8**	**Shelter 9**
Number of personnel	10	12	14
Personnel activity level	At rest	At rest	Moderate work
Desired internal humidity [%]	60	60	60
Ventilation / infiltration $[ft^3/min]$	100	120	140
Electrical load $[BTU/hr]$	682	682	7506
Shelter volume $[m^3]$	90.4	90.4	126.6
U factor $[BTU/(hr \cdot ft^3 \cdot^\circ F)]$	0.2342	0.2342	0.2342
Solar absorption	0.2	0.2	0.2

Table A.2: Baseline grid configuration shelter characteristics and internal conditions.

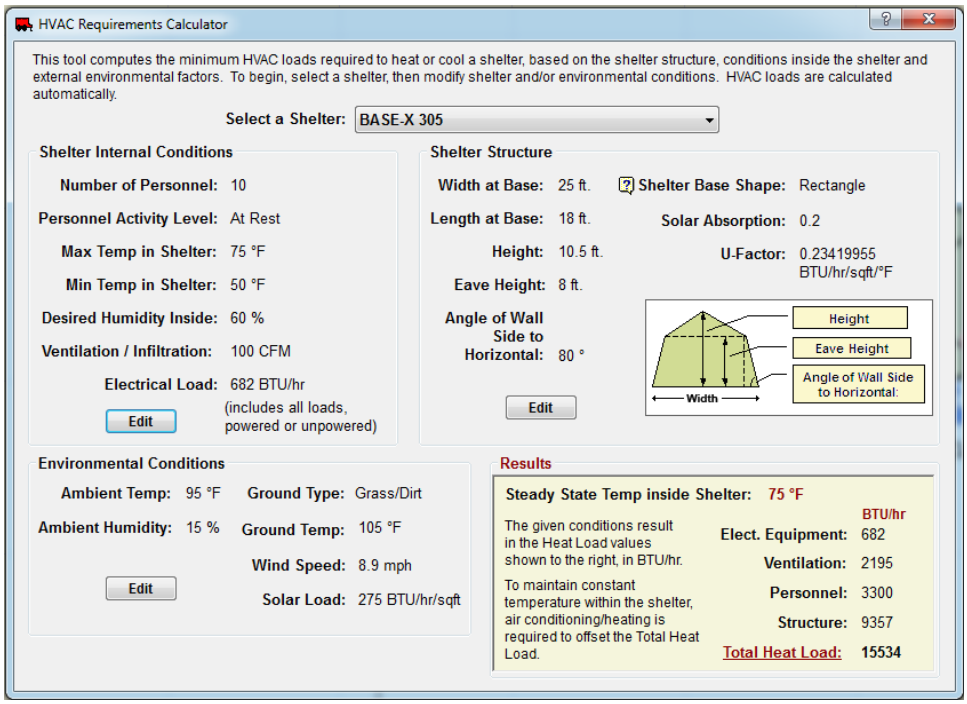

Figure A.1: AutoDISE calculated thermal load for shelters 1-7 at 75F, from [77].

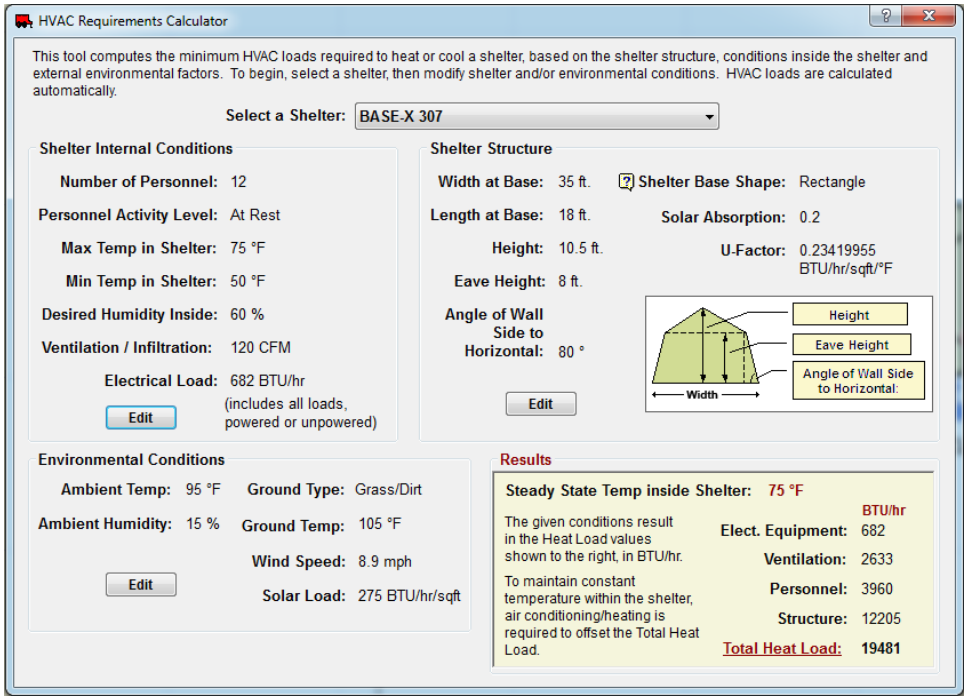

Figure A.2: AutoDISE calculated thermal load for shelter 8 at 75F, from [77].

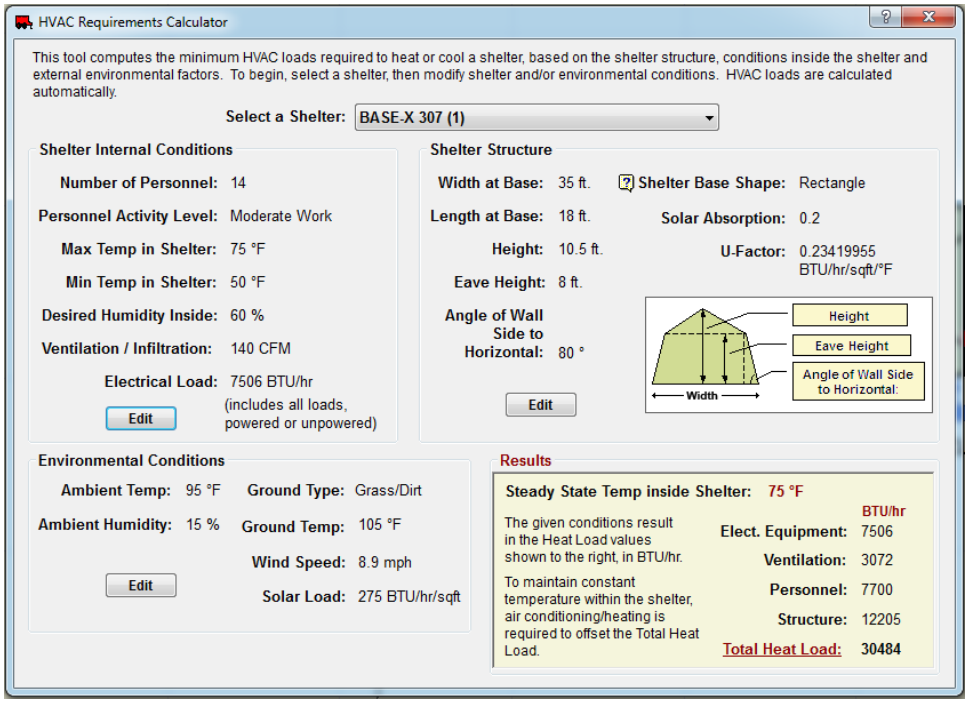

Figure A.3: AutoDISE calculated thermal load for shelter 9 at 75F, from [77].

Cooling Required to Maintain Temperature				
Max Temp		Required cooling [BTU/hr]		
°F	°C	Shelters 1-7	Shelter 8	Shelter 9
70	21.1	18,122	22,869	33,981
72	22.2	17,087	21,514	32,582
74	23.3	16,052	20,159	31,183
76	24.4	15,016	18,804	29,785
78	25.6	13,981	17,449	28,386
80	26.7	12,946	16,094	26,987
82	27.8	11,911	14,739	25,588
84	28.9	10,876	13,384	24,189
86	30.0	9,841	12,029	22,970
88	31.1	8,805	10,674	21,392
90	32.2	7,770	9,139	19,993

Table A.3: Results of AutoDISE thermal analysis.

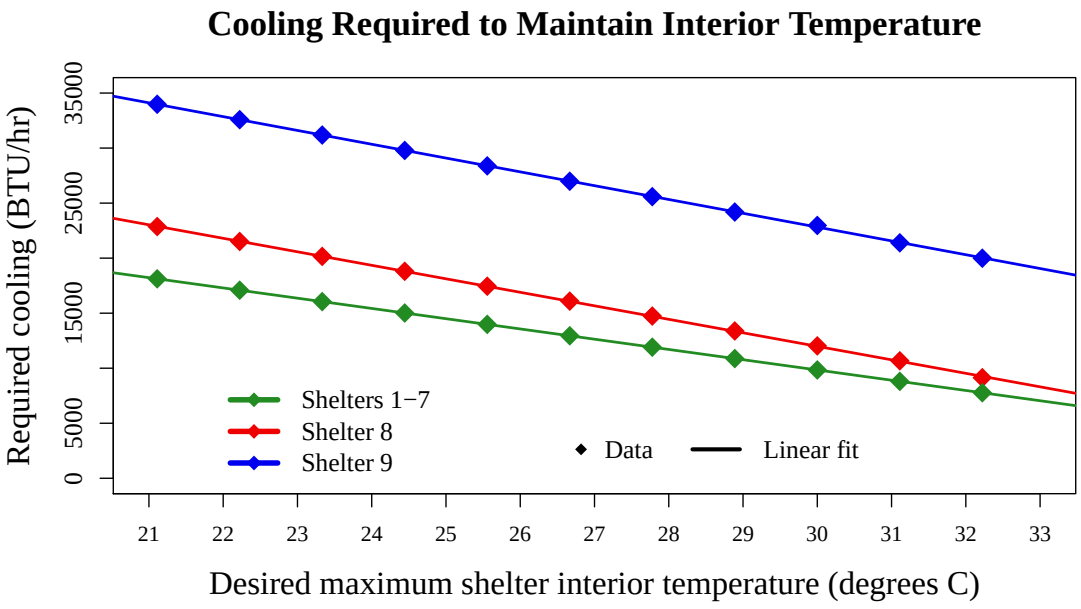

Figure A.4: AutoDISE results for required cooling for shelters 1-9 from 21.1C to 32.2C.

Shelter Heat Transfer Fitted Values			
	Shelters 1-7	**Shelter 8**	**Shelter 9**
Slope $[BTU/hr \cdot ^\circ C]$	-931	-1,226	-1,254
Intercept $[BTU/hr]$	37,790	48,794	60,456

Table A.4: Fitted values for the baseline configuration of shelters 1-9.

THIS PAGE INTENTIONALLY LEFT BLANK

APPENDIX B: Computational Data

Optimization was performed in GAMS running in Windows 7 on a Dell Precision T7500 workstation equipped with dual Intel Xeon X5675 3.06 GHz processors and 64 gigabytes (GBs) of memory. Problem size, solution time, rolling horizon parameters, and optimization stopping conditions are listed in Tables B.1 through B.3.

Optimization Dimensions and Solution Times					
			Variables		
Variant	**Time**	**Constraints**	**Total**	**Binary**	**SOS2**
LGCY	< 2 sec	2,408	6,897	-	-
PFK-SOM	< 10 sec	3,000	8,160	-	-
PFK-GSM	< 3 min	18,596	14,437	3,604	1,204
RH-PFK	8 to 19 min[†]	3,711	2,527	1,183	124
RH-U	12 to 20 min[†]	3,711	2,527	1,183	124
RMIP	< 10 sec	37,461	24,005	-	-

Table B.1: Solution times and problem dimensions for the baseline configuration.

[†]Rolling horizon times are for the entire ten-hour optimization period.

Stopping Conditions		
Relative Optimality Gap	**Absolute Optimality Gap**	**Time**
4%	0.15 gallons[‡]	30 minutes

Table B.2: Optimization stopping conditions for the baseline configuration.

[‡]The absolute optimality gap was selected to prevent excessive solution times in the early horizons of RH-PFK and RH-U.

Stopping Conditions		
Number of Intervals	**Minutes per Interval**	**Number of Horizons**
300	2 (*10 hours total*)	20 (*30 minutes each*)

Table B.3: Parameters for rolling horizon optimization.

THIS PAGE INTENTIONALLY LEFT BLANK

List of References

[1] "Environmental medicine: heat, cold, and altitude," in *Military Preventive Medicine: Mobilization and Deployment*, R. Burr, Ed. Natick, MA: Office of the Surgeon General, United States Army, 2003, vol. 1, ch. 19, pp. 363–416.

[2] M. Schwartz, K. Blakely, and R. O'Rourke, "Department of Defense Energy initiatives: Background and issues for Congress," Congressional Research Service, Washington, DC, CRS Report R42558, June 2012.

[3] *10 U.S. Code § 2924(5)*, July 2015.

[4] Office of the Assistant Secretary of Defense (Energy, Installations, and Environment), "Department of Defense annual energy management report for fiscal year 2014," Department of Defense, Washington, DC, Report, May 2015.

[5] Office of the Assistant Secretary of Defense (Energy, Installations, and Environment), "Department of Defense annual energy management report for fiscal year 2013," Department of Defense, Washington, DC, Report, Oct. 2014.

[6] The CIA World Factbook. [Online]. Available: https://www.cia.gov/library/publications/the-world-factbook/rankorder/2246rank.html

[7] A. M. Andrews, W. Bryzik, R. Carlin, J. M. Feigley, W. E. Harrison III, D. J. Katz, J. Y. Rodriquez, R. L. Snead, J. C. Sommerer, J. T. Tozzi, G. E. Webber, W. Weldon, and J. Wolbarsht, "Future fuels," Naval Research Advisory Committee, Arlington, VA, Tech. Rep. NRAC 06-1, Apr. 2006.

[8] T. C. Moore, B. H. Newell, J. L. Alderman, R. Dickson, D. Nolan, and J. W. Barnett, "Report of the Afghanistan Marine energy assessment team," Tech. Rep., Jan. 2011.

[9] *United States Marine Corps Expeditionary Energy Strategy Implementation Planning Guidance*, Office of the Commandant of the Marine Corps, Washington, DC, Feb. 2011.

[10] M. Gillman, W. M. Singleton, R. A. Wilson, W. Cotta, J. Donnal, J. Paris, and S. Leeb, "Accounting for every kilowatt," *Defense AT&L*, vol. XLIII, no. 5, pp. 44–49, September-October 2014.

[11] U.S. Government Accountability Office, "Defense management: Steps taken to better manage fuel demand but additional information sharing mechanisms are needed," U.S. Government Accountability Office, Washington, DC, GAO Report GAO-12-619, June 2012.

[12] U.S. House. 111th Congress, 1st Session. (2009, Mar 3), *Department of Defense Fuel Demand Management at Forward-Deployed Locations and Operational Energy Initiatives*. [Online]. Available: http://www.gpo.gov/fdsys/pkg/CHRG-111hhrg51161/pdf/CHRG-111hhrg51161.pdf

[13] D. S. Eady, S. B. Siegel, R. S. Bell, and S. H. Dicke, "Sustain the mission project: Casualty factors for fuel and water resupply convoys," Army Environmental Policy Institute, Arlington, VA, Final Technical Report CTC-CR-2009-163, Sep. 2009.

[14] A. Edwards and M. Schwartz, "Department of Defense fuel costs in Iraq," Congressional Research Service, Washington, DC, CRS Report RS22923, July 2008.

[15] S. B. Siegel, S. Bell, S. Dicke, and P. Arbuckle, "Sustain the mission project: Energy and water costing methodology and decision support tool," Army Environmental Policy Institute, Arlington, VA, Final Technical Report, Mar. 2008.

[16] *Guide to Contingency Electrical Power System Installation*, Air Force Handbook 10-222, vol 5, U.S. Dept. of the Air Force, Washington, DC, Sep. 2008.

[17] P. Bulanow, P. Tabler, and S. Charchan, "Expeditionary energy assessment environmental control unit alternatives study," U.S. Marine Corps Expeditionary Energy Office, Quantico, VA, Final Report, July 2011.

[18] S. B. Van Broekhoven, E. Shields, S. V. T. Nguyen, E. R. Limpaecher, and C. M. Lamb, "Tactical power systems study ," Lincoln Laboratory, Massachusetts Institute of Technology, Lexington, MA, Technical Report 1181, May 2014.

[19] G. Dogum, "Village stability operations VS-platform: Power site surveys," U.S. Army Research, Development, and Engineering Command (RDECOM) Field Assistance in Science and Technology Center (FAST-C), Trip Report, July 2012.

[20] C. Bolton, July 2015, private communication.

[21] M. Rooney, "Advanced Medium Mobile Power Sources (AMMPS) program overview," Presentation, Nov. 2009. [Online]. Available: http://jocotas.natick.army.mil/Nov09/rooney%20advanced%20medium%20mobile%20power%20sources%20(ammps)%20program.pdf

[22] *Military Generator*, Cummins Power Generation Corp., Minneapolis, MN, 2013.

[23] U.S. Marine Corps Expeditionary Energy Office. [Online]. Available: http://www.hqmc.marines.mil/e2o/Fleet.aspx

[24] B. Frounfelker and T. Wilke, "Tent foam insulation cost benefit analysis," US Army Material Systems Analysis Activity, Aberdeen, MD, Technical Report TR-2010-14, Apr. 2010.

[25] J. Hampel, "Fabric structures team overview," presented at the 6th Bi-Annual DOD JOCOTAS Meeting with Rigid Soft Wall Shelter Industry and Indoor & Outdoor Exhibition, Panama City, FL, Nov. 2009. [Online]. Available: http://dtic.mil/docs/citations/ADA514946

[26] J. Taylor, "Improved environmental control unit (IECU) program overview," presented at the 6th Bi-Annual DOD JOCOTAS Meeting with Rigid Soft Wall Shelter Industry and Indoor & Outdoor Exhibition, Panama City, FL, Nov. 2009. [Online]. Available: http://dtic.mil/docs/citations/ADA514486

[27] E. Thompson. (2012, Oct.). Army successfully demonstrates tactical operations smart grid. Aberdeen, MD. [Online]. Available: http://www.army.mil/article/88440/

[28] Lockheed Martin receives $3.5 million hybrid intelligent power microgrid contract. (2010, Oct.). [Online]. Available: http://www.lockheedmartin.com/us/news/press-releases/2010/october/LMReceives35MillionHybrid.html

[29] E. Anderson, M. Antkowiak, R. Butt, J. Davis, J. Dean, M. Hillesheim, E. Hotchkiss, R. Hunsberger, A. Kandt, J. Lund, K. Massey, R. Robichaud, B. Stafford, and C. Visser, "Broad overview of energy efficiency and renewable energy opportunities for Department of Defense installations," National Renewable Energy Laboratory (NREL), Golden, CO, Tech Report NREL/TP-7A20-50172, Aug. 2011. [Online]. Available: http://www.osti.gov/servlets/purl/1023698-6alCol/

[30] National Research Council, "Force multiplying technologies for logistics support to military operations," The National Academies, Washington, DC, Tech. Rep., Dec. 2014.

[31] H. Bouaicha, "Optimal day-ahead scheduling of a hybrid electric grid using weather forecasts," master's thesis, Ops. Research Dept., Naval Postgraduate School, Monterey, CA, Dec. 2013.

[32] N. A. Ulmer, "Optimizing microgrid architecture on department of defense installations," master's thesis, Ops. Research Dept., Naval Postgraduate School, Monterey, CA, Sep. 2014.

[33] A. M. Newman, "Energy resource planning tool for the Office of Naval Research," presented at Naval Postgraduate School, Monterey, CA, June 2015.

[34] M. Sadiqi, A. Pahwa, and R. D. Miller, "Basic design and cost optimization of a hybrid power system for rural communities in Afghanistan," in *North American Power Symposium (NAPS)*, Champaign, IL, 2012, pp. 1–6.

[35] J. S. Vardakas, N. Zorba, and C. V. Verikoukis, "A survey on demand response programs in smart grids: Pricing methods and optimization algorithms," *Communications Surveys & Tutorials, IEEE*, vol. 17, no. 1, pp. 152–178, 2015.

[36] M. Alizadeh, G. Kesidis, and A. Scaglione, "Clustering consumption in queues: A scalable model for electric vehicle scheduling," *Signals*, May 2013. [Online]. Available: http://ieeexplore.ieee.org/xpls/abs_all.jsp?arnumber=6810299

[37] S. Chen, Y. Ji, and L. Tong, "Deadline scheduling for large scale charging of electric vehicles with renewable energy," in *IEEE 7th Sensor Array and Multichannel Signal Processing Workshop (SAM)*, Hoboken, NJ, 2012, pp. 13–16. [Online]. Available: http://acsp.ece.cornell.edu/papers/ChenJiTong12SAM.pdf

[38] H. Mohsenian-Rad and M. Ghamkhari, "Optimal charging of electric vehicles with uncertain departure times: A closed-form solution," *IEEE Transactions on Smart Grid*, vol. 6, no. 2, pp. 940–942, Mar. 2015. [Online]. Available: http://ieeexplore.ieee.org/xpls/abs_all.jsp?arnumber=6960074&tag=1

[39] Y. Xu and F. Pan, "Scheduling for charging plug-in hybrid electric vehicles," in *IEEE 51st Annual Conference on Decision and Control (CDC)*, Maui, HI, 2012, pp. 2495–2501.

[40] H. Sherif, Z. Zhu, and S. Lambotharan, "An optimization framework for home demand side management incorporating electric vehicles," in *2014 IEEE Innovative Smart Grid Technologies - Asia (ISGT ASIA)*, 2014, pp. 57–61.

[41] Energy Storage Association, "Spinning Reserve," Washington, DC, n.d. [Online]. Available: http://energystorage.org/energy-storage/technology-applications/spinning-reserve

[42] M. C. Vlot, J. D. Knigge, and J. G. Slootweg, "Economical regulation power through load shifting with smart energy appliances," *IEEE Transactions on Smart Grid*, vol. 4, no. 3, pp. 1705–1712, 2013. [Online]. Available: http://ieeexplore.ieee.org/xpls/abs_all.jsp?arnumber=6513322

[43] D. T. Nguyen and L. B. Le, "Optimal bidding strategy for microgrids considering renewable energy and building thermal dynamics," *IEEE Transactions on Smart Grid*, vol. 5, no. 4, pp. 1608–1620, July 2014. [Online]. Available: http://ieeexplore.ieee.org/xpls/abs_all.jsp?arnumber=6839078

[44] P. Tarasak, C. C. Chai, and Y. S. Kwok, "Demand bidding program and Its application in hotel energy management," *IEEE Transactions on Smart Grid*, vol. 5, no. 2, pp. 821–828, 2014. [Online]. Available: http://ieeexplore.ieee.org/xpls/abs_all.jsp?arnumber=6732972

[45] Southern California Edison, "Demand Bidding Program," 2010. [Online]. Available: https://www.sce.com/wps/wcm/connect/96702c0a-c759-4efe-b302-f874e4407c32/090217_Demand_Bidding_Fact_Sheet.pdf?MOD=AJPERES

[46] G. Wilkenfeld, "A national demand management strategy for small airconditioners: The role of the national appliance and equipment energy efficiency program," National Appliance and Equipment Energy Efficiency Committee Report 2004/22, November 2004.

[47] I. Koutsopoulos and L. Tassiulas, "Challenges in demand load control for the smart grid," *IEEE Network*, vol. 25, no. 5, pp. 16–21, 2011. [Online]. Available: http://ieeexplore.ieee.org/xpls/abs_all.jsp?arnumber=6033031

[48] J. Vavrin, "Power and energy considerations at forward operating bases (FOBs)," presented at the NDIA Environment, Energy Security & Sustainability (E2S2) Symposium & Exhibition, Denver, CO, June 2010.

[49] *Engineer Prime Power Operations*, TM 3-34.45, U.S. Dept. of the Army, Washington, DC, Aug. 2013.

[50] "Earl Energy FlexGen Power Systems," n.d. [Online]. Available: http://www.earlenergy.com/uploads/4/5/3/3/45338487/flexgen_battlefield_energy_spec_sheet_3kw.pdf

[51] "ZeroBase: Energy to the Tactical Edge," May 2015. [Online]. Available: http://thezerobase.com/wp-content/uploads/mdocs/CaseStudyARMYREFE2E_v1_14-05-15.pdf

[52] B. Bloodworth, "COP Chak DC trip report," U.S. Army Corps of Engineers, Champaign, IL, Trip Report, Nov. 2011.

[53] B. Bloodworth, "COP Nerkh trip report," U.S. Army Corps of Engineers, Champaign, IL, Trip Report, Nov. 2011.

[54] W. M. Solis, "Defense management: DOD needs to increase attention on fuel demand management at forward-deployed locations," U.S. Government Accountability Office, Washington, DC, GAO Report GAO-09-300, Feb. 2009.

[55] J. Whitmore, "Intelligent Power Management Distribution Systems (IPMDS)," presented at the 2011 Joint Service Power Expo, Myrtle Beach, SC, May 2011. [Online]. Available: http://www.dtic.mil/ndia/2011power/Session2_12093_Whitmore.pdf

[56] U.S. Dept. of Energy, "2014 smart grid system report," U.S. Department of Energy, Washington, DC, Report to Congress, Aug. 2014. [Online]. Available: http://energy.gov/sites/prod/files/2014/08/f18/SmartGrid-SystemReport2014.pdf

[57] E. Shaffer, P. Roege, and T. Zheleva, "Advanced microgrid concepts and technologies workshop," US Army Research Laboratory, Adelphi, MD, Tech Report ARL-TR-6407, Apr. 2013.

[58] Large power sources (n.d.). U.S. Army Program Director for Large Power Sources. Warren, MI. [Online]. Available: http://www.peocscss.army.mil/PdDLPS.html. Accessed Aug. 18, 2015.

[59] L. Murphy, "Creating energy efficiency on the battlefield," DRASH Systems, White Paper, (n.d.), Accessed Aug. 5, 2015. [Online]. Available: http://www.drash.com/userfiles/File/White%20Paper/IPT%20White%20Paper.pdf

[60] Medium power sources (n.d.). U.S. Army Product Manager Medium Power Sources. Warren, MI. [Online]. Available: http://www.peocscss.army.mil/PdMMPS.html. Accessed Aug. 18, 2015.

[61] Cummins Power Generation. (2010). Advanced Medium Mobile Power Sources (AMMPS). [Online]. Available: https://cumminspower.com/www/literature/brochures/F-2254-MilitaryAdvancedMediumMobilePowerSources-en.pdf. Accessed Sep. 2, 2015.

[62] C. Hedelt. (2012, Dec.). MCSC helps Marines go green. [Online]. Available: http://www.marcorsyscom.marines.mil/News/PressReleaseArticleDisplay/tabid/8007/Article/509517/mcsc-helps-marines-go-green.aspx

[63] National Solar Radiation Data Base 1991-2010 Update. Four Corners, NM data. [Online]. Available: http://rredc.nrel.gov/solar/old_data/nsrdb/1991-2010/hourly/siteonthefly.cgi?id=723658. Accessed Aug. 12, 2015.

[64] X3-20 portable power system (n.d.). X3 Energy. [Online]. Available: http://www.x3energy.net/X3-20.php. Accessed Jul. 19, 2015.

[65] J. Andrews and N. Jelley, *Energy Science: Principles, Technologies, and Impacts*. Oxford, UK: Oxford Univ. Press, 2013.

[66] *Bare Base Assests*, Air Force Handbook 10-222, Volume 2, Department of the Air Force, Washington, DC, Feb. 2012.

[67] Program Manager, Expeditionary Power Systems, "Environmental Control Equipment (ECE)," in *Environmental Control and Power Sources Equipment*. Quantico, VA: U.S. Marine Corps Systems Command, 2011, no. TM 12359A-OD, Ch. 4, ch. 4. [Online]. Available: http://www.marcorsyscom.marines.mil/Portals/105/pdmeps/docs/ECE/TM%2012359A-OD-C%20JUNE2011%20ECU.pdf

[68] NPR Staff. (2011, June). Among the costs of war: Billions a year in A.C.? [Online]. Available: http://www.npr.org/2011/06/25/137414737/among-the-costs-of-war-20b-in-air-conditioning

[69] U.S. Army Natick Soldier Research, Development, and Engineering Center, *Commanders' Smartbook Equipment Catalog*, Natick, MA, Apr. 2013.

[70] Joint Committee OnTactical Shelters (JOCOTAS), *Department of Defense Standard Family of Tactical Shelters (Rigid/Soft/Hybrid)*, Natick, MA, May 2012.

[71] U.S. Army Natick Soldier Research, Development and Engineering Center, "Fabric structures team technology update," presented at the 7th Bi-Annual DOD JOCOTAS Meeting with Rigid Soft Wall Shelter Industry and Indoor & Outdoor Exhibition, Natick, MA, Nov. 2011.

[72] W. M. Solis, "Increased attention on fuel demand management at DOD's forward-deployed locations could reduce operational risks and costs," Government Accountability Office, Washington, DC, Testimony Before the Subcommittee on Readiness, Committee on the Armed Services, House of Representatives GAO-09-388T, Mar. 2009.

[73] *Operation/Maintenance Manual for Mobile Electric Power Distribution System Replacement (MEPDIS-R)*, TM 6110-OI-1, U.S. Marine Corps Systems Command, Quantico, VA, Feb. 2012.

[74] *Operator and Field Maintenance Manual for Power Distribution Illumination Systems, Electrical (PDISE)*, TM 9-6150-226-13, U.S. Army Headquarters, Washington, DC, Apr. 2012.

[75] J. Antonetti, "Low-sulfur diesel fuel (DL)-2 and jet propellant (JP)-8 fuel consumption test Advanced Medium Mobile Power Sources (AMMPS)," Program Manager, Expeditionary Energy and Sustainment Systems, Fort Belvoir, VA, Tech. Rep. ATC-11590, Aug. 2014.

[76] BRTRC Federal Solutions, Inc, *AutoDise 6.2.3.7 User Manual*, Vienna, VA, Feb. 2015. [Online]. Available: https://www.autodise.net

[77] AutoDISE 6.2.3.7. BRTRC Federal Solutions, Inc. [Online]. Available: https://www.autodise.net/default.asp

[78] P. D. Howard, "Capabilities of the generic systems assessment model," United States Army Belvoir Research, Development and Engineering Center, Fort Belvoir, VA, Tech. Rep. USA-BRDEC-TR//2530, July 1992.

[79] E. Shields and B. H. Newell, "Current power and energy requirements of forward deployed USMC locations," presented at the NDIA Environment, Energy Security & Sustainability (E2S2) Symposium & Exhibition, May May 22, 2012.

[80] B. H. Newell and E. B. Shields, "USMC expeditionary energy office report on expeditionary energy data collection within Regional Command Southwest, Afghanistan," USMC Expeditionary Energy Office, Tech. Rep., Sep. 2012.

Initial Distribution List

1. Defense Technical Information Center
   Ft. Belvoir, Virginia

2. Dudley Knox Library
   Naval Postgraduate School
   Monterey, California